Project Photogator

NASA Student Launch 2023 Preliminary Design Review

University of Florida
Swamp Launch Rocket Team
939 Center Dr, Gainesville, FL 32611
MAE-A 324
October 26, 2022

Table of Contents

Table of Figures

Table of Tables

1. Summary of Report

1.1 Team Summary

Swamp Launch Rocket Team
University of Florida – MAE-A 324
939 Center Drive
Gainesville, FL 32611

1.1.1 Team Mentor

Jimmy Yawn
NAR #85660, TRA #09266 Level 3 Certified
jimmy.yawn@sfcollege.edu
(352) 281-2025

1.1.2 Hours

The total amount of hours the team spent developing PDR was 572 hours. This time was spent designing, performing tests, writing PDR, and holding meetings.

1.1.3 Team Social Media

Instagram	Facebook	YouTube	LinkedIn
@swamplaunch	Swamp Launch Rocket Team	Swamp Launch Rocket Team	Swamp Launch Rocket Team

Table 1: Team Social Media

1.2 Launch Vehicle Summary

The launch vehicle is 4 in. in diameter with an overall length of 115 in and overall mass of 398 oz, including the motor. There are three sections: the forward section, the central section, and aft section. An avionics bay is in the central section. A payload is in the aft section and remains securely contained throughout flight. The launch vehicle has a dual deploy recovery system comprised of a 72 in main and 24 in. drogue parachute. Based on simulations, the center of gravity and center of pressure are located 73.175 in and 84.035 in from the tip of the nosecone respectively, resulting in a stability margin of 2.71. The selected motor is an Aerotech K1000T-P motor. The target altitude is 4600 ft. The overall lengths and masses of each main section of the launch vehicle are listed in Table 2.

Section	Exterior Length (in)	Overall Mass (oz)
Forward	45	77.9
Central	21	74.0
Aft	49	246.1
Total	**115**	**398.0**

Table 2: Lengths and Masses of Launch Vehicle

1.3 Payload Summary

Payload Title: InvestiGator

The payload consists of three camera systems that will be positioned 120° apart so that one will always be aligned with the z-axis, normal to the ground, upon landing. Each camera system will have a camera housing that integrates a camera, camera mount, and motors. An Inertial Measurement Unit (IMU) will detect the orientation of the launch vehicle and determine which camera to activate so that only one camera will be in use when taking photos of the surroundings. A Software Defined Radio (SDR) dongle will be incorporated in the payload to receive Automatic Package Reporting System (APRS) commands from NASA.

2. Changes Made Since Proposal

2.1 Changes Made to Launch Vehicle

2.1.1 Changes to Vehicle Design

The payload will be located in a dedicated payload airframe that is part of the aft section. Changes were made to the vehicle design to improve the structural integrity of the payload airframe. The payload airframe will have three rectangular holes that the camera system deploys out of upon landing. The radius of the hole's fillets at its corners was increased to reduce the stress concentrations in those areas. The holes in the airframe were also made larger to allow for unobstructed rotation of the camera systems and movement of the spring for the camera housing. The holes in the payload were changed from 3.89 x 1.78 in to 4.524 x 1.732 with a 0.1 in fillet on each corner to reduce stress concentrations. The payload forward coupler length increased from 4 in to 8 in to take in consideration the separation point occurring between the central and aft sections of the launch vehicle. The length of payload airframe was changed from 22 in to 25 in, so the payload housings can fit inside of the airframe. To take in consideration the size of the forward airframe was decreased from 30 in to 27 in. The size of the fins changed as well in order for the launch vehicle to stay within the required altitude. The dimensions of the fins were changed from a height of 4.5 in to 4 in, a tip chord length of 7 in to 0.5 in, and a sweep length of 4.984 in was changed to 8.984 in.

2.1.2 Changes to Avionics and Recovery System

Changes were made to the layout of the avionics bay to ensure that the batteries and arming switches are secure. The mounts for the keylock switches, which will act as arming switches, were separated into two parts that will be fastened together to prevent motion of the switches. Similarly, caps were added to the battery holders that will fasten the battery in place.

2.2 Changes Made to Payload

2.2.1 Changes to Mechanical Design

Changes were made to ensure the validity of the concept as modeled in aerodynamic simulations. The size of the housings were increased to allow for unobstructed rotation. The camera mounts that cover the holes in the airframe were modified in length to minimize exposed surface area. The original design's camera mount did not extend past the camera, so the hole in the airframe was exposed above the camera. The housing 3D print was changed from rectangular to curved on the surface that aligns with the airframe to match the curvature of the airframe.

2.2.2 Changes to Electronics Design

The shape of the solenoid motor shaft was changed to allow the camera arm to be retracted into the payload bay. The wiring and placement of the electronics in the payload bay was changed to allow easier assembly on the launch field. Instead of placing the Raspberry Pi in the center of the payload bay, it was moved to the end of the airframe to allow for easy access when wiring the electronics.

2.2.3 Changes to Software Design

The initial software design had one singular motor controller subsystem. Now, it will be split into two different systems, one for the solenoid motors and one for the stepper motors. This is because the motors have different input requirements, and they occur at different stages in the launch vehicle's lifecycle. Splitting them into two additional systems makes it easier to test and manage each motor individually. Finally, in the proposal, it was mentioned that the software will either be written Python or C++, but that has changed to just being solely C++.

2.3 Changes Made to Project Plan

There have been changes to the project plan that was established in the proposal. These changes were made to improve the timeline of the project's development. The changes are:

- The subscale manufacturing and launch have been changed to the week of November 14, 2022, and Saturday, December 3, 2022, respectively. This change increases the time to receive component deliveries and to manufacture the vehicle.
- The team's preferred CAD software is now Fusion 360 instead of SolidWorks 2022.

3. Vehicle Criteria

3.1 Selection, Design, and Rationale of Launch Vehicle

3.1.1 Mission Statement

The launch vehicle's mission is to perform a flight that is safely recoverable. The launch vehicle will be able to carry the payload camera housings without causing damage to the launch vehicle. The launch vehicle must be able to be relaunch and not sustain irreparable damage that would prevent recovery.

3.1.2 Design Alternatives

An alternative design incorporated externally mounted camera systems. The external mounts would have simplified the design in comparison to the selected design. Despite this, the external camera mount concept was not selected since the launch vehicle would become over-stable causing complications with the aerodynamics of the flight.

The launch vehicle would consist of a forward section, central section, and aft section (Figure 1). The cameras would be mounted to the aft section and would be positioned directly above the fins to minimize their impacts on the launch vehicle's aerodynamics. Since there are three fins, one of the external cameras would be oriented normal to the ground upon landing and would then be free to rotate within the external camera housing. The external camera housings would be made of a transparent material, allowing the cameras to take images without having to remove the housings.

The avionics bay would be located in the coupler between the forward and aft sections, and the main parachute and drogue parachute would be housed forward and aft of the bay, respectively. The drogue parachute would be located in the central airframe and would be deployed by separating the central and aft sections. The main parachute would be located in the forward airframe and would be deployed by separating the forward and central sections.

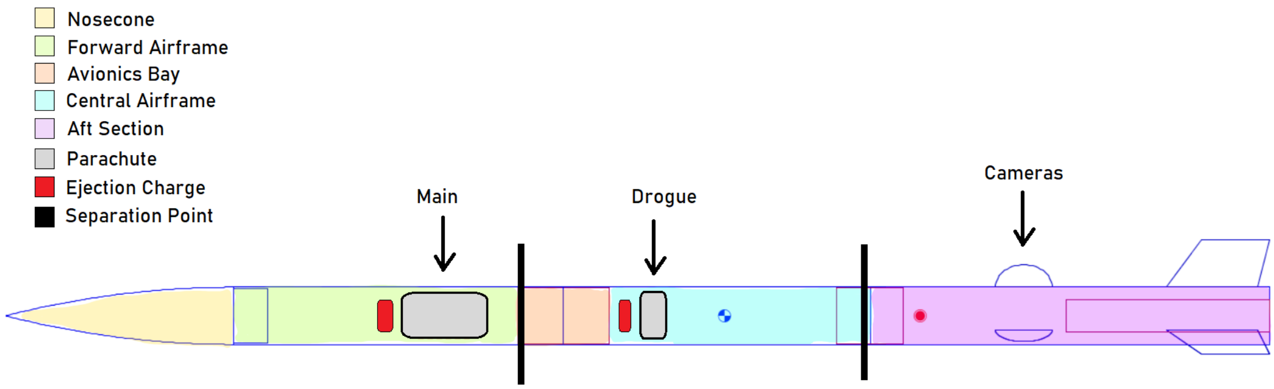

Figure 1: Launch Vehicle Design for Externally Mounted Cameras Alternative

Another alternative design that was considered was to have three cameras that would be contained next to each other in the aft airframe that would move radially outward from the airframe after landing using linear motion. They would then be able to photograph the launch vehicle's surroundings. The launch vehicle layout, parachute locations, ejection charge locations, and separation points are identical to the previously discussed design alternative (Figure 2).

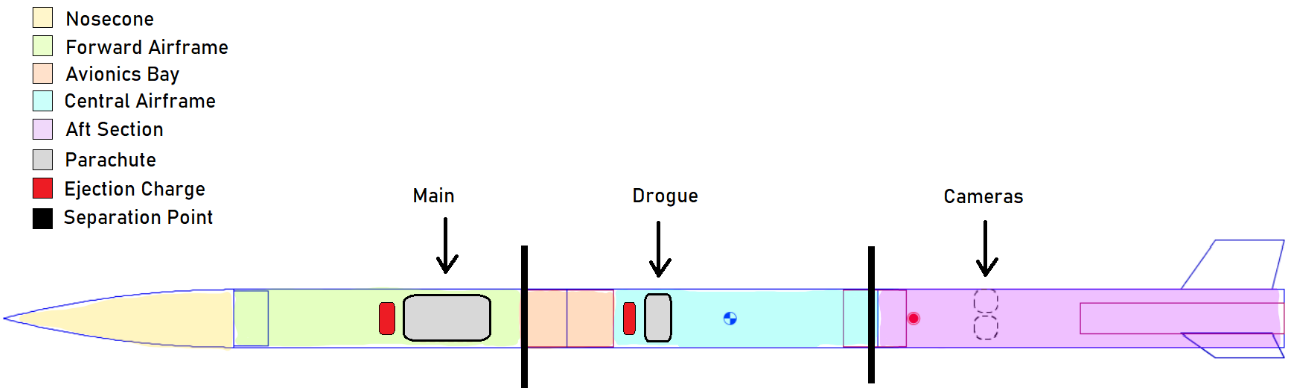

Figure 2: Launch Vehicle Design for Linear Cameras Alternative

The cameras would be radially offset within the aft airframe and be located 120° from each other (Figure 3). After landing, linear actuators within the aft airframe would extend, pushing the cameras out of the launch vehicle through the holes in the airframe. Because this launch vehicle would have three fins, one of the fins would be oriented vertically and the camera aligned with that vertical fin would be in the correct orientation to photograph the launch vehicle's surroundings.

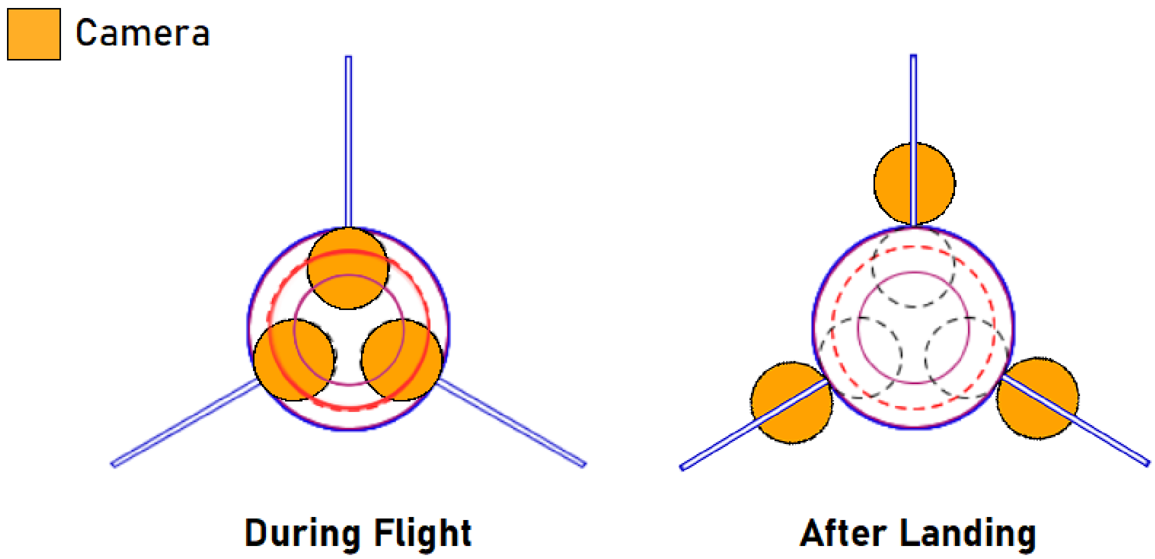

Figure 3: Camera Positions for Linear Camera Alternative Design

Ultimately, the linear motion design was not selected due to complications with fitting the cameras, the linear actuators, and other electronics and batteries in the airframe. The linear actuators were the largest complication as even linear actuators that move very little were big enough to not fit in the airframe. Additionally, the linear actuators would have to be positioned directly next to the cameras, which there was not sufficient space for in neither a 4 in or 5 in diameter airframe.

3.1.3 Material Selection

Material selection was justified by completing objectives and decision matrices that assessed material options for each component. Each objective was compared and had a weighting factor relating to its importance added into the decision matrices.

Design matrices were used to evaluate the different possible materials. The magnitudes described in the design matrices explain the numerical or qualitative value which relates to an objective. Qualitative scores were determined based on the assignment table (Table 3). A score was found by comparing the magnitudes on a linear scale where a score of 10 out of 10 is the best. Lastly, a final value was found by multiplying each objective's score and weighting factor, which was compared to find the highest overall value. The material with the largest value was the selected material.

Qualitative Score	
Great	10
Good	8
Okay	6
Fair	4
Poor	2

Table 3: Qualitative Scoring Assignments

3.1.3.1 Nosecone

Potential materials for the nosecone were compared using defined evaluation criteria to select a final material for the launch vehicle.

3.1.3.1.1 Evaluation Criteria

Decision matrices were used to evaluate potential nosecone materials. Scores were calculated linearly, and the best score was assigned 10 out of 10 points (Table 4).

Nosecone			Polypropylene			G12 Fiberglass		
Objective	Weighting Factor	Parameter	Mag.	Score	Value	Mag.	Score	Value
Cost	0.1	USD	24.75	10.0	1.00	75.90	3.3	0.33
Density	0.30	lb/in^3	0.03	4.9	1.48	0.067	10.0	3.00
Tensile Strength	0.60	ksi	6.50	0.6	0.34	115	10.0	6.00
Overall value					**2.82**			**9.33**

Table 4: Nosecone Material Decision Matrix

Cost is the price of each component (USD). Cost was taken into consideration to pick the best nosecone while also keeping overall costs of the vehicle low. Due to the cost of the nosecone being relatively low in the overall cost of the launch vehicle, the cost was weighted at only 10%. The nosecone with the lowest cost received a score of 10 out of 10.

Density is the mass per unit volume (lb/in^3) of the material. Using a denser material for a nosecone will shift the center of gravity forward, creating a more stable launch vehicle. It also helps to ensure that the launch vehicle follows it predicted path. Density was weighted at 30% because of its importance to flight stability. As a result, the material with the highest density received a score of 10 out of 10.

Tensile strength is the maximum strength, measured in ksi, that can be applied to the nosecone without damage to the launch vehicle. The nosecone must withstand several forces from air resistance, ejection charges, the recovery harness, and ground impact. If the nosecone were to fail the launch vehicle would sustain damage such that it would be unrecoverable. For this reason, tensile strength is ranked at 60% and the design with the highest tensile strength received a score of 10 out of 10.

3.1.3.1.2 Alternative Materials

Polypropylene and G12 Fiberglass were the two materials considered for the nosecone. Polypropylene scored the lowest in both the areas of density and tensile strength. As a result, this material was not strongly considered as an option for the nosecone.

3.1.3.1.3 Selected Material

G12 fiberglass scored the highest in both areas of density and tensile strength. The larger value of density means that the center of gravity will be moved forward on the launch vehicle and will enable a more stable flight than the polypropylene alternative. The strength of this material and its effects on stability were the reasons it was chosen.

3.1.3.2 Airframe and Couplers

Potential airframe and coupler materials were evaluated using various criteria to select a final material.

3.1.3.2.1 Evaluation Criteria

Decision matrices were used to evaluate the airframe and coupler material. The scores were calculated linearly with 10 out of 10 being the highest score (Table 5).

Airframe			Blue Tube			G12 Fiberglass		
Objective	Weighting Factor	Parameter	Mag.	Score	Value	Mag.	Score	Value
Cost	0.17	USD/in	0.92	8.04	1.34	2.12	3.49	0.58
Density	0.17	lb/in^3	0.05	10.00	1.67	0.07	6.19	1.03
Compressive Strength	0.50	ksi	4.28	1.43	0.71	30.00	10.00	5.00
Machinability	0.17	experience	good	8.00	1.34	okay	6.00	1.00
Overall value					**5.1**			**7.6**
Airframe			**Phenolic**			**Quantum Tube**		
Objective	Weighting Factor	Parameter	Mag.	Score	Value	Mag.	Score	Value
Cost	0.17	USD/in	0.74	10.00	1.67	0.87	8.51	1.42
Density	0.17	lb/in^3	0.05	9.83	1.64	0.05	9.42	1.57
Compressive Strength	0.50	ksi	13.50	4.50	2.25	18.20	6.07	3.03
Machinability	0.17	experience	good	8.00	1.34	good	8.00	1.34
Overall value					**6.9**			**7.4**

Table 5: Airframe and Couplers Materials Decision Matrix

Cost is the price per inch of the material (USD/in). Cost was considered because it needs to be minimized in order to stay within the project budget. Airframe and couplers are usually the largest cost factor when taking in consideration the cost of the launch vehicle. However, the performance of the airframe is very important as well, which is why the cost is only weighted at 16.7%. Cost was weighted less compared to compressive strength because if the airframe is not strong enough to withstand the forces from flight and landing, the launch vehicle will fail. The material with the lowest cost received a score of 10 out of 10.

Density is the mass per unit volume (lb/in^3) of the material. The density should be minimized to decrease the overall mass of the launch vehicle. This will optimize its flight and ensure the launch vehicle has a safe thrust to weight ratio. Since the airframe contributes significantly to the overall weight of the launch vehicle, it is weighted at 16.7%. The material with the lowest density received a score of 10 out of 10.

Compressive Strength is the maximum amount of compressive stress (ksi) a material can withstand before it fractures. The compressive strength must be high enough to withstand significant compressive stresses during takeoff and landing. For example, after takeoff the motor applies an upward force on the airframe which compresses the body of the launch vehicle. The airframe needs to be able to withstand these compressive stresses for multiple flights. For the current design of the launch vehicle, the airframe needs to be able to withstand large compressive forces due to having rectangular holes in the airframe. The corners are susceptible to failure if the material is not able to withstand the forces from flight. Compressive strength is weighted as 50% since the airframe and couplers need to withstand forces applied or the launch vehicle may not be recoverable. The material with the highest compressive strength received a score of 10 out of 10.

Machinability is the ease at which a material can be manufactured. Machinability is important because certain materials that are more easily machined take less time and are less dangerous to manufacture. Machinability is evaluated based on the necessary machines used to manufacture the material and the safety risks associated with the manufacturing of the material. Machinability is weighted at 16.7% and the scoring of machinability will be determined using a qualitative scale of poor, fair, okay, good, and great. Their quantitative values will be 2, 4, 6, 8, and 10 respectively. The material with the best machinability will receive a score of 10 out of 10.

3.1.3.2.2 Alternative Materials

Alternative materials for the airframe included blue tube, G12 fiberglass, phenolic, and quantum tubing. Regarding machinability, blue tube, Phenolic, and Quantum tubing are relatively easier to manufacture and assemble, however during flight they are the most likely to perform poorly compared to fiberglass. Cost is also important because the airframe makes up most of the exterior material. Although Phenolic scored the best in this category, how it responds to forces during flight takes precedence.

3.1.3.2.3 Selected Material

Due to the large weighting of the compressive strength of the airframe, G12 fiberglass was chosen even though it did not score as high in the other sections. The airframe is subject to many of the compressive forces during flight, so it needs to be structurally sound. The cost of the material was relevant to this component due to the team needing to pick a design which the most efficient in price and performance.

3.1.3.3 Motor Tube

Materials for the motor tube were analyzed with defined evaluation criteria.

3.1.3.3.1 Evaluation Criteria

Decision matrices were used to evaluate potential motor mount materials (Table 6). Scores were calculated linearly with the highest possible score of 10 out of 10.

Motor Tube			**G12 Fiberglass**			**Blue Tube**		
Objective	Weighting Factor	Parameter	Mag.	Score	Value	Mag.	Score	Value
Cost	0.17	USD/in	1.20	3.33	0.56	0.40	10.00	1.67
Density	0.17	lb/in^3	0.07	6.87	1	0.06	7.80	1.30
Compressive Strength	0.50	ksi	37.10	10.00	5	5.08	1.37	0.68
Machinability	0.17	experience	fair	4.00	0.67	good	8.00	1.34
Overall value					**7.37**			**4.99**

Motor Tube			**Phenolic**		
Objective	Weighting Factor	Parameter	Mag.	Score	Value
Cost	0.17	USD/in	0.71	5.63	0.94
Density	0.17	lb/in^3	0.05	10.00	1.67
Compressive Strength	0.50	ksi	13.50	3.64	1.82
Machinability	0.17	experience	fair	4.00	0.67
Overall value					**5.10**

Table 6: Motor Tube Decision Matrix

Cost is the price per unit inch (USD/in) of the material. It is necessary to take cost into account to avoid exceeding the project budget. Although the materials are typically used for motor tubes tend to cost more than the other components of the vehicle, the amount on material required for the motor tube is minimal, resulting in a low weighting for cost. As a result, the cost was weighted at 16.7%. The material with the lowest cost received a score of 10 out of 10.

Density is the measurement of mass per unit volume (lb/in^3) of a material. Since the mass of the vehicle needs to be optimized, density of the motor tube was weighted at 16.7%. The material with the lowest density received a score of 10 out of 10.

Compressive Strength is the measurement of the amount of compressive stress (ksi) a material can withstand before fracture. The motor tube must be able to withstand the impulse produced by the motor during its flight. Therefore, it was weighted at 50.0%. The material with the highest compressive strength received a score of 10 out of 10 possible points.

Machinability is the time, safety, and resources required to manufacture the component while taking the safety concerns of manufacturing the material into account. Materials that require more safety concerns and resources were scored lower. The scoring for machinability was determined using a qualitative scale of poor, fair, okay, good, and great, with its corresponding quantitative values being 2, 4, 6, 8, and 10, respectively. Machinability was weighed at 16.7% and the material with the best machinability received a score of 10 out of 10.

3.1.3.3.2 Alternative Materials

Blue tube and phenolic were considered as materials for the motor tube. However, these were not selected due to their lower compressive strength when compared to G12 fiberglass. Blue tube and phenolic both had a significantly lower score for the compressive strengths and received a score of 0.46 and 1.21, respectively. Although blue tube and phenolic received higher scores for cost and machinability, the compressive strength was weighted as one of the higher objectives. As a result, blue tube and phenolic were not selected as the materials for the motor tube.

3.1.3.3.3 Selected Material

G12 fiberglass was selected as the material for the motor tube. Higher compressive strength is desired to withstand the stresses experienced by the motor tube throughout multiple launches. Although fiberglass received a lower score in cost, the compressive strength was weighted as the most significant objective for the motor tube.

3.1.3.4 Bulkheads

Potential bulkhead materials were evaluated using defined evaluation criteria.

3.1.3.4.1 Evaluation Criteria

Decision matrices were used to evaluate potential materials for the bulkheads (Table 7). Scores were calculated linearly with the highest possible score of 10 out of 10.

Bulkhead			**Structural FRP Fiberglass**			**Plywood**		
Objective	Weighting Factor	Parameter	Mag.	Score	Value	Mag.	Score	Value
Density	0.22	lb/in^3	0.06	3.3	0.7	0.02	10.0	2.2
Tensile Strength	0.56	ksi	18.50	10.0	5.6	9.20	4.3	2.4
Machinability	0.22	experience	Fair	4.0	0.9	Fair	4.0	0.9
Cost	0.11	USD/ft^2	27.89	1.50	0.2	20.41	10.00	1.1

Overall value					**7.3**			**6.6**

Bulkhead			**Type II PVC**		
Objective	Weighting Factor	Parameter	Mag.	Score	Value
Density	0.22	lb/in^3	0.05	3.9	0.9
Tensile Strength	0.56	ksi	6.15	6.7	3.7
Machinability	0.22	experience	Great	10.0	2.2
Cost	0.11	USD/ft^2	8.42	4.90	0.5
Overall value					**7.4**

Table 7: Decision Matrix for Bulkheads

Density is the measurement of the mass per unit of volume (lb/in^3) of the material. It is important to reduce the mass of the launch vehicle wherever possible. Compared to other parts, the mass of the bulkheads is relatively low, so it is weighted at 22.2%. The material with the lowest density will receive a score of 10 out of 10.

Tensile strength is the maximum amount of pull (ksi) that the bulkhead can withstand without failing. Since the bulkheads act as a barrier between each section of the launch vehicle, it is important that they be able to withstand stresses from ejection charges at different points during the flight. This is weighted at 55.6% because failure of the bulkheads will lead to improper parachute deployment and then recovery failure. The material with the highest tensile strength will receive a score of 10 out of 10 points.

Machinability is the time, safety, and resources that go into manufacturing the bulkheads. The assembly also considers putting manufactured components to develop the bulkheads. The scoring for machinability was determined using a qualitative scale of poor, fair, okay, good, and great, with its corresponding quantitative values being 2, 4, 6, 8, and 10, respectively. Machinability was weighted at 22.2% because the team has access to the tools necessary, for example, a lathe, bandsaw, and drill.

Cost is the price per square foot (USD/ft^2) of the material. It is necessary to take in account the cost in order to remain within budget. Cost was given a weight as 11.1%. The material with the lowest cost will receive a score of 10 out of 10.

3.1.3.4.2 Alternative Materials

Plywood and Structural FRP fiberglass were not chosen as the bulkhead material due to their poor performance in the decision matrices and the added complexity of manufacturing. One important factor to consider was tensile strength, and even though polycarbonate scored the best in the matrix, the other factors such as cost, and assembly prevented it from scoring the best. Plywood scored the best in the cost and density sections, however its tensile strength performance was low, so it was not heavily considered. Fiberglass had high tensile strength and low density however it reflected high costs in the decision matrix.

3.1.3.4.3 Selected Material

Type II PVC was selected as the final material for the bulkheads because it had the best performance in the decision matrices. Its relatively high scores in the areas of cost, assembly, tensile strength, and density mean that it will be the best option for the subscale and full-scale launch vehicle.

3.1.3.5 Centering Rings

Potential centering ring materials were evaluated with defined evaluation criteria.

3.1.3.5.1 Evaluation Criteria

Decision matrices were used to evaluate potential centering ring materials. Scores were calculated linearly with the highest magnitude for each objective being scored 10 out of 10 points (Table 8).

Centering rings			Structural FRP Fiberglass			Plywood		
Objective	Weighting Factor	Parameter	Mag.	Score	Value	Mag.	Score	Value
Density	0.30	lb/in^3	0.06	3.3	0.99	0.02	10.0	3.00
Cost	0.10	USD/in^2	4.67	0.7	0.07	0.31	10.0	1.00
Shear Strength	0.30	ksi	21.50	10.0	3.00	2.00	0.9	0.28
Machinability	0.30	mins	13.00	3.8	1.15	5.00	10.0	3.00
Overall value					**5.2**			**7.3**
Centering rings			**Type II PVC**					
Objective	Weighting Factor	Parameter	Mag.	Score	Value			
Density	0.30	lb/in^3	0.05	4.0	1.21			
Cost	0.10	USD/in^2	2.18	4.7	0.47			
Shear Strength	0.30	ksi	1.50	0.7	0.21			
Machinability	0.30	mins	25.00	2.0	0.60			
Overall value					**2.5**			

Table 8: Centering Rings Decision Matrix Assessment

Density is the measurement of the mass per unit volume (lb/in^3) of the material. The mass of the components in the launch vehicle should be minimized where possible. Compared to the other components, the centering rings accounted for a very small percentage of the launch vehicle mass. As a result, density was weighted at 30%. The lowest density will score a 10 out of 10.

Shear strength is the upper bound of how much internal sliding force (ksi) a material can withstand without experiencing a shear failure. The centering rings in a launch vehicle experience shear force in the form of static friction against the body tube which allows the launch vehicle to propel itself. If the centering rings fail, the motor may not be able to propel the launch vehicle, disabling it. Shear strength has been given a weight of 30%. The highest shear strength will score 10 out of 10.

Manufacturing time is the amount of time (min) required to manufacture the centering rings. Ease of manufacturing is not included as easily workable materials are used for centering rings, so the manufacturing process for the rings will be similar for every material. The centering rings will be made with the abrasive waterjet, so the time it takes to manufacture the rings are dependent on the type of material. Centering rings are not complex so the time to manufacture is estimated to be low. Machinability has been given a weight of 30%. The lowest manufacturing time will be given a score of 10 out of 10.

3.1.3.5.2 Alternative Materials

Materials which were considered for the centering rings included structural FRP fiberglass, plywood, and TYPE II PVC. Structural FRP fiberglass had a high shear strength, however, the machinability and density are not as desirable as plywood, the selected material. Type II PVC was not considered due to its relatively low shear strength and high density and machinability time.

3.1.3.5.3 Selected Material

Plywood was selected as the material for the centering rings. Plywood scored the highest in density, cost, and machinability which makes it the ideal material for centering rings. Although the shear strength of the material is lower compared to other materials, it is still sufficiently strong enough to withstand the forces applied to the centering rings.

3.1.3.6 Fins

An evaluation was completed to justify the material selection for the fins.

3.1.3.6.1 Evaluation Criteria

A decision matrix was developed for the fins to evaluate potential materials for the fins (Table 9). Scores were calculated linearly with the highest possible score of 10 out of 10.

Fins			**Structural FRP**			**Plywood**		
Objective	Weighting Factor	Parameter	Mag.	Score	Value	Mag.	Score	Value
Shear Strength	0.33	ksi	21.50	10.0	3.3	2.00	0.9	0.3
Cost	0.17	USD/ft^2	27.89	1.5	0.2	4.10	10.0	1.7
Density	0.17	lb/in^3	0.06	4.0	0.7	0.02	10.0	1.7
Impact Strength	0.33	ft-lb/in	8.00	6.7	2.2	3.70	3.1	1.0
Overall value					6.5			**4.7**

Fins			**G10 Fiberglass**		
Objective	Weighting Factor	Parameter	Mag.	Score	Value
Shear Strength	0.33	ksi	21.50	10.0	3.3
Cost	0.17	USD/ ft^2	62.75	0.7	0.1
Density	0.17	lb/in^3	0.07	3.7	0.6
Impact Strength	0.33	ft-lb/in	12.00	10.0	3.3
Overall value					**7.4**

Table 9: Fin Material Decision Matrix Assessment

Cost is the price per square foot (USD/ft^2) for each selected material. This is relevant to the launch vehicle since the component needs to be within the budget, however, there are other factors which are more crucial to the success of the launch vehicle. The fin's cost was weighted as 17% and the lowest cost will receive a score of 10 out of 10.

Density measures a material's mass per unit of volume (lb/in^3). The weight of the fins must be considered because it is important to keep the launch vehicle's weight at a minimum. However, since the fin's mass is not significant to the launch vehicle, fin density is weighted at 17%. The material with the lowest density will receive a 10 out of 10.

Shear strength of a material is the maximum stress (ksi) it can withstand until it fractures parallel to itself. Since the fins are usually the first component to contact the ground upon impact, they must possess enough shear strength to not deform. As a result, shear strength is weighted at the highest of 33%. The material with the highest shear strength will receive a 10 out of 10.

Impact strength is measured as the energy that a material can withstand when a load is applied to it. For the fins to be reusable and recoverable it needs a high impact toughness to withstand collision with the ground. Therefore, the impact strength is weighted at 33%. The material with the highest impact strength will receive a 10 out of 10.

3.1.3.6.2 Alternative Materials

Structural FRP and plywood were alternative materials considered for fins. While the cost and density of plywood were scored highly in the decision matrix, the shear and impact strength are relatively low. It is important for the fins to have this strength to withstand the landing of the launch vehicle. For structural FRP the tensile and shear strength are notable, but the G10 fiberglass had an efficient strength for a cost within the planned budget.

3.1.3.6.3 Selected Material

G10 fiberglass was selected for the fin material since it had the greatest impact and shear strength, while also being within the budget. The weighting factors determined which objectives were of more importance for the launch vehicle in each objective. For this reason, G10 fiberglass was the chosen material for the fins.

3.1.3.7 Epoxy

Potential epoxy options were evaluated using various criteria.

3.1.3.7.1 Evaluation Criteria

Epoxy will be used to attach the fins and centering rings to the launch vehicle. The epoxy needs to have high tensile strength and withstand high temperatures from the motor. If the epoxy were to fail it would result in failure of the launch vehicle.

3.1.3.7.3 Selected Material

JB Weld was selected to epoxy the centering rings to the motor tube and the inside the airframe, as well as to create the interior fillets. JB Weld was selected due to its high tensile strength of 5.0 ksi and high maximum temperature threshold of 550 °F. RocketPoxy was chosen for the exterior fin fillets due to its higher tensile strength, despite its lower temperature threshold. This is because heat resistance was not as important as the tensile strength for the exterior fin fillets due to their distance from the motor. RocketPoxy has a tensile strength of 7.6 ksi and low temperature threshold of 225° F.

3.1.4 Leading Vehicle Design

The leading vehicle design was modeled using OpenRocket (Figure 4).

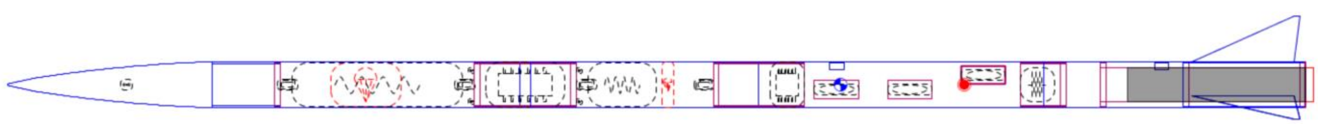

Figure 4: Leading Vehicle Design Modeled in OpenRocket

Additionally, the leading vehicle design was modeled using Fusion 360 (Figure 5)

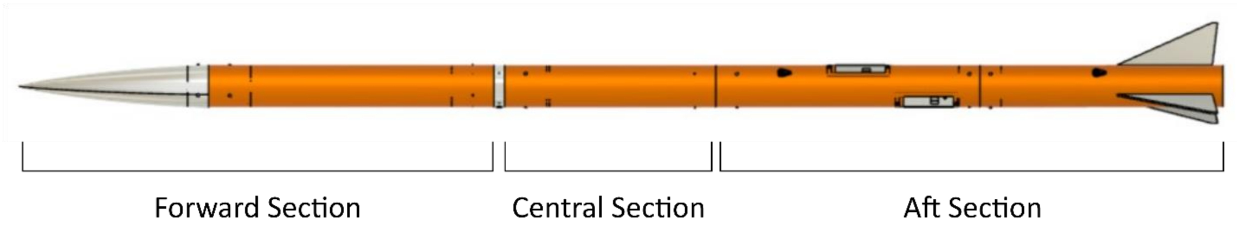

Figure 5: Leading Vehicle Design Modeled in Fusion 360

3.1.4.1 Forward Section

The forward section includes a nosecone, nosecone coupler, nosecone bulkhead, eyebolt, and forward airframe (Figure 6).

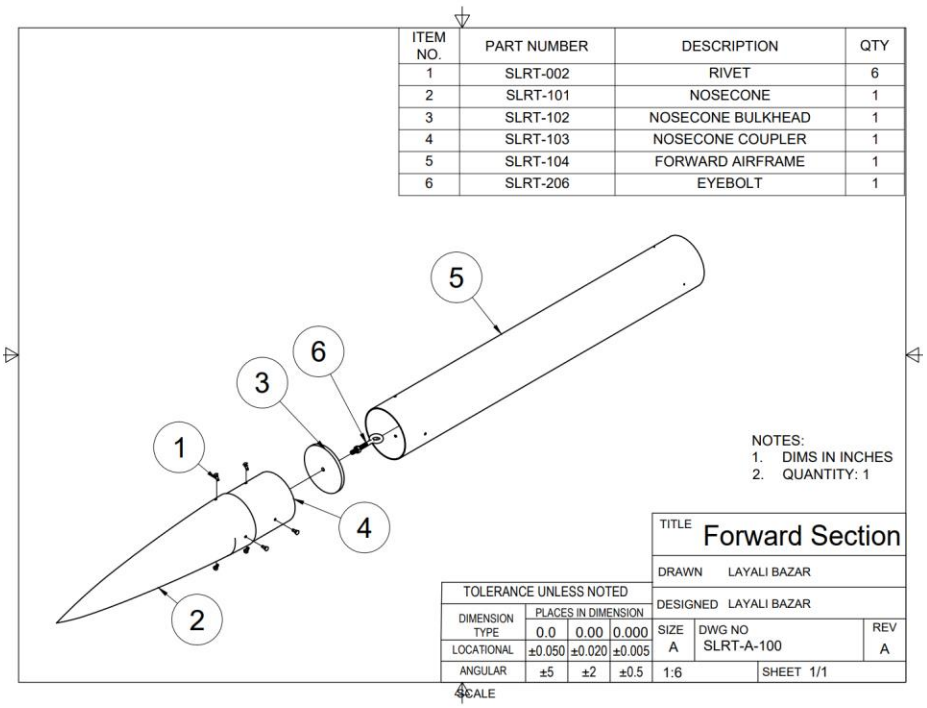

Figure 6: Forward Section

The selected nosecone is a 4.5:1 Von Karman made of G12 fiberglass. The nosecone has a stepped aluminum tip attached to the nosecone. The nosecone is 4 in. in diameter and is 18 in long. The nosecone has three holes for three plastic 0.154 in diameter rivets, 1 in from the aft end of the nosecone. The rivets connect the nosecone to the nosecone coupler. The holes are spaced equally, 120 degrees apart (Figure 7).

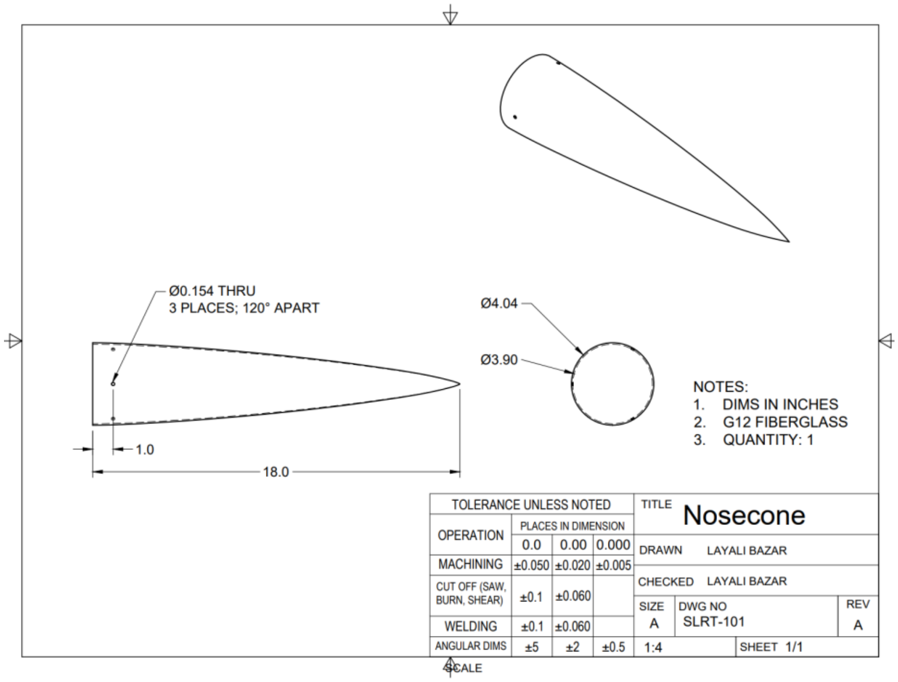

Figure 7: Nosecone

The nosecone coupler has a length of 6.0 in. The selected material for the coupler was G12 fiberglass. Two sets of three equally spaced, nylon rivets with a diameter of 0.154 in, connect the nosecone to the nosecone coupler, and the nosecone coupler to the forward airframe. The two sets of rivets are located 2.00 in and 5.00 in away from the aft end of the nosecone coupler, respectively (Figure 8).

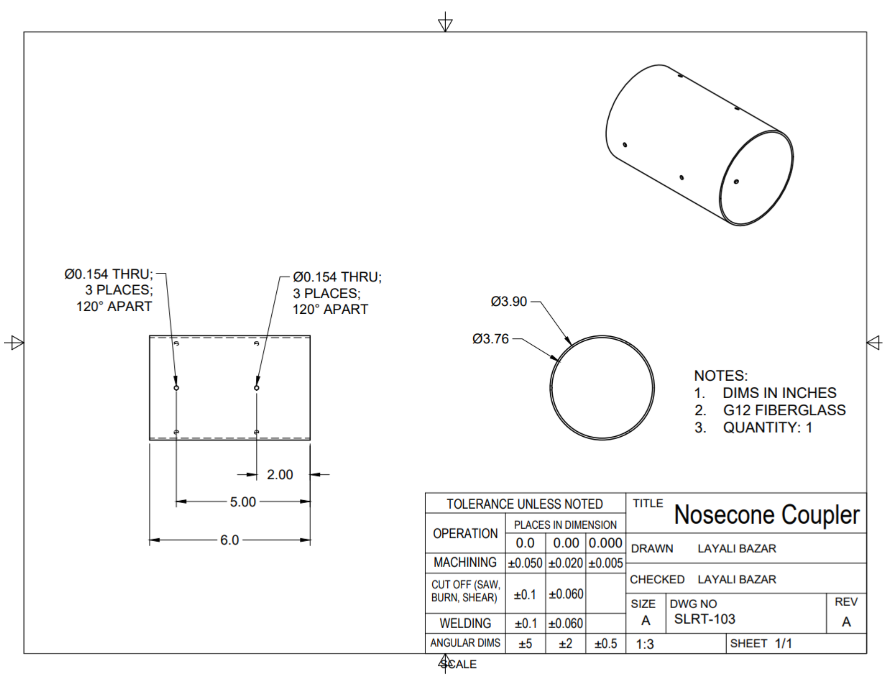

Figure 8: Nosecone Coupler

The nosecone bulkhead has a diameter of 3.8 in and a thickness of 0.25 in (Figure 9). The bulkhead is made of Type II PVC. Connected to the bulkhead, is an eyebolt which is designed to connect the forward and central sections with a recovery harness. The eyebolt is located in the center of the of the bulkhead through a 0.257 in diameter hole.

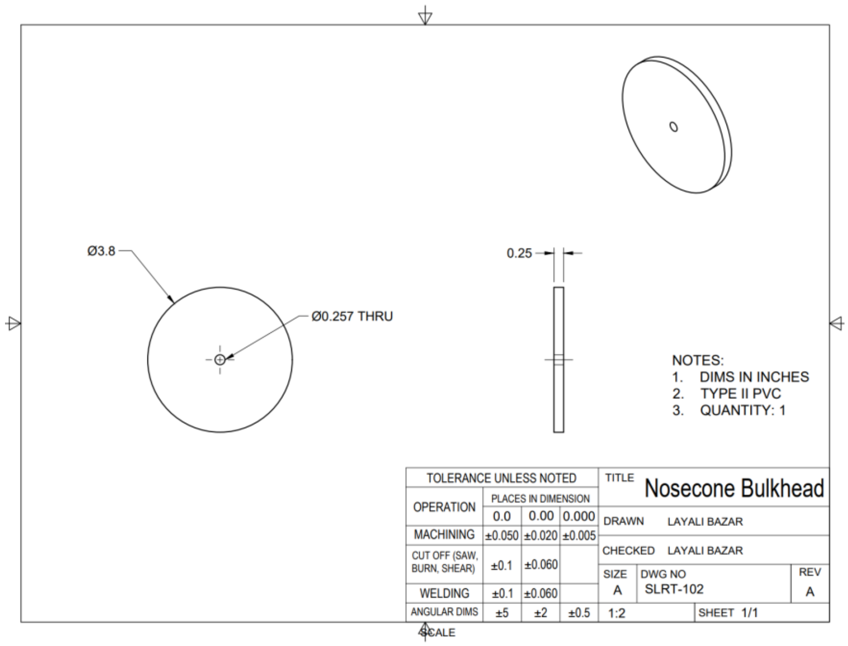

Figure 9: Nosecone Bulkhead

G12 fiberglass was the selected material for the airframe. The airframe has a diameter of 4 in and length of 27 in (Figure 10). The forward airframe has three 0.154 in diameter holes, spaced equally apart, for three plastic rivets. These holes are located 2 in from the forward end of the airframe. The rivets connect the forward airframe to the nosecone coupler. There are three 0.086 in diameter holes, spaced equally apart, for three nylon shear pins. The holes are located 2 in from the aft end of the airframe. These shear pins connect the forward airframe to the central section.

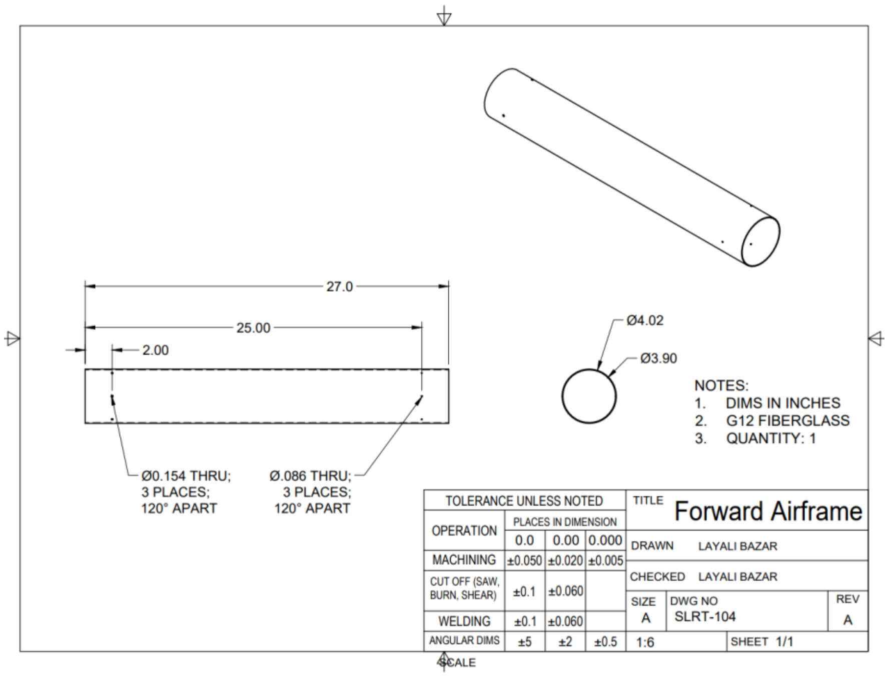

Figure 10: Forward Airframe

3.1.4.2 Central Section

The central section contains a central airframe, an avionics bay, bulkheads, and rivets (Figure 11).

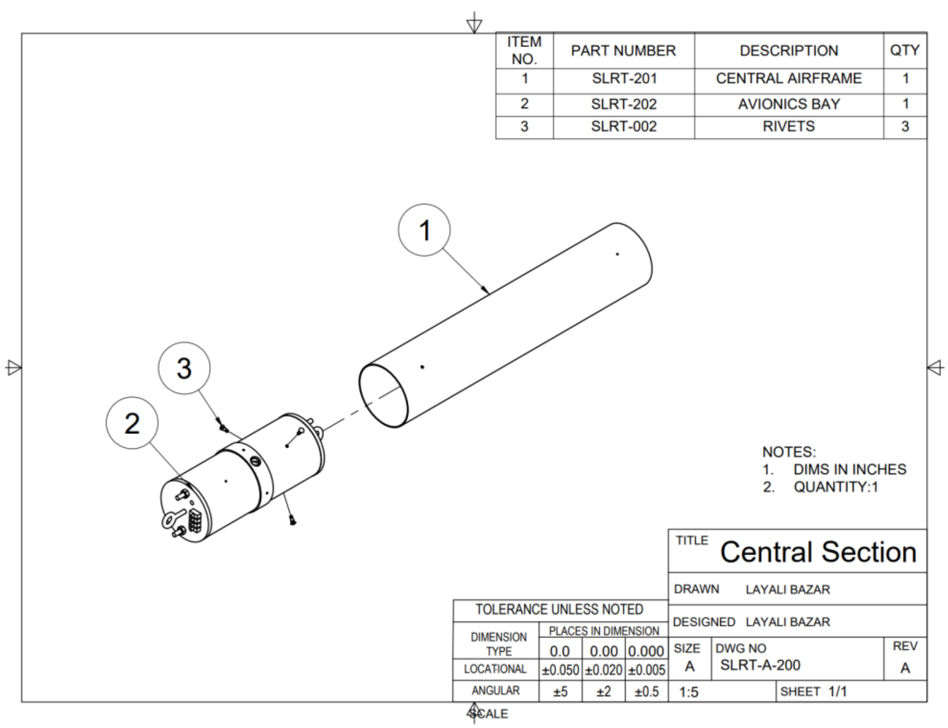

Figure 11: Central Section

The central airframe is made of G12 fiberglass. It has a diameter of 4.02 in and a length of 20 in (Figure 12). The central airframe has three 0.154 in diameter holes, spaced equally apart, for three plastic rivets. The rivets connect the central airframe to the avionics bay. The central airframe also has three 0.086 in diameter holes, spaced equally apart, for the three nylon shear pins that connect the central section to the forward section.

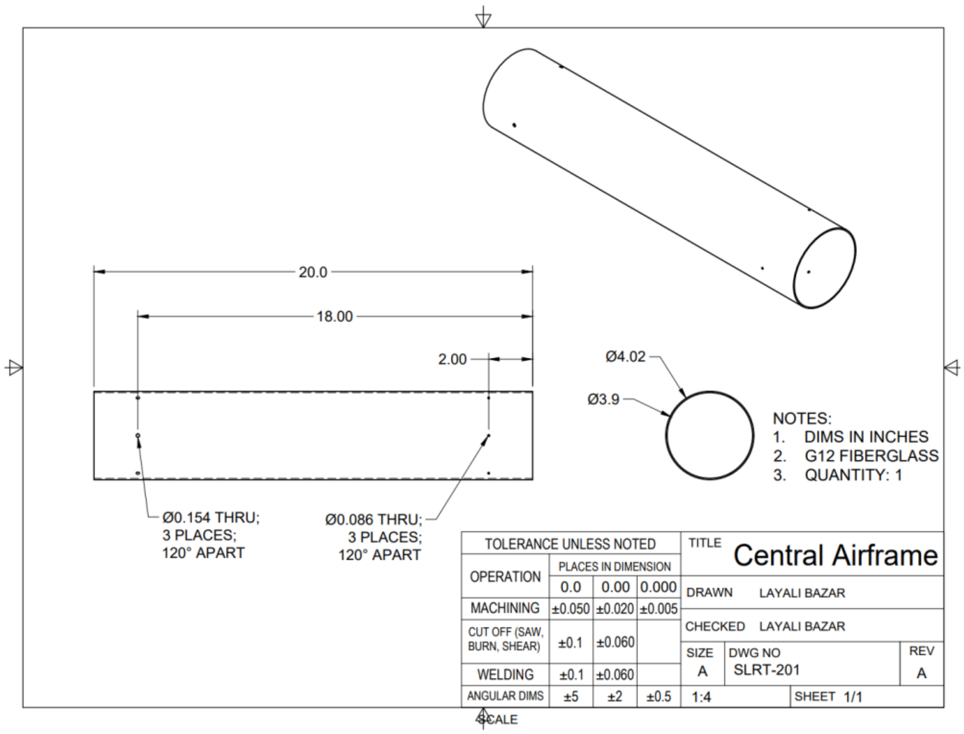

Figure 12: Central Airframe

The avionics bulkheads have an outer diameter of 3.9 in and inner diameter of 3.7 in (Figure 13). The overall thickness of the bulkhead is 0.5 in and are made of Type II PVC. The bulkheads cap both the forward and aft ends of the avionics bay, to protect the electronics from ejection charge gasses. The bulkheads both have an eyebolt that is the connection point for the main recovery harness to the fore, and the drogue recovery harness to the aft.

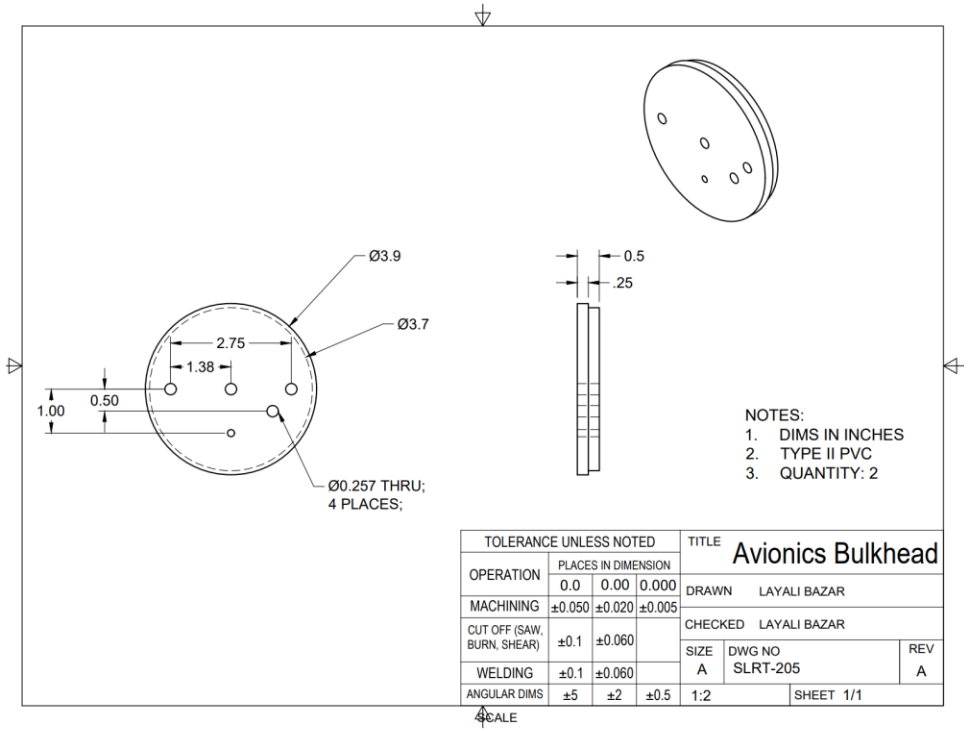

Figure 13: Avionics Bay Bulkheads

The selected material for the avionics coupler is G12 fi

berglass (Figure 14). The coupler is 9 in long and will house the avionics components. There are three 0.086 in diameter holes, spaced 120 degrees apart, for three nylon shear pins. The holes are located 2 in from the forward end of the coupler. The shear pins connect the forward airframe to the avionics coupler. Three 0.154 in diameter holes, spaced 120 degrees apart, are located 2 in from the aft end of the coupler. The holes are for three rivets that connect the avionics bay to the central airframe.

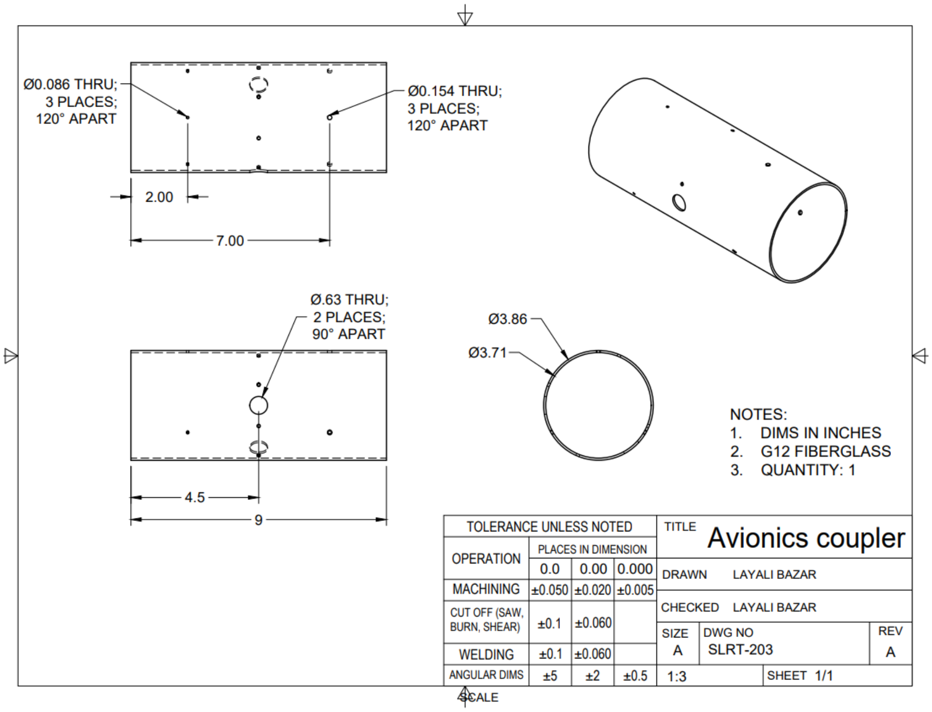

Figure 14: Avionics Coupler

3.1.4.3 Aft Section

The aft sections contain the payload airframe, aft airframe, forward and aft couplers, motor tube, centering rings, and fins (Figure 15). Components relating to the payload's mission are also present.

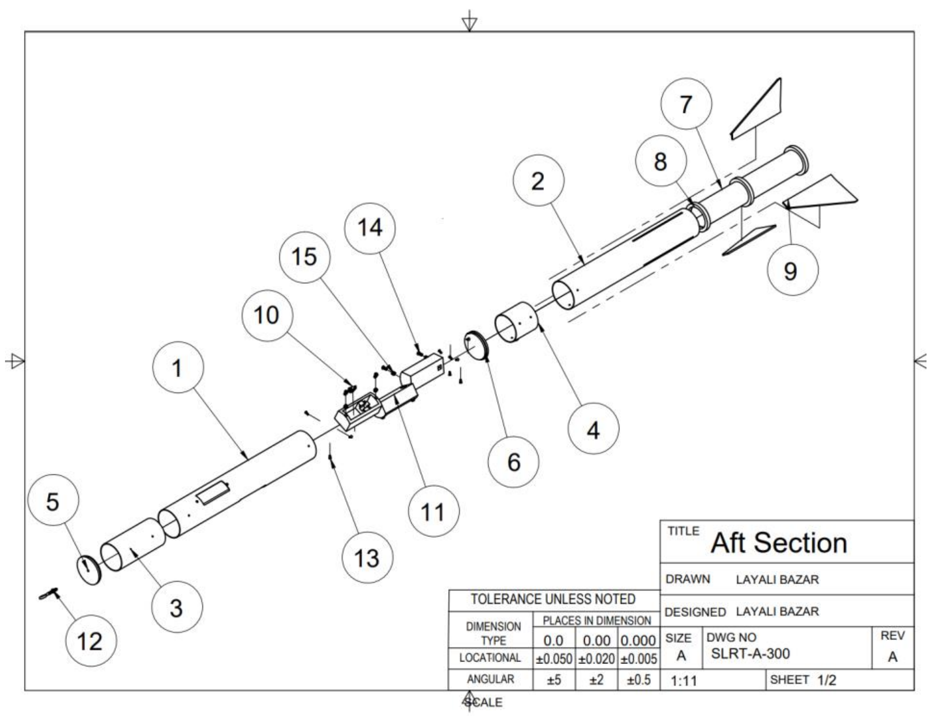

Figure 15: Aft Section

ITEM NO.	PART NUMBER	DESCRIPTION	QTY.
1	SLRT-301	PAYLOAD AIRFRAME	1
2	SLRT-302	AFT AIRFRAME	1
3	SLRT-303	PAYLOAD FORWARD COUPLER	1
4	SLRT-304	PAYLOAD AFT COUPLER	1
5	SLRT-305	PAYLOAD FORWARD BULKHEAD	1
6	SLRT-306	PAYLOAD AFT BULKHEAD	1
7	SLRT-308	MOTOR TUBE	1
8	SLRT-309	CENTERING RINGS	3
9	SLRT-310	FINS	3
10	SLRT-003	RAIL BUTTONS	2
11	SLRT-312	PAYLOAD HOUSING	3
12	SLRT-206	EYEBOLT	1
13	SLRT-002	RIVETS	9
14	SLRT-314	1/4-20 SCREW	6
15	SLRT-315	1/4-20 THREADED ROD	6

TITLE **Aft Section**

DRAWN LAYALI BAZAR

DESIGNED LAYALI BAZAR

SIZE A | DWG NO SLRT-A-300 | REV A

SHEET 2/2

TOLERANCE UNLESS NOTED			
DIMENSION TYPE	PLACES IN DIMENSION		
	0.0	0.00	0.000
LOCATIONAL	±0.050	±0.020	±0.005
ANGULAR	±5	±2	±0.5

SCALE

Figure 16: Aft Section Bill of Materials

The payload airframe has a length of 25 in with a diameter of 4.02 in (Figure 17). It is made of G12 fiberglass. There are two sets of three 0.154 in diameter holes, spaced 120 degrees apart, for three plastic rivets. The two sets of three rivets connect the payload airframe to the forward and aft payload couplers. These sets of holes are located 1 in from the forward end, and 2 in from the aft end of the payload airframe respectively. The payload airframe also has three 4.72 in by 1.73 in holes, spaced 120 degrees apart radially, and spaced 0.5 in apart along the length of the airframe. These holes are what the payload camera assemblies will extend out of.

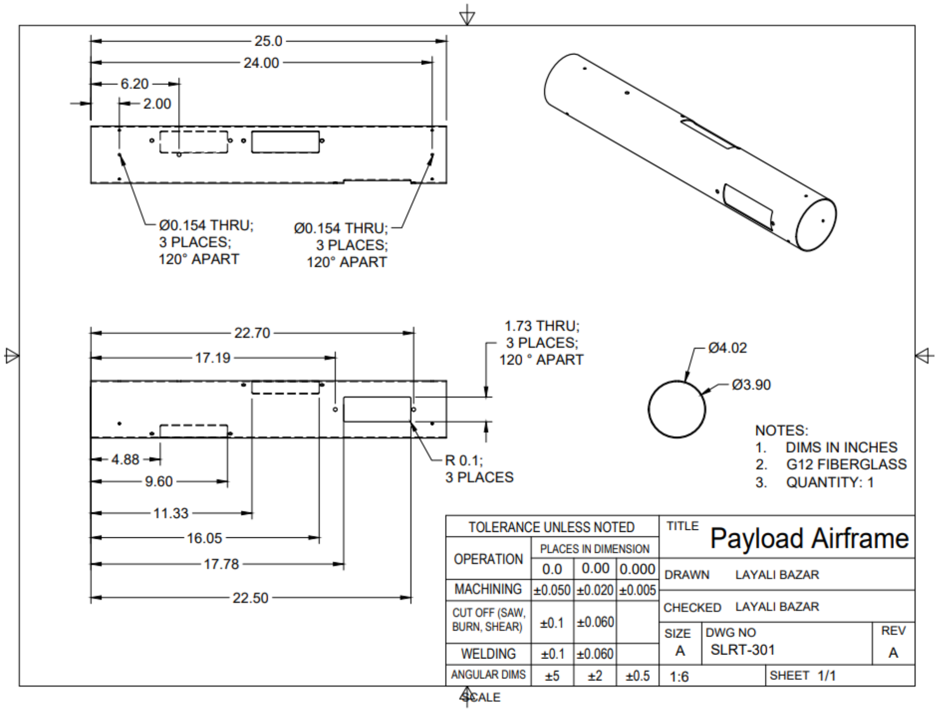

Figure 17: Payload Airframe

The aft airframe is made of G12 fiberglass. It is 23 in long and has a diameter of 4.02 in (Figure 18). The aft airframe has three 0.154 in diameter holes, spaced 120 degrees apart, for three rivets. The three rivets connect the aft airframe to the aft payload coupler. There are three, 9 in long fin slots in the aft airframe, through which the fins will be secured to the airframe and motor tube. 11 in from the forward end of the aft airframe, there is a 0.257 in diameter hole for a ¼-20 threaded insert. A 15-15 rail button will be installed with this threaded insert.

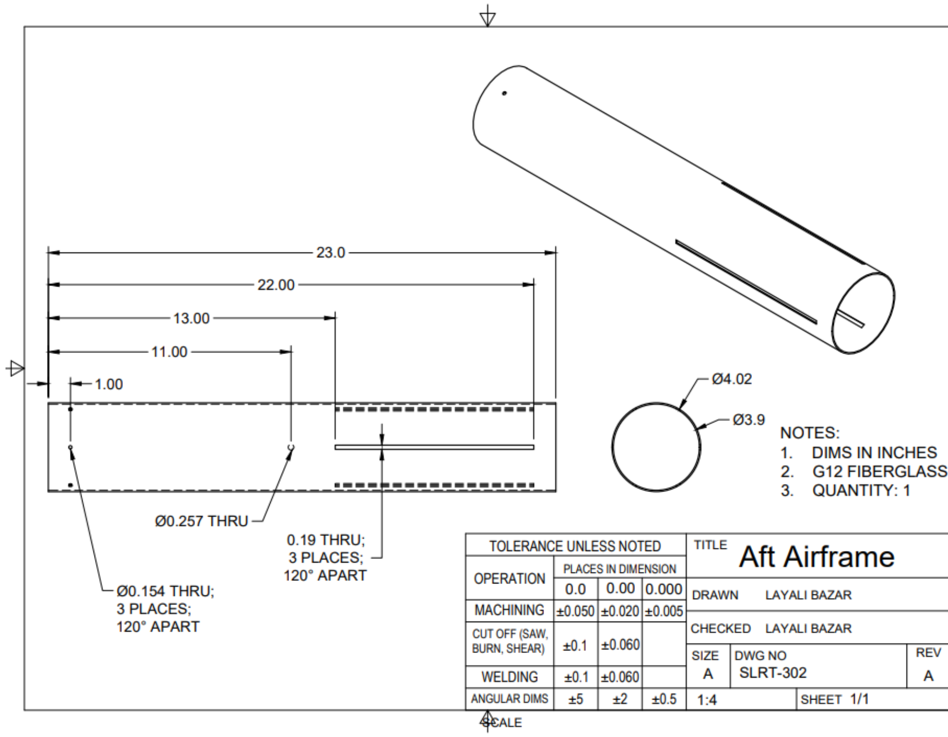

Figure 18: Aft Airframe

The payload's forward coupler is 8 in long with a diameter of 3.9 in (Figure 19). The couplers are made of G12 fiberglass. The payload forward coupler has three shear pins which connect the aft section to the central section and three rivets which connect the coupler to the payload airframe. The payload forward coupler contains the electronics relevant to the three camera systems that are stored in the payload airframe.

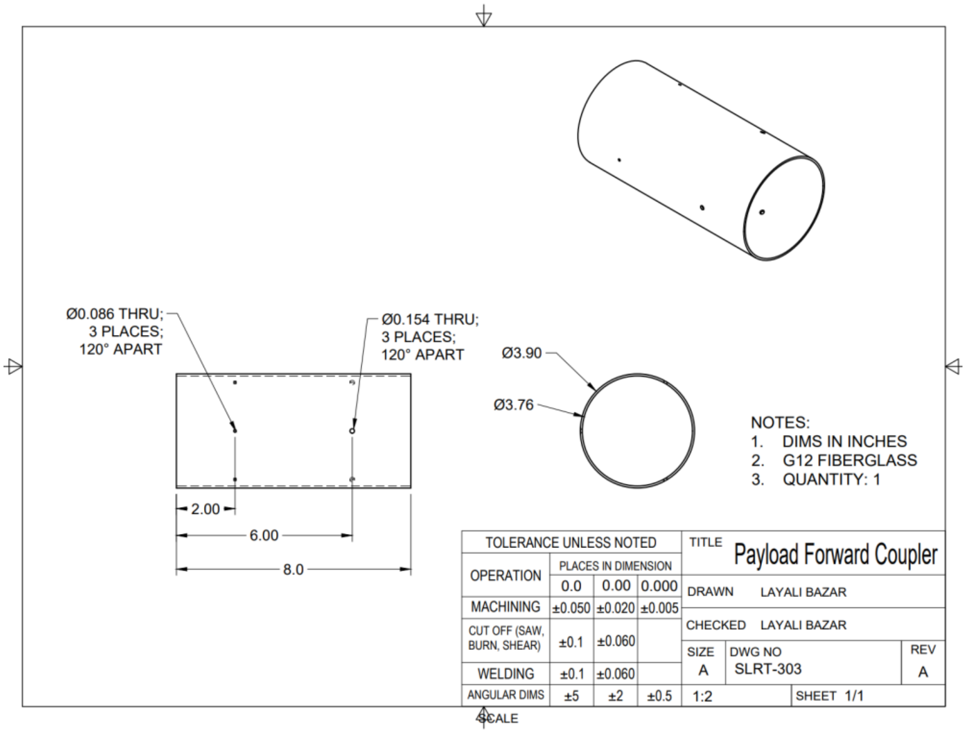

Figure 19: Payload Forward Coupler

The payload aft coupler has a length of 4.0 in and a diameter of 3.9 in (Figure 20). Three rivets are located 2 in from the forward and aft ends of the coupler. These rivets connect the payload airframe to the aft airframe.

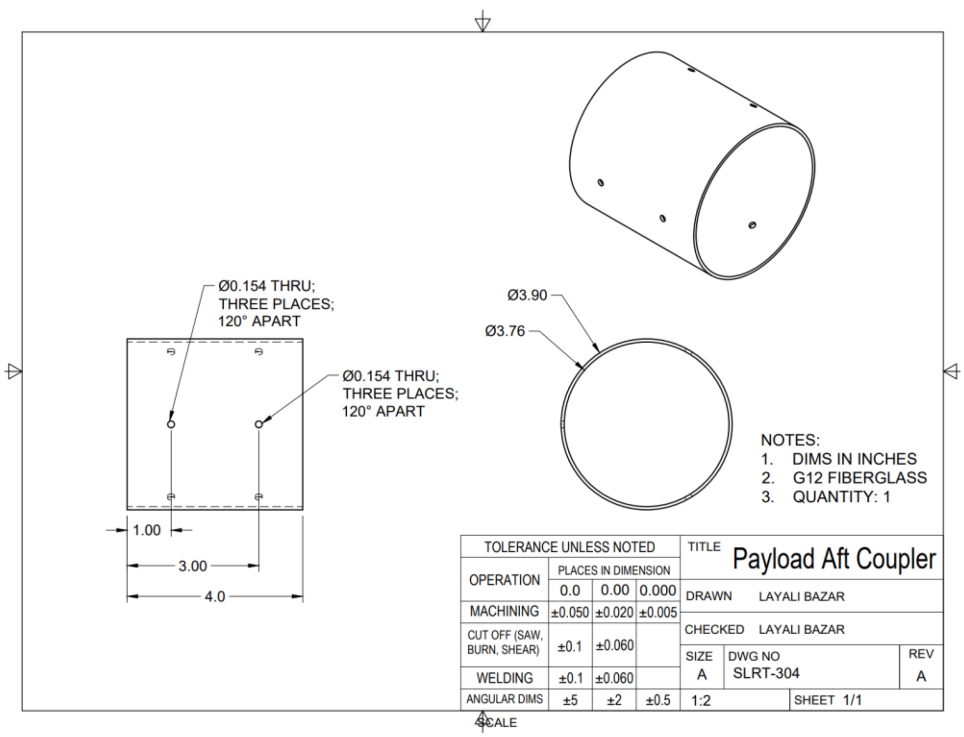

Figure 20: Payload Aft Coupler

The payload coupler bulkheads are made of Type II PVC. The forward bulkhead, which caps the forward end of the forward payload coupler, has an eyebolt that serves as the aft connection point of the drogue recovery harness (Figure 21). The aft bulkhead caps the aft end of the aft payload coupler (Figure 22). The bulkheads have an outer diameter of 4 in, inner diameter of 3.8 in, and thickness of 0.5 in.

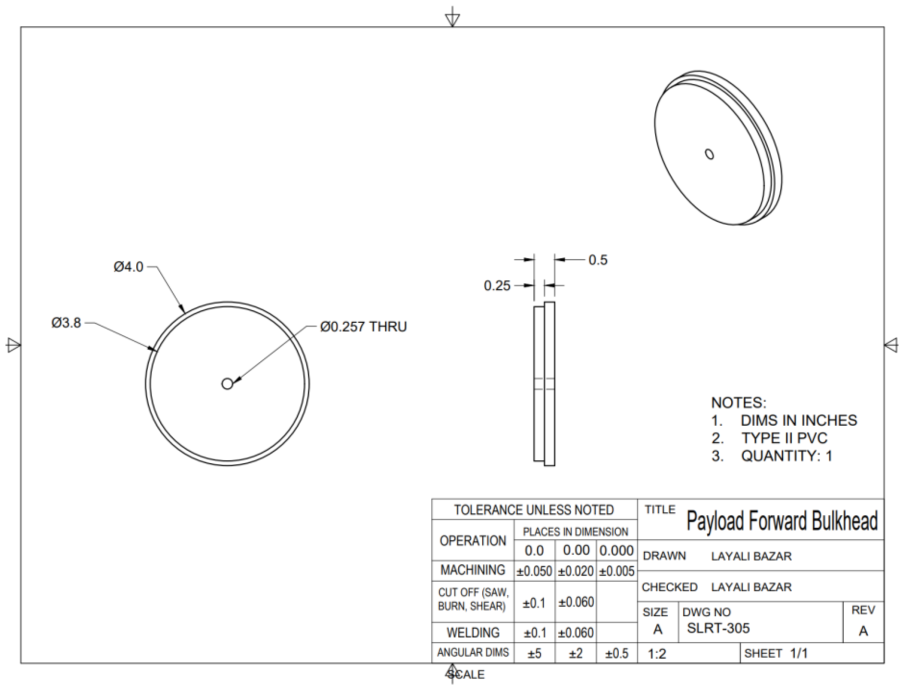

Figure 21: Payload Forward Bulkhead

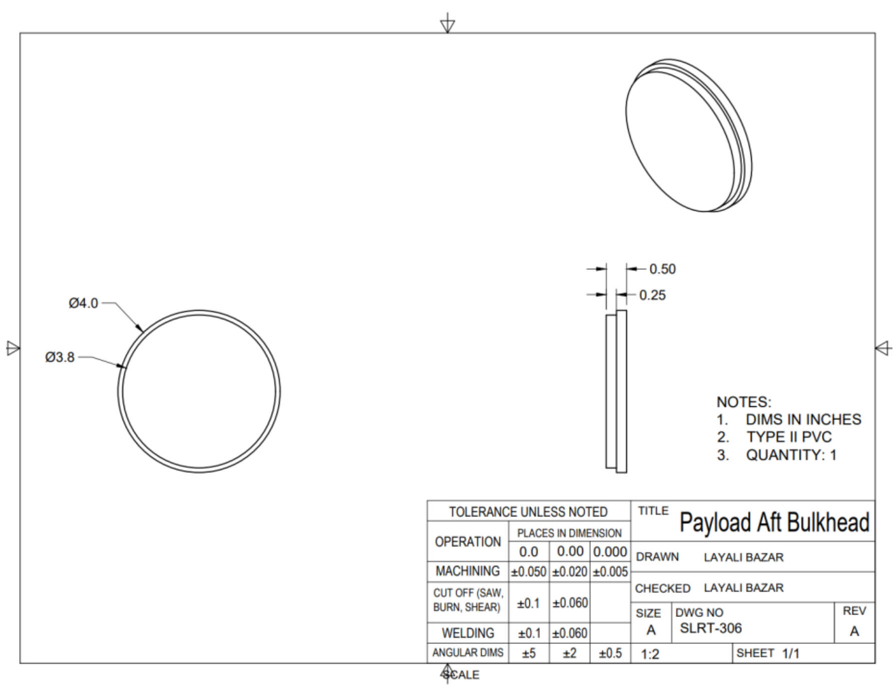

Figure 22: Payload Aft Bulkhead

The motor is 18 in long with an outer diameter of 3.12 in and inner diameter of 3 in (Figure 23). The selected material of the motor tube was G12 fiberglass.

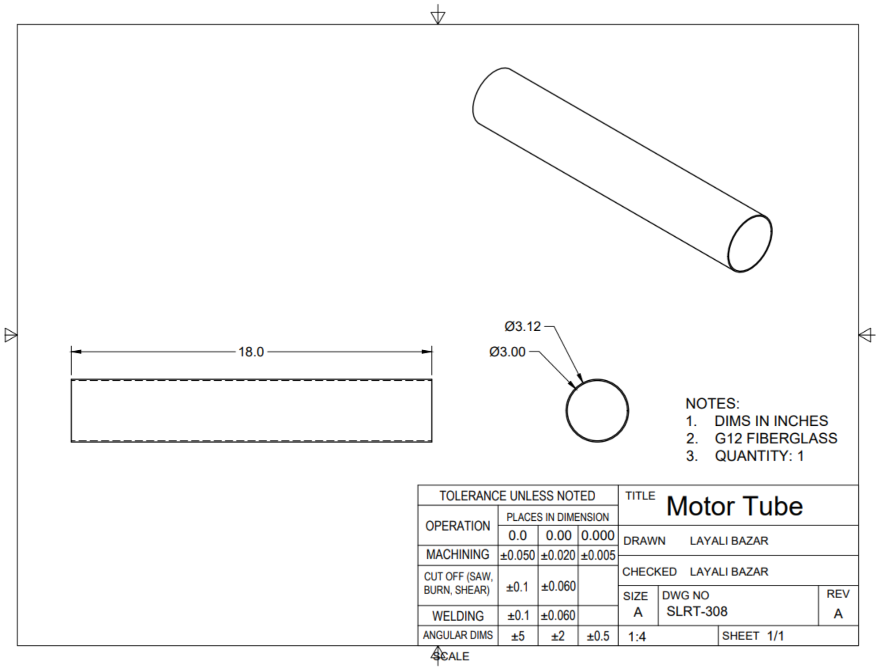

Figure 23: Motor Tube

The centering rings are designed to keep the motor tube aligned in center of the aft section. There is a total of three 0.5 in thick plywood centering rings. The centering rings have an outer diameter of 4 in and inner diameter of 3 in (Figure 24). The centering rings are epoxied to the outside of the motor tube and to the inside of face of the aft airframe.

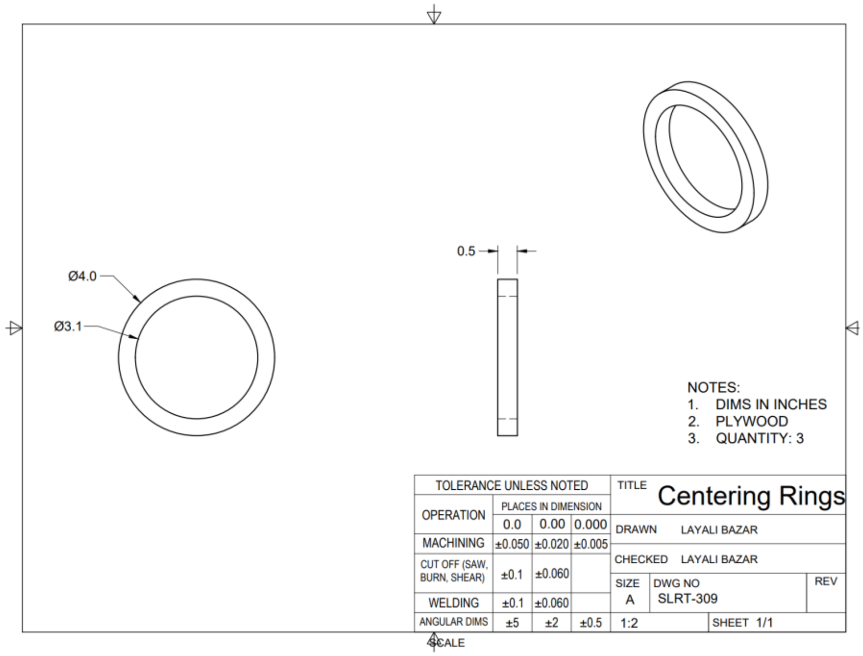

Figure 24: Centering Rings

The three fins are 0.19 in thick, 9 in long at the root, and 9.5 in long overall (Figure 25). The fins are 0.5 in from the aft end of the aft airframe. The fins will be epoxied to the outside and inside faces of the aft airframe and to the outside face of the motor tube.

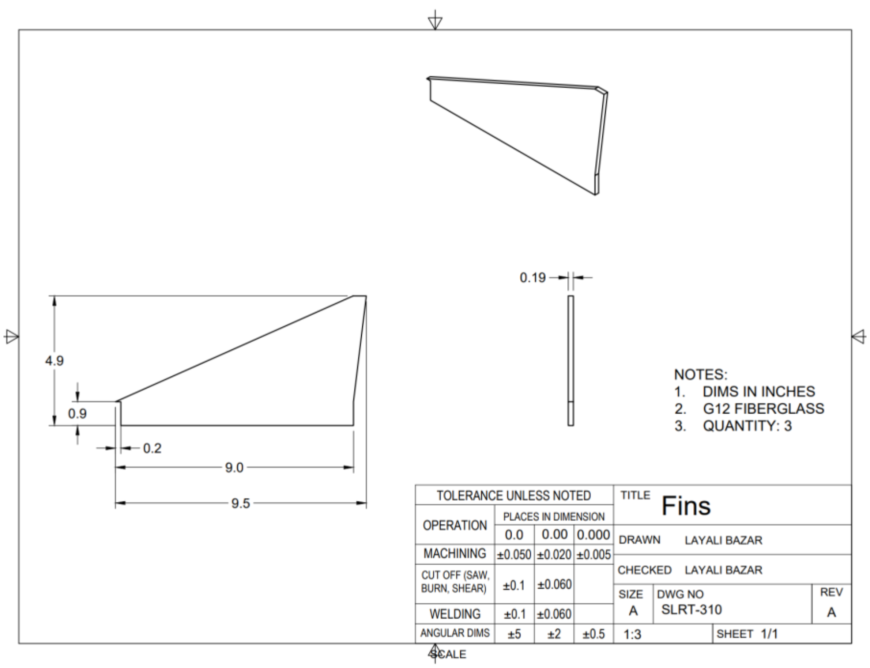

Figure 25: Fins

3.1.4.4 Component Masses

The following table lists the masses of each component in each section of the launch vehicle (Table 10).

Forward Section		
Subteam	**Component**	**Mass (oz)**
Structures	Nosecone	21.1
Structures	Nosecone Bulkhead	4.8
Structures	Eyebolt	1.0
Structures	Forward Airframe	21.6
Avionics and Recovery	Main Parachute	13.4
Avionics and Recovery	Recovery Harness	16.0
Total		77.9
Central Section		
Subteam	**Component**	**Mass (oz)**
Structures	Switchband	0.8
Avionics and Recovery	Eyebolts	2.0
Structures	Bulkheads	9.6
Avionics and Recovery	Sled and Electronics	20.2
Structures	Central Airframe	16.0
Structures	Coupler	8.3
Avionics and Recovery	Drogue Parachute	1.1
Avionics and Recovery	Recovery Harness	16.0
Total		74.0
Aft Section		
Subteam	**Component**	**Mass (oz)**
Structures	Payload Airframe	20.0
Structures	Rail Buttons	0.7
Structures	Couplers	11.0
Avionics and Recovery	Eyebolt	1.0
Payload Electronics	Electronics	14.2
Payload Mechanics	Camera Housing	13.0
Payload Mechanics	Payload Housing	12.2
Structures	Bulkheads	9.6
Structures	Aft Airframe	18.4
Structures	Centering Rings	2.9
Structures	Epoxy	22.2
Structures	Motor Retainer	4.9
Structures	Thrust Plate	2.5
Structures	Fins	11.4
Flight Dynamics	Motor and Motor Casing	91.0
Structures	Motor Tube	11.1
Total		246.1
Overall Total		**398.0**

Table 10: Launch Vehicle Mass Table

3.2 Avionics and Recovery Subsystem

The avionics and recovery subsystem will deploy a drogue and main parachute to safely recover the launch vehicle. The subsystem will consist of two redundant altimeters, redundant ejection charges, drogue and main parachutes, recovery hardware, recovery harnesses, and a GPS. Decision matrices were used to select the components for the avionics and recovery subsystem.

3.2.1 Preliminary Parachute Analysis

Target descent rates of 85 ft/s and 18 ft/s were chosen for the drogue and main parachute, respectively. The target descent rates were determined using Equations 1-3. A descent with these values enables the rocket to descend in less than 90 seconds (84.82s predicted descent time) and drift less than the allowed 2500 ft in 20 mph wind conditions (2488 ft predicted drift). It will also land with the aft section, the heaviest section, experiencing less than 75 ft-lb of kinetic energy (58.08 ft-lb predicted kinetic energy). The descent values were calculated with the following formulas:

$$descent\ time = \frac{apogee - main\ deployment\ height}{drogue\ descent\ rate} + \frac{main\ deployment\ height}{main\ descent\ rate}$$

Equation 1: Estimate Total Descent Time

$$drift = descent\ time * \ wind\ speed$$

Equation 2: Estimate Total Drift

$$kinetic\ energy = \frac{1}{2} m_{section} * main\ descent\ rate^2$$

Equation 3: Estimate Kinetic Energy of a Section Upon Landing

OpenRocket simulations were used to obtain predicted descent rates for common sizes and coefficients of drag (Table 11, Table 12).

Coefficient of Drag	Diameter (in)	Descent Rate (ft/s)
1.0	108	17.0
1.2	96	17.7
1.6	84	17.2
2.0	72	18.5
2.2	72	17.7

Table 11: Main Parachute Estimated Sizes

Coefficient of Drag	Diameter (in)	Descent Rate (ft/s)
0.8	24	92.1
1.0	24	79.7
1.2	24	72.7
1.6	12	126

Table 12: Drogue Parachute Estimated Sizes

The simulated descent rate values from OpenRocket for the main and drogue parachutes selected in Table and Table are 17.2 ft/s and 80.1 ft/s, respectively. These values are close enough to the target descent rate to ensure that the launch vehicle will meet recovery and flight time requirements.

3.2.2 Component Selection

3.2.2.1 Altimeter

A decision matrix was used to evaluate some common commercially available altimeters (Table 13).

Altimeter			Eggtimer Classic			Stratologger CF		
Objective	Weighting Factor	Parameter	Mag.	Score	Value	Mag.	Score	Value
Cost	0.2	USD	35	10	2	54.96	6.4	1.3
Resolution	0.3	ft	1	5	1.5	1	5	1.5
PCB Size	0.3	In^2	3.9	4.3	1.3	1.68	10	3
Weight	0.2	oz	0.71	5.4	1.1	0.38	10	2
Overall value					**5.9**			**7.8**
Altimeter			**Altus Metrum Telemega**			**Entacore AIM**		
Objective	Weighting Factor	Parameter	Mag.	Score	Value	Mag.	Score	Value
Cost	0.2	USD	400	0.9	0.2	115	3	0.6
Resolution	0.3	ft	0.5	10	3	1	5	1.5
PCB Size	0.3	In^2	4.1	4.1	1.2	2.5	6.7	2
Weight	0.2	oz	1	3.8	0.8	0.4	9.5	1.9
Overall value					**5.2**			**6.0**
Altimeter			**Altus Metrum Easymega**			**RRC3 "Sport"**		
Objective	Weighting Factor	Parameter	Mag.	Score	Value	Mag.	Score	Value
Cost	0.2	USD	341.3	1	0.2	96.5	3.6	0.7
Resolution	0.3	ft	1	5	1.5	unknown	0	0
PCB Size	0.3	In^2	2.9	5.8	1.7	3.6	1	0.3
Weight	0.2	oz	0.5	7.6	1.5	0.6	6.3	1.3
Overall value					**5.0**			**2.3**

Table 13: Altimeter Decision Matrix

3.2.2.1.1 Objective Definitions and Weighting Factors

Cost is the price of each altimeter, in USD. Cost was considered because more advanced altimeters can be very expensive and significantly impact the team's budget. As a result, cost will be weighted at 20%. The altimeter with the lowest cost will be assigned a maximum score of 10, and the others will be linearly assigned lower scores.

Size is the area that the PCB of the altimeter takes up and is measured in in^2. This objective was weighted relatively high at 30% because the altimeters will be secured to the avionics sled with fasteners that will protrude through it, reducing the available space for other components. The altimeter with the smallest size will receive the highest score.

Resolution refers to the accuracy of an altimeter's altitude measurements in ft. For instance, if an altimeter has a resolution of 10 ft, its measurements will be within 10ft of the launch vehicle's actual altitude when the measurement was taken. This objective was weighted at 30% because accurate measurement of the launch vehicle's altitude is crucial to ensure that parachutes are deployed at the correct times. The altimeter with the smallest resolution (most accuracy) will score a 10, and the rest will be scored linearly from that minimum value. Some altimeter manufacturers don't provide the altimeter resolution; those altimeters will receive a score of 0.

Mass, which is the mass of each altimeter in oz, was weighted at 20% because it is important to ensure that the weight of the altimeters won't significantly impact the performance of the launch vehicle. However, it isn't weighted as high relative to the other objectives because altimeters typically weigh less than an ounce, limiting the effects of altimeter weight on the launch vehicle. The altimeter with the smallest mass will receive a score of 10.

3.2.2.1.2 Alternative Components

The Entacore AIM altimeter, which scored the second highest with a score of 6.0, will be used as the secondary altimeter. This altimeter is more expensive than the Stratologger CF and has a larger size but has a similar accuracy and thus should perform similarly to the primary altimeter.

The Eggtimer Classic altimeter was considered. It has a very low cost of $35 and an accuracy of 1 ft but was not chosen because of its large PCB size and mass.

The Telemega altimeter by Altus Metrum was also considered. It is the most accurate of all the altimeters assessed with an accuracy of 0.5 ft. However, it is also the most expensive altimeter considered with a cost of $400, has a large PCB size, and has a mass of 1 oz. The Telemega altimeter wasn't chosen because of these drawbacks.

The Easymega altimeter, also by Altus Metrum, was considered. It is one of the lighter altimeters assessed with a mass of 0.5 oz and has an accuracy of 1 ft but is also one of the most expensive and had a larger PCB size. The Easymega was not selected because of this.

The RRC3 "Sport" altimeter by Missile Works was also considered. It was among the least expensive of the assessed altimeters with a cost of $96.5 and has a small mass of 0.6 oz, but its accuracy could not be determined from the manufacturer's website or the altimeter's manual. It was not chosen for use in the launch vehicle for this reason.

3.2.2.1.3 Selected Component

The Stratalogger CF, which scored the highest overall with a score of 7.8, will be used as the primary altimeter. It is one of the cheapest altimeters, being only more expensive than the Eggtimer Classic, and has the smallest size of the assessed altimeters. It is also accurate, with an accuracy of 1ft.

3.2.2.2 Recovery Harness

A decision matrix was used to evaluate recovery harnesses (Table 14).

Recovery Harness			Kevlar Cord 1500#			1/2" Nylon Tubular Webbing		
Objective	Weighting Factor	Parameter	Mag.	Score	Value	Mag.	Score	Value
Cost	0.2	USD/ft	1.3	5.0	1.0	0.7	10.0	2.0
Thermal Resistivity	0.2	K·m/W	0.3	0.9	0.2	3.0	10.0	2.0
Thickness	0.1	in	0.2	3.1	0.3	0.5	8.0	0.8
Mass	0.3	oz/ft	0.1	10.0	3.0	0.2	3.5	1.0
Strength	0.2	lb	1500	2.3	0.5	500	0.8	0.2
Overall value					**4.9**			**6.0**
Recovery Harness			**Tubular Kevlar - LOC Precision**			**Kevlar Shock Cord - Fruity Chutes**		
Objective	Weighting Factor	Parameter	Mag.	Score	Value	Mag.	Score	Value
Cost	0.2	USD/ft	1.2	5.5	1.1	2.3	2.8	0.6
Thermal Resistivity	0.2	K·m/W	0.3	0.9	0.2	0.3	0.9	0.2
Thickness	0.1	in	0.3	4	0.4	0.6	10	1
Mass	0.3	oz/ft	unknown	0.0	0.0	0.2	24.6	7.4
Strength	0.2	lb	1900	2.9	0.6	6600	10	2
Overall value					**2.3**			**11.1**

Table 14: Recovery Harness Decision Matrix

3.2.2.2.1 Objective Definitions and Weighting Factors

Cost is the price of the recovery harness per foot. Cost is weighted at 20% because the recovery harnesses will be long at 18-20 ft, so the cost per foot adds up quickly. The recovery harness with the lowest cost per foot will receive the highest possible score of 10, and the others will be scored linearly.

Thermal Resistivity is a measure of a material's ability to resist a heat flow and is measured in K·m/W. Materials with a higher thermal resistivity are less likely to burn or melt when exposed to heat generated when the ejection charges are detonated. This objective is weighted at 20% because recovery harness failure due to burning or melting could cause sections of the launch vehicle to fall freely and be damaged. Recovery harness made of the material with the highest thermal resistivity will receive a score of 10.

Thickness, which refers to the width (in) of each recovery harness, was considered because thinner recovery harnesses have a higher chance of zippering through the airframe due to forces during separation being applied over a smaller area. The recovery harness with the largest thickness will receive the highest score of 10, and others will be scaled linearly. However, this objective will have a relatively low weight of 10% because the airframe will be made of fiberglass, which has a low chance of zippering even when thinner recovery harnesses are used.

Mass refers to the mass per foot of each recovery harness, in oz/ft. It has a high weight of 30% due to the long length of the recovery harnesses, which will result in the overall recovery mass significantly impacting the launch vehicle. The recovery harness with the lowest mass with receive the highest possible score of 10.

Strength, the maximum force (lbs) that the recovery harness can be subjected to before breaking, was chosen as an objective to ensure that the selected recovery harness will be sufficiently strong to withstand separation forces. This objective was weighed at 20% since a recovery harness failure would untether a section of the launch vehicle, causing it to fall freely and potentially be damaged. The recovery harness with the highest strength was assigned a score of 10.

3.2.2.2.2 Alternative Component

The Kevlar Cord from Apogee Components was also considered and received the second highest score overall in the decision matrix. It is significantly cheaper than the selected component and made of heat-resistant Kevlar but was ultimately not chosen due to its relatively small thickness and strength.

3.2.2.2.3 Selected Component

The 5/8 in Kevlar Shock Cord by Fruity Chutes scored the highest overall with a score of 11.1. It is significantly stronger than the other assessed recovery harnesses and is also the thickest, and thus has a low risk of failure and damage.

Both recovery harnesses will be 24 ft in length to ensure that they are at least 2.5 times longer than the height of the launch vehicle. The launch vehicle will have an overall height of 9.58 ft, so the minimum recovery harness length is 9.58ft * 2.5 = 23.95 ft. The manufacturer of the selected recovery harness, Fruity Chutes, sells recovery harness in length increments of yards, so recovery harness lengths of 24 ft will be used.

3.2.2.3 Recovery Hardware

A decision matrix was used to evaluate recovery hardware (Table 15). All the bolts considered are from McMaster-Carr.

Recovery Hardware			**Galvanized Steel Eyebolt (0.5 ID)**			**Galvanized Steel Eyebolt (0.625 ID)**		
Objective	Weighting Factor	Parameter	Mag.	Score	Value	Mag.	Score	Value
Cost	0.3	USD	4.9	10	3	6.2	7.9	2.4
Height	0.3	in	3	7.7	2.3	3.5	6.6	2.0
Weight	0.2	oz	0.96	10	2	1.9	5	1
Carrying Capacity	0.2	lb	500	6.25	1.3	800	10	2
Overall value					**8.6**			**7.3**
Recovery Hardware			**316 Stainless Steel (0.5 ID)**			**304 Stainless Steel U-Bolt (2.0 ID)**		
Objective	Weighting Factor	Parameter	Mag.	Score	Value	Mag.	Score	Value
Cost	0.3	USD	24.3	2.0	0.6	7.0	7.0	2.1
Height	0.3	in	2.3	10.0	3.0	3.5	6.6	2.0
Weight	0.2	oz	1.0	10.0	2.0	2.8	3.5	0.7
Carrying Capacity	0.2	lb	500.0	6.3	1.3	425.0	5.3	1.1
Overall value					**6.9**			**5.8**

Table 15: Recovery Hardware Decision Matrix

3.2.2.3.1 Objective Definitions and Weighting Factors

Height is the total height of the bolt (including threads), in in. Height was chosen as an objective and assigned a high weight of 30% because longer bolts protrude farther out from the avionics bulkheads, taking up valuable space in the parachute compartments and potentially making the sections containing parachutes longer than necessary. The bolt with the shortest height was assigned the highest possible score of 10.

Mass refers to the mass of each bolt in oz. This objective was given a weight of 20% because eyebolts and U-bolts are smaller components and have a limited effect on vehicle performance. Scores were assigned linearly, with the lightest bolt receiving the highest score.

Carrying Capacity is the amount of weight that the bolt can hold, in lbs, and was weighted at 20% to ensure that the selected bolt is sufficiently strong to withstand forces during separation. The bolt with the highest carrying capacity received the highest score of 10.

Cost is the price of each bolt. This objective was given a weight of 30% because individual bolts are generally inexpensive, but at least four will be needed for the launch vehicle, making cost more significant. The bolt with the lowest cost was assigned the highest score.

3.2.2.3.2 Alternative Component

The Galvanized Steel Eyebolt with a 0.625 in inner diameter from McMaster-Carr was considered for its high carrying capacity of 800lbs, which made it the strongest of all assessed hardware. However, it was ultimately not chosen because of its higher mass and height.

The 316 Stainless Steel Eyebolt with a 0.5 in inner diameter from McMaster-Carr was also considered. It is very light and short but was not chosen because it is significantly more expensive than the other assessed hardware with a cost of $24.29.

A 304 Stainless Steel U-Bolt with a 2.0 in inner diameter from McMaster-Carr was considered but was ultimately not chosen because of its high 2.8 oz mass and its relatively small carrying capacity of 425 lbs.

3.2.2.3.3 Selected Component

The Galvanized Steel Eyebolt with a 0.5 in inner diameter from McMaster-Carr, which received the highest score overall, was selected. This bolt weighs less than 1 oz and is the cheapest of the assessed bolts.

3.2.2.4 GPS

A decision matrix was used to select the GPS (Table 16).

GPS			**BRB 900**			**TeleGPS - Altus Metrum**		
Objective	Weighting Factor	Parameter	Mag.	Score	Value	Mag.	Score	Value
Cost	0.3	USD	199.99	10	3	242.3	8.3	2.5
Resolution	0.3	ft	8.2	10	3	Unknown	0	0
Range	0.2	mi	6	1.9	0.4	30	9.7	1.9
Current Draw	0.2	mA	115	9.7	1.9	Unknown	0	0
Overall value					**8.3**			**4.4**
GPS			**Featherweight GPS Tracker**					

Objective	Weighting Factor	Parameter	Mag.	Score	Value
Cost	0.3	USD	365	5.5	1.6
Resolution	0.3	ft	Unknown	0	0
Range	0.2	mi	31.1	10	2
Current Draw	0.2	mA	112	10	2
Overall value					**5.6**

Table 16: GPS Decision Matrix

3.2.2.4.1 Objective Definitions and Weighting Factors

Cost is the price of each GPS. Cost was weighted at 30% because GPS is a more expensive component and thus has more significant impacts on the overall budget. The GPS with the lowest cost will receive a score of 10.

Resolution is the accuracy of the measurements made by the GPS, in ft. A GPS with a higher resolution will give readings that are closer to the actual location of the launch vehicle. This objective is weighted at 30% to ensure that the selected GPS is accurate enough to give location data that is useful for recovering the launch vehicle. The GPS with the highest resolution will receive the highest score of 10.

Range is the maximum distance between the GPS transmitter and receiver for which the GPS will function, in mi. This objective was weighted at 20% because while it is important that signals from the GPS transmitter can reach the receiver, the launch vehicle is required to drift less than 2500 ft from the launch vehicle, so a range of only about a mile is needed. The GPS with the longest range will receive a score of 10.

Current Draw is a measure of the power consumption of the GPS transmitter in mA. Current draw was assigned a weight of 20%. A GPS with a lower current draw will function longer than a high current draw GPS with the same battery, so current draw is an important objective as the launch vehicle may remain on the launch pad for up to two hours. The GPS with the smallest current draw will receive the highest score.

3.2.2.4.2 Alternative Components

The GPS Tracker by Featherweight Altimeters was considered as the GPS for the launch vehicle. It has an extremely long range of 31.1 mi and the lowest current draw among the assessed components but was ultimately not chosen because of its relatively high cost and the lack of information on its resolution.

The TeleGPS by Altus Metrum was also considered. It has a long range of 30 mi but was not chosen because its resolution and current draw could not be determined from the manufacturer’s website and GPS manual.

3.2.2.4.3 Selected Component

The Big Red Bee (BRB) 900 was selected as the GPS. It has the lowest cost of the assessed components, a sufficiently long range, and has a resolution of 8.2 ft, which is small enough for the team to accurately find and recover the launch vehicle upon landing.

3.2.2.5 Main Parachute

A decision matrix was used to select the main parachute (Table 17).

Main Parachute			Fruity Chutes 84" Iris Ultra			Rocketman 72" Elliptical		
Objective	Weighting Factor	Parameter	Mag.	Score	Value	Mag.	Score	Value
Cost	0.2	USD	326.7	4.1	0.8	135	10	2
Mass	0.1	oz	19	6.6	0.7	12.6	10	1
Packed Length	0.1	in	8.8	5.7	0.6	5	10	1
Descent Rate	0.35	ft/s	15.5	9	3.2	20.4	8.4	3
Shroud Line Quality	0.25	qualitative	great	10	2.5	okay	6	1.5
Overall value					**7.7**			**8.5**
Main Parachute			**SkyAngle Cert 3 X Large**			**Fruity Chutes 72" Iris Ultra**		
Objective	Weighting Factor	Parameter	Mag.	Score	Value	Mag.	Score	Value
Cost	0.2	USD	189	7.1	1.4	248.3	5.4	1.1
Mass	0.1	oz	34	3.7	0.4	13.4	9.4	0.9
Packed Length	0.1	in	12	4.2	0.4	6.2	8.1	0.8
Descent Rate	0.35	ft/s	16.7	9.7	3.4	17.2	10	3.5
Shroud Line Quality	0.25	qualitative	good	8	2	great	10	2.5
Overall value					**7.6**			**8.8**

Table 17: Main Parachute Decision Matrix

3.2.2.5.1 Objective Definitions and Weighting Factors

Cost is the price of the parachute in USD. Cost was weighted at 20% because parachutes can be expensive and significantly impact the budget. The parachute with the lowest cost will receive a score of 10, and the others will be assigned scores linearly.

Mass refers to the mass of each parachute, in oz. This objective was assigned a relatively low weight of 10% because parachutes typically don't weigh enough to significantly impact the performance of the launch vehicle. The parachute with the lowest weight will receive a score of 10, and the other parachutes will be scored linearly.

Packed Length, the length of the parachute when it is in its parachute compartment, in in., was chosen as an objective. The parachute must be able to fit inside its compartment in the launch vehicle, so the packed length of the selected parachute may impact the length of the launch vehicle. This objective was weighted at 10% because parachute manufacturers provide dimensions for the packed parachutes, allowing parachute sizes to be accounted for before beginning manufacturing. The parachute with the shortest packed length will receive the highest score.

Descent Rate, the speed in ft/s at which the launch vehicle will descend under, was considered. This objective was given a high weight of 35% because it is important that the selected parachute causes descent that is close to the target descent rate, which was the descent rate used to calculate recovery values. The parachute with the descent rate that is closest to the target descent rate will receive the maximum score of 10, and the other parachutes will be assigned scores linearly relative to that highest-scoring parachute. The target descent rates are 85 ft/s for the drogue parachute and 18 ft/s for the main parachute.

Shroud Line Quality is a qualitative objective that measures how well the shroud lines are attached to the parachute. This objective was weighted at 25% because parachutes with weakly attached shroud lines could be damaged during deployment, reducing the lifespan of the parachute, and potentially altering the launch vehicle's descent rate. Parachutes with shroud lines that are sewn farther up the parachute will receive a higher score, with parachutes with shroud lines sewn high up the parachute canopy receiving a qualitative score of "great" and a numerical score of 10. Lesser score assignments are shown in Table 3.

3.2.2.5.2 Alternative Components

A 72" elliptical parachute from Rocketman was considered as the main parachute. It is the cheapest of the assessed parachutes, has a light weight, and is close to the target main descent rate of 18 ft/s with a simulated descent rate of 20.4 ft/s. However, it was ultimately not chosen because its shroud lines are not sewn far up the parachute.

An 84" Iris Ultra parachute from Fruity Chutes was also considered. It has a predicted descent rate of 15.5 ft/s and a high shroud line quality but is expensive and more massive than many of the other alternatives and was not chosen as a result.

The SkyAngle Cert 3 X Large parachute was considered. It has a predicted descent rate that is very close to the main parachute target descent rate but was not chosen because it is also significantly more massive than the other alternatives with a mass of 34 oz. The next largest parachute, the 84" Iris Ultra, has a mass of 19 oz.

3.2.2.5.3 Selected Component

The 72" Iris Ultra parachute from Fruity Chutes had the highest overall score of 8.8. It has a higher cost than many of the alternatives but has a simulated descent rate that most closely matches the target descent rate, has a light weight, and has shroud lines that are securely attached.

3.2.2.6 Drogue Parachute

A decision matrix was used to select the drogue parachute (Table 18). The objectives and objective weights in the following matrix are identical for those of the main parachute.

Drogue Parachute			**Rocketman 24" Standard**			**24" Spherachute**		
Objective	Weighting Factor	Parameter	Mag.	Score	Value	Mag.	Score	Value
Cost	0.2	USD	28.5	7.7	1.5	22	10	2
Mass	0.1	oz	1.5	7.3	0.7	1.1	10	1
Packed Length	0.1	in	1.5	6.7	0.7	1.75	5.7	0.6
Descent Rate	0.35	ft/s	80.1	9.2	3.2	90.6	9.4	3.3
Shroud Line Quality	0.25	qualitative	great	10	2.5	okay	6	1.5
Overall value					**8.7**			**8.4**

Drogue Parachute			Rocketman 24" Elliptical			Fruity Chutes 18" Elliptical		
Objective	Weighting Factor	Parameter	Mag.	Score	Value	Mag.	Score	Value
Cost	0.2	USD	50	4.4	0.9	62.89	3.5	0.7
Mass	0.1	oz	2.1	5.2	0.5	1.7	6.5	0.6
Packed Length	0.1	in	1	10	1	3.5	2.9	0.3
Descent Rate	0.35	ft/s	63.4	7.3	2.6	86.9	10	3.5
Shroud Line Quality	0.25	qualitative	okay	6	1.5	good	8	2
Overall value					**6.5**			**7.1**

Drogue Parachute			Skyangle C3 Drogue		
Objective	Weighting Factor	Parameter	Mag.	Score	Value
Cost	0.2	USD	27.5	8	1.6
Mass	0.1	oz	3.1	3.5	0.4
Packed Length	0.1	in	6	1.7	0.2
Descent Rate	0.35	ft/s	98.9	8.6	3
Shroud Line Quality	0.25	qualitative	great	10	2.5
Overall value					**7.6**

Table 18: Drogue Parachute Decision Matrix

3.2.2.6.1 Alternative Component

The 24” parachute from Spherachutes was considered as the drogue parachute. It is relatively inexpensive, has a small weight and has a simulated descent rate that is close to the target drogue descent rate of 85 ft/s. However, it was ultimately not chosen because its packed length is longer than most of the other parachutes assessed and because its shroud lines were not as securely attached as many of the other alternatives.

The Skyangle C3 Drogue parachute was also considered. It has securely attached shroud lines, a descent rate of 98.9 ft/s that is somewhat close to the drogue target descent rate, and a relatively low cost of $27.5. It is also the most massive of the drogue parachute assessed and has the longest packed length, which is why it was not selected.

An 18” Elliptical parachute from Fruity Chutes was considered. It has a predicted descent rate of 86.9 ft/s, which is closest to the target drogue descent rate of 85 ft/s and has securely attached shroud lines. However, it was not chosen because of its long, packed length and high cost.

A 24” Elliptical parachute from Rocketman was considered. This parachute has the shortest packed length of all of the considered alternatives with a packed length of 1 in, but was not chosen because of its high cost and mass and its predicted descent rate, which is farthest from the target drogue descent rate with a predicted descent rate of 63.4 ft/s.

3.2.2.6.2 Selected Component

The 24” standard parachute from Rocketman received the highest overall score of 8.7 and was selected as the drogue parachute for the launch vehicle. Its simulated descent rate is close to the target descent rate, and the shroud lines are sewn all the way around the parachute, minimizing the risk of damage to the parachute during deployment.

3.2.3 Recovery System Layout

The recovery system consists of an avionics bay, a main parachute, and a drogue parachute. The avionics bay is located in in the coupler between the forward and central sections. The parachutes are located in the sections adjacent to the avionics bay; the main parachute is located in the forward section, and the drogue parachute is located in the central section (Figure 26).

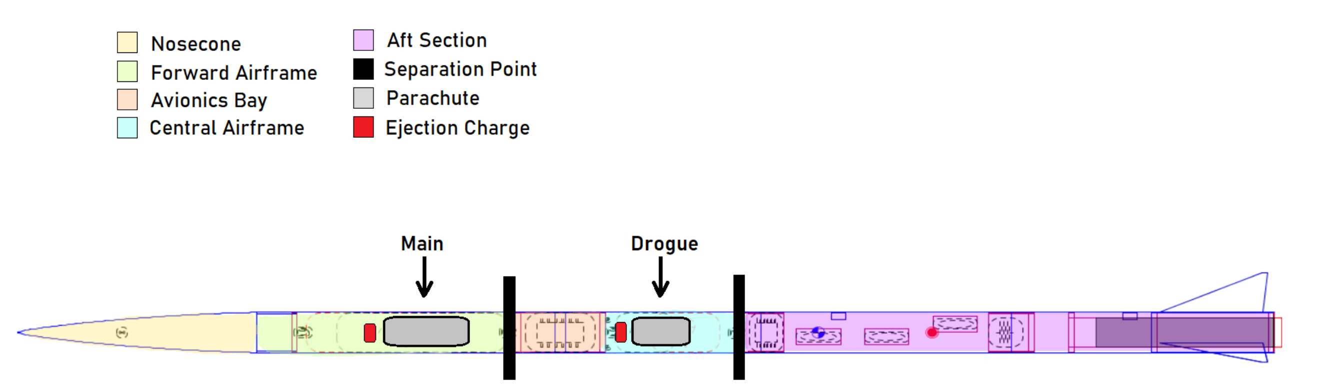

Figure 26: Recovery System Location in Launch Vehicle

During the first separation event, which will take place at apogee, the central and aft sections will separate, deploying the drogue parachute (Figure 27).

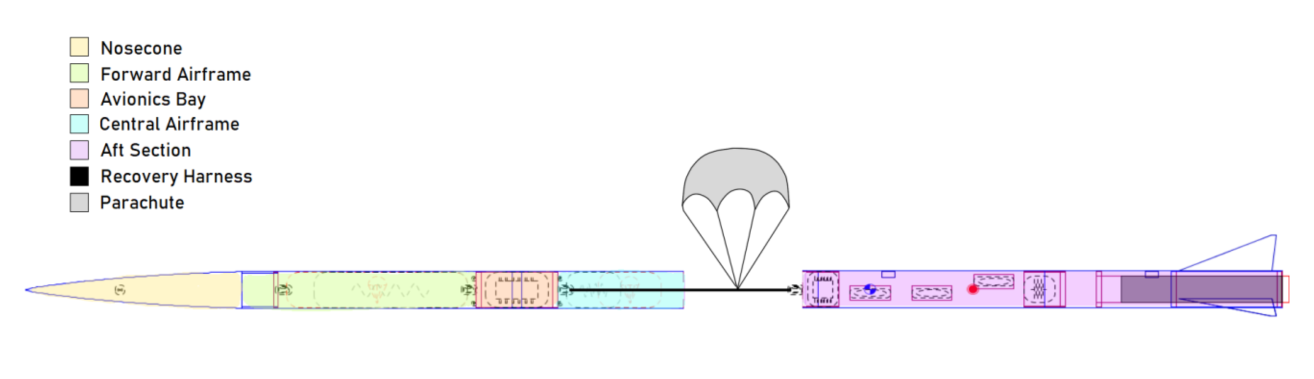

*Figure 27: First Separation Event**

**Not to scale*

The launch vehicle will descend under the drogue parachute from apogee until it reaches an altitude of 600 ft. At 600 ft, the forward section and avionics bay will separate, deploying the main parachute (Figure 28).

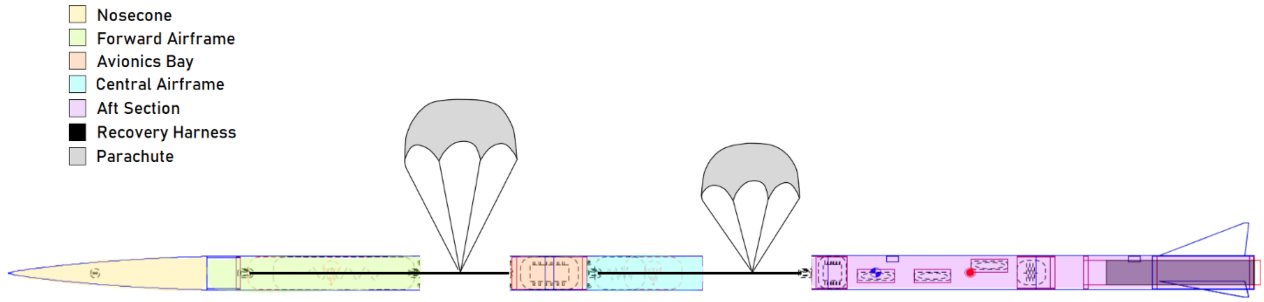

*Figure 28: Second Separation Event**

**Not to scale*

The avionics bay consists of the primary and secondary altimeters, 9V batteries for each altimeter, and two keylock switches to arm each altimeter. The components will be secured in the avionics bay with fasteners, mounts for the arming switches, and casings for the batteries (Figure 29).

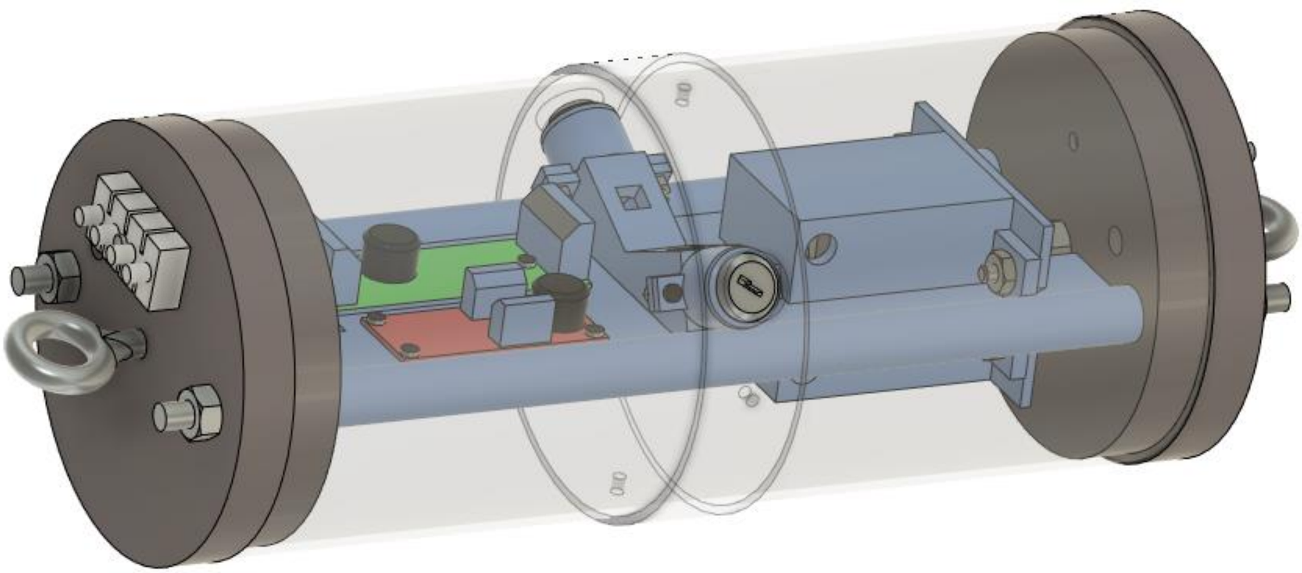

Figure 29: Avionics Bay Layout

3.2.4 Redundancy in the System

To ensure that the recovery system continues to function in the case of an altimeter or power failure, a redundant set of two separately wired altimeters with separate power sources will be used. Each altimeter will have a separate set of drogue and main ejection charges, with the charges for the secondary altimeter being 25% larger than the corresponding primary charge to ensure that separation occurs if the primary ejection charge is unable to separate the launch vehicle sections. The secondary ejection charge for the drogue parachute will ignite 1 s after apogee is reached and the secondary ejection charge for the main parachute will ignite at an altitude of 550ft, 50ft below the primary ejection charge ignition. Additionally, the primary and secondary altimeters will be from different manufacturers to minimize the impact of an altimeter failure on the launch vehicle. The wiring for the redundant components is shown in Figure 30.

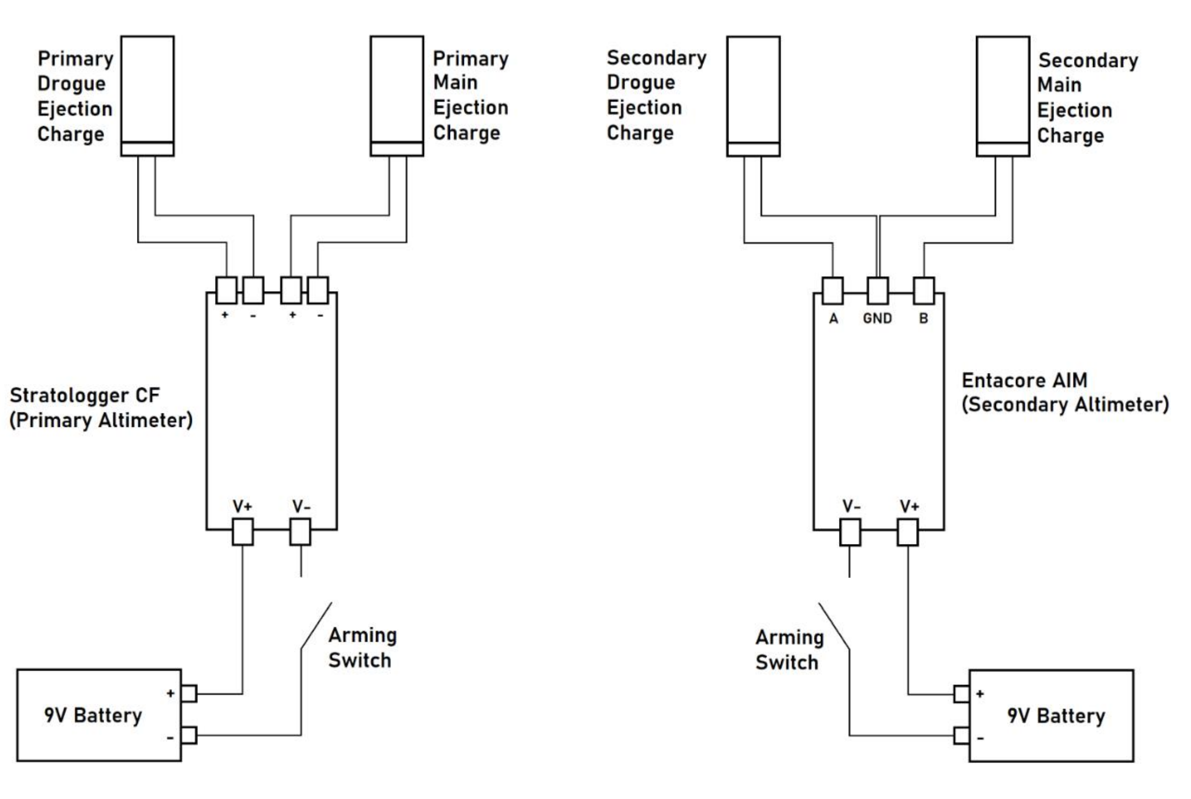

Figure 30: Altimeter Wiring Diagram

3.3 Mission Performance Predictions

3.3.1 Target Altitude

The launch vehicle's official competition launch target altitude is expected to be 4600 ft. This altitude is determined through Monte Carlo Simulations to account for the vehicle's susceptibility to environmental conditions. The results are summarized in section 3.3.6.

3.3.2 Flight Profile Simulations

Based on the launch conditions defined in Table 19, the vehicle's apogee is predicted to be 4644 ft in this simulation. The drogue is expected to deploy at apogee and the main is expected to deploy at 600 ft. The total flight time is expected to be 89 seconds The flight profile of the launch is shown in Figure 31.

Launch Conditions in Huntsville, Alabama	
Wind	5 mph
Launch Angle	5 deg
Launch Rod Length	144 in

Latitude	34.6 °N
Longitude	-86.7 °E
Altitude	800 ft
Temperature	80 °F
Pressure	1 atm

Table 19: Launch Conditions for Simulation

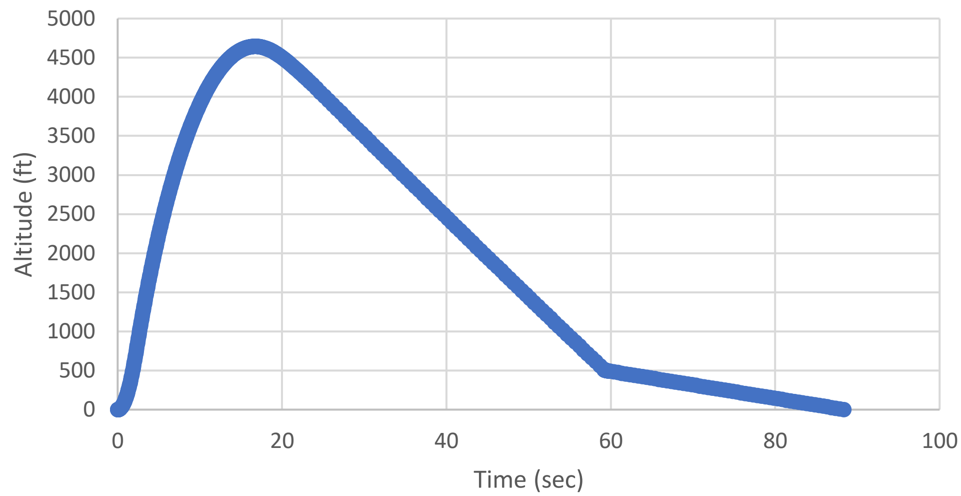

Figure 31: Launch Vehicle's Altitude vs Time

The velocity of the launch vehicle is shown in Figure 32. The initial spike is due to the motor ignition and the maximum thrust. The maximum velocity is expected to be 639 ft/s, equivalent to Mach 0.58. The initial velocity off the rail is expected to be 86.3 ft/s, meeting the competition's requirement of at least 52 ft/s. The ground hit velocity is expected to be 17.1 ft/s.

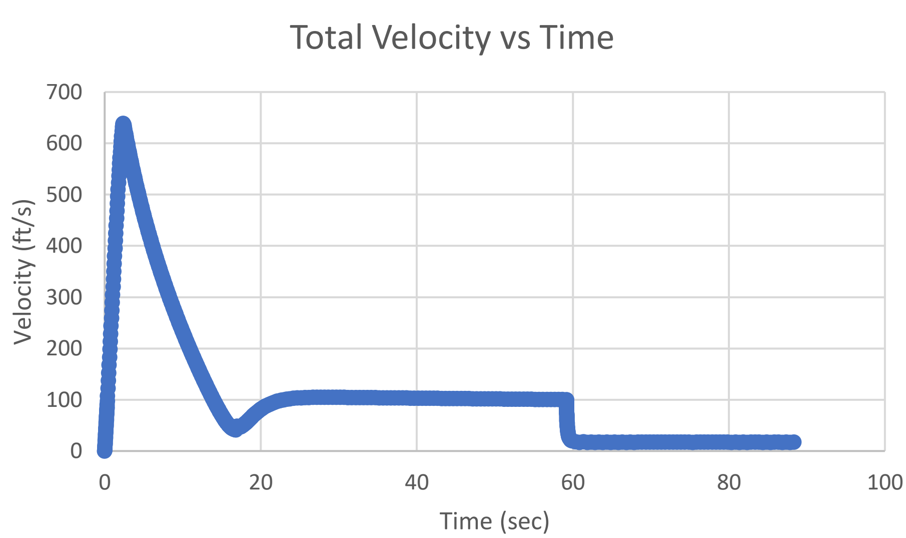

Figure 32: Launch Vehicle's Velocity vs Time

The acceleration of the launch vehicle is shown in Figure 33. The initial spike is due to motor ignition. The second spike is due to the main parachute deploying. The maximum acceleration is expected to be 305 ft/s^2.

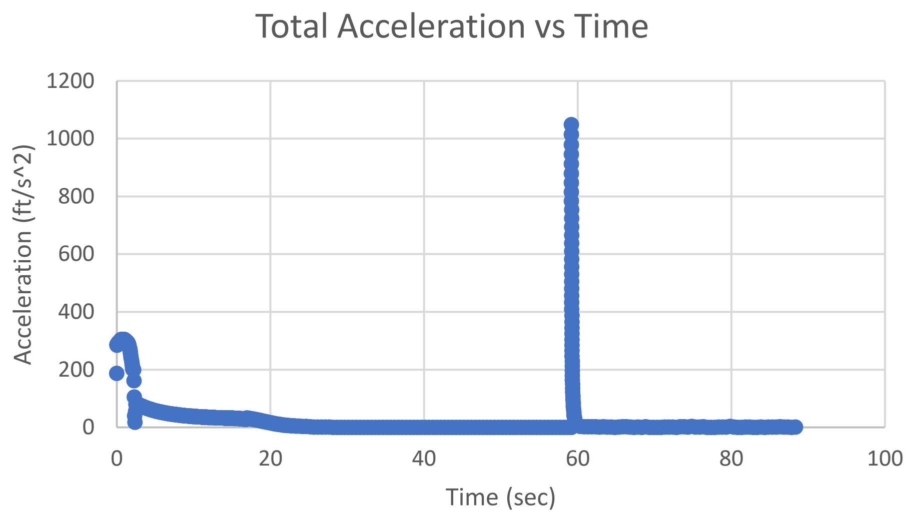

Figure 33: Launch Vehicle's Acceleration vs Time

3.3.3 Motor: Aerotech K1000

The motor selected is the Aerotech K1000, which has a maximum thrust of 1674 N and a total impulse of 2512 Ns. The maximum thrust occurs at the launch rod to propel the vehicle to 86.3 ft/s off the rail. The motor has a burn time of 2.35 seconds and uses 1234 grams of propellant. It provides a thrust to weight ratio of 9.04:1, fulfilling the competition's requirement of 5:1. The thrust vs time of the motor is shown in Figure 34.

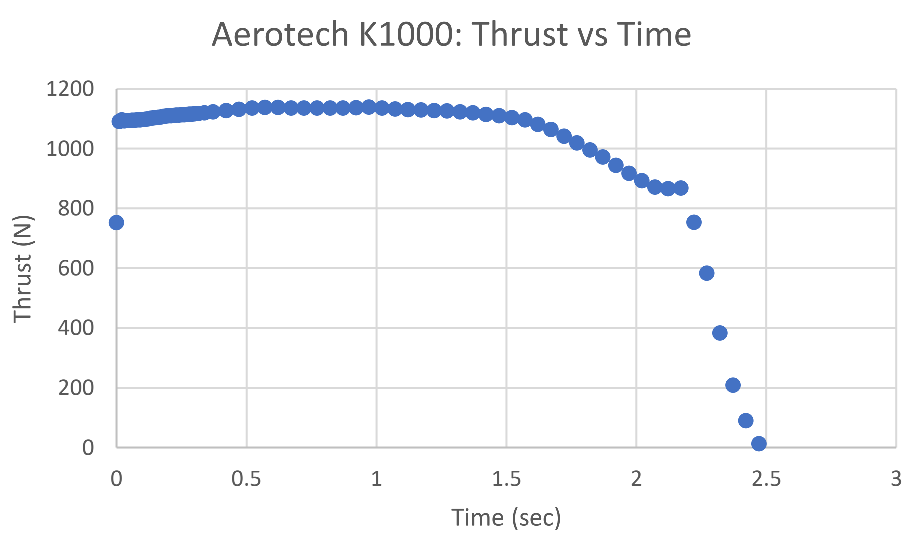

Figure 34: Aerotech K1000 Thrust Curve

3.3.4 Stability

The vehicle is considered stable when the center of pressure is located at least 1 body caliber behind the center of gravity. However, it is recommended you have a stability margin within 7-15% of the length of the rocket. In other words, at least a minimum of 2 body calibers as per competition guidelines. The center of gravity of the rocket with the motor is 73.2 inches from the tip of the nosecone. The center of pressure of the rocket with the motor is 84 inches from the tip of the nosecone. Therefore, the static stability of the vehicle (loaded) on the launch pad is 2.62 calibers. The static stability at the rail exit is 2.73 calibers. During flight, the stability gradually increases to a maximum of 3.75 calibers, due to the motor decreasing the mass. After the motor burns out, the stability decreases to a minimum of 2.1 as the velocity is decreasing up till apogee. Figure 35 displays the change in stability over time where the oscillations are an indication of simulated wind gusts.

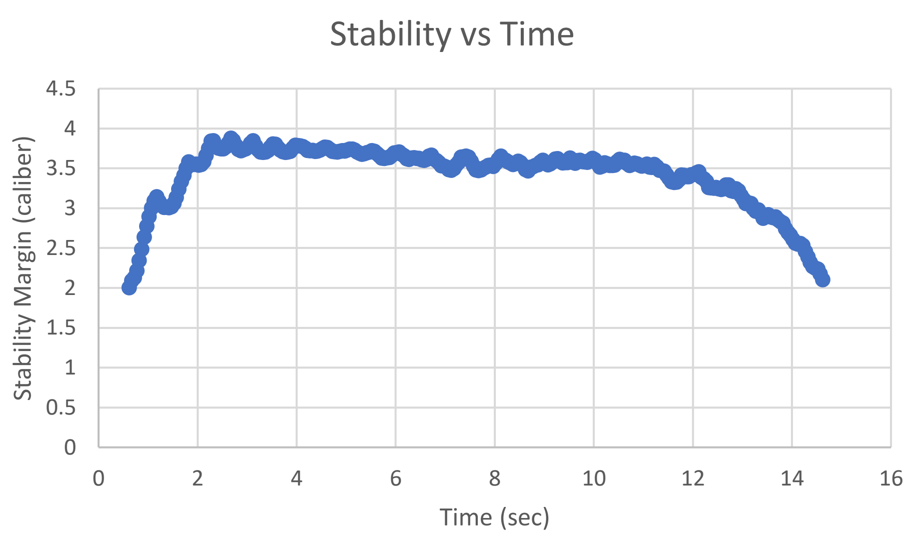

Figure 35: Launch Vehicle's Stability vs Time

3.3.5 Descent Simulations

Equation 3 was used to calculate the kinetic energy of each section of the launch vehicle upon landing. The launch vehicle will be descending under the main parachute prior to landing, so the main parachute descent rate of 17.2 ft/s was used. It was assumed that the descent rate of the launch vehicle was constant. The masses of each section were obtained from Table 10.

$$K_{Forward} = \frac{1}{2} * (0.1714\ slug) * \left(17.2 \frac{ft}{s}\right)^2 = 25.35\ ft \cdot lb$$

$$K_{Central} = \frac{1}{2} * (0.1438\ slug) * \left(17.2 \frac{ft}{s}\right)^2 = 21.27\ ft \cdot lb$$

$$K_{Aft} = \frac{1}{2} * (0.3927\ slug) * \left(17.2 \frac{ft}{s}\right)^2 = 58.08\ ft \cdot lb$$

Equation 1 was used to calculate the expected descent time for the launch vehicle, with the first term of the equation corresponding to descent time under the drogue parachute and the second term corresponding to descent time under the main parachute. These terms were then summed to obtain the total descent time.

$$Descent\ time_{\ drogue} = \frac{4600ft\ - 600ft}{80.1\frac{ft}{s}} = 49.94s$$

$$Descent\ time_{\ main} = \frac{600ft}{17.2\frac{ft}{s}} = 34.88s$$

$$Total\ Descent\ Time = 49.94s + 34.88s = 84.82s$$

OpenRocket simulations were also used to verify the accuracy of the original calculations (Table 20). OpenRocket simulations account for the time spend accelerating to the terminal descent rates used in the above calculations, which results in them being more accurate as a real launch vehicle will not move at constant velocities. To avoid introducing additional variables that would result in the simulation results being drastically different from the original calculations, the angle of the launch rod was set to 0° and the wind speed was set to 0 mph.

Descent Times from OpenRocket Simulations	
Total Flight Time (s)	99.5
Time to Apogee (s)	16.8
Total Descent Time (s)	82.7

Table 20: Descent Times from OpenRocket Simulations

Equation 2 was used to calculate the drift of the launch vehicle in five different wind conditions: no wind, 5 mph wind, 10 mph wind, 15 mph wind, and 20 mph wind (Table 21). It was assumed that apogee was reached directly above the launch pad, that wind speed and direction were constant, and that the launch vehicle descended at a constant velocity. These constant velocities were the terminal velocities under each parachute, which was 80.1 ft/s for the drogue parachute and 17.2 ft/s for the main parachute.

Drift from Equation 2			
Wind Speed (mph)	Total Drift (ft)	Drogue Drift (ft)	Main Drift (ft)
0	0	0	0
5	622.02	366.21	255.81
10	1244.05	732.42	511.63
15	1866.07	1098.63	767.44
20	2488.10	1464.84	1023.26

Table 21: Drift Calculations from Equation 2

Drift was also calculated using OpenRocket simulations (Table 22). Unlike the original calculations, OpenRocket accounts for the time needed for the launch vehicle to accelerate to terminal velocity and variations in wind speed. As a result, the drift values obtained from OpenRocket simulations are more likely to match the launch vehicle's drift during descent. The angle of the launch rod was set to 0° so that the launch vehicle reaches apogee as close to directly above the launch pad as possible. Additionally, to account for the launch vehicle sometimes travelling upwind, the drift value used was the sum of the distance between the landed launch vehicle and the launch pad and the maximum distance travelled upwind.

Drift from OpenRocket Simulations	
Wind Speed (mph)	Total Drift (ft)
5	596.1
10	1163.7
15	1696.3
20	2270.4

Table 22: Drift Calculations from OpenRocket Simulations

Because the simulations accounted for variations in wind speed, results were slightly different every time the simulations were run. However, these variations were minimal; apogee varied by less than 5 ft and the total flight time varied by less than 2 s.

3.3.6 Robustness & Monte Carlo Simulations

A Monte Carlo Simulation was conducted in MATLAB to test the sensitivity of the launch vehicle to wind conditions and launch angle to the effects on apogee. A total of 10,000 simulations were conducted with wind profiles based on the probability weight as shown in the table. The probability weights were assigned after reviewing the launch site's climate trend around the time of the competition. Figure 36 displays the results of the Monte Carlo Simulation. Table 23 quantifies the data in the figure to quantify the average altitude for each wind condition and the most probable altitude given the range of launch conditions.

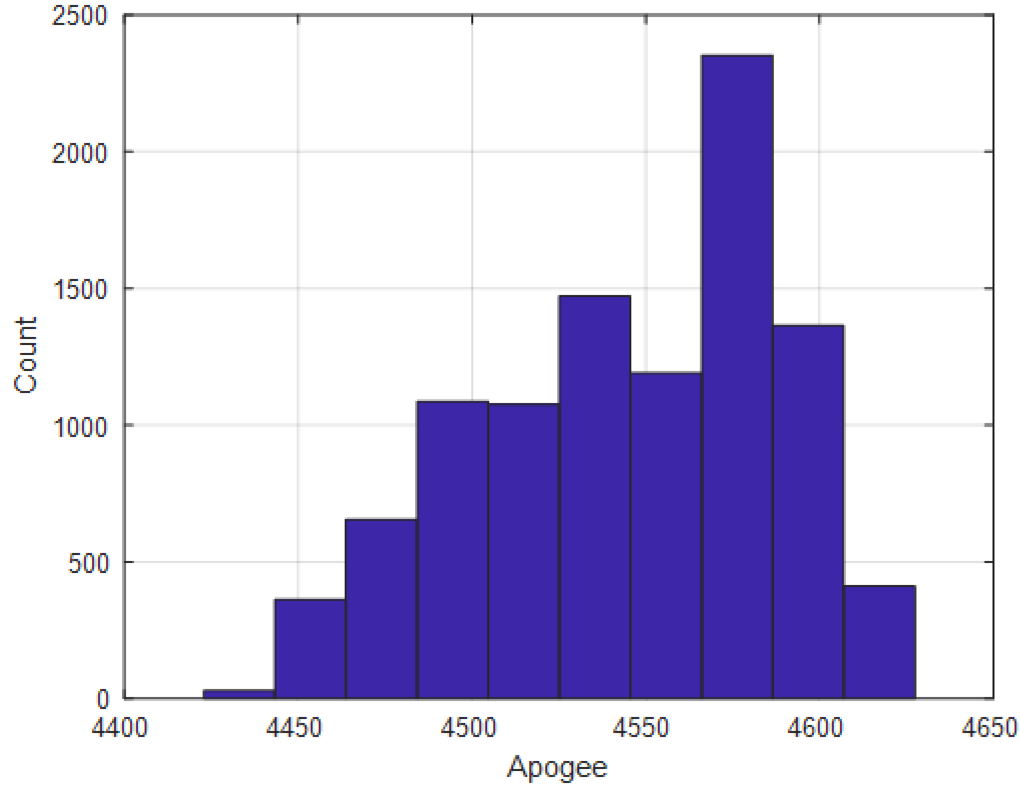

Figure 36: Monte Carlo Simulation Results

Monte Carlo Simulation: Altitude			
Launch Angle	Wind Condition	Probability Weight	Predicted Average Altitude
0	0 mph	5%	4670
5 deg	5 mph	10%	4646
5 deg	10 mph	70%	4620
10 deg	15 mph	10%	4459
10 deg	20 mph	5%	4444
Most Probable Altitude			**4600 ft**

Table 23: Monte Carlo Simulation Altitude Determination

Additionally, the adverse effects of the long and skinny nature of the rocket were considered to ensure robustness. The concern is that a long skinny rocket that has a high fineness ratio is susceptible to fracturing due to forces and perturbations during fight. The body tube is then capable of buckling. To mitigate that, our launch vehicle is made of carbon fiber to ensure structural integrity. Since our rocket will not be flying supersonic, we also don't have many of the concerns such as oblique shocks. A slightly larger fineness ratio has been tested twice by the team, each using fiberglass as the body tube. Experimentally, it tested that fiberglass could provide the structural integrity for this rocket.

4. Payload Criteria

4.1 Selection, Design and Rationale of Payload

4.1.1 Payload Objectives and Success Criteria

The objective of the payload is to receive RF commands and output the corresponding responses. The payload consists of three cameras mounted 120° apart from each other, aligned with the three fins. The cameras are aligned so that regardless of the orientation of the rocket upon landing, one of the cameras will be positioned so it can take the pictures and output the correct responses to the RF commands.

The IMU must determine the orientation of the rocket and relay that to the Raspberry Pi so the correct camera will rotate outwards. The mini solenoid tongue will retract, and the locking lug will no longer hold the camera mount system down. The camera mount will swing out 90° on the spring-loaded hinge so that it is perpendicular to the ground. The stepper motor on the camera's mount will rotate the camera about the z-axis after receiving the RF commands.

4.1.2 System Level Design Alternatives

4.1.2.1 Orientation System

The team first considered various systems to orient the camera to be perpendicular to the ground. The team decided that the simplest and most efficient way to ensure this design requirement was to utilize the naturally occurring orientation of a launch vehicle after landing. A launch vehicle with three fins will always land so that one fin points up, meaning that there are three possible orientations the launch vehicle could be in upon landing.

4.1.2.1.1 Externally Mounted Camera Concept

The first concept was an externally mounted camera design. It consisted of clear teardrop-shaped mounts containing cameras on the outside of the airframe. Each one would have been aligned with a fin so that one of the mounts would be vertically oriented upon landing. This is because the launch vehicle would land with two fins contacting the ground and with the third fin and its corresponding camera oriented normal to the ground. The design advantages were its low motor count, complexity, and cost. It only requires three motors which minimizes cost and does not require many components to implement the concept. The most significant disadvantage for the externally mounted camera idea was the effects it had on the aerodynamics of the launch vehicle. The added mounts on the surface of the launch vehicle could make it over stable. The teardrop-shaped domes could be modeled as fins in OpenRocket, but they could behave in a significantly opposing way without testing. Other disadvantages were the environmental factors that could affect the quality of the images. For example, dirt could stick to the external mounts or there may be glare from the sun that could negatively impact the image quality.

4.1.2.1.2 Linear Camera Extension Concept

The second concept involved radially extending out of the airframe using linear motion. It would have used linear actuators to push the cameras out of the airframe through milled cut outs in the airframe using a lead screw. The linear extension design had no environmental risks, which was one of its main advantages. It also required a small exterior panel that could provide aerodynamic risk, but not nearly as much as cut outs would. The primary disadvantage for linear extension concept is that it would require three times as many motors which intrinsically increases complexity and cost; the design introduces too many potential points of failure. If the linear camera extension were to fail, the launch vehicle's aerodynamics would be negatively affected. The mechanism would not risk aerodynamic stability with airframe protrusions like the externally mounted camera idea but there could be problems with the effects of the holes in the airframe on aerodynamic stability.

4.1.2.1.3 Spring Hinge Extension Concept

The third concept required a spring hinge to rotate a camera and a camera housing out of the airframe. It would have cameras mounted inside the airframe in housings that would be flush with milled cut-outs in the airframe. The camera aligned with the vertical fin would spring out of the airframe on a hinge. The spring hinge design's advantages solve the challenges posed by the other ideas. The design protects the cameras during flight, has no external protrusions during flight, and could be designed such that the holes in the airframe are covered by the camera mount flush with the airframe and that the hinge is oriented in the direction opposite of the flight direction to prevent premature extension of the cameras during flight. The design only requires two motors per subsystem totaling six motors and has a cost within the range of affordable and necessary. This became the leading design. All other decisions, including material selection and electronics, were then made on this basis.

4.1.2.1.1 Orientation System Objectives

To determine which design to implement for the rockets final design, multiple decision matrices were used. For each design, certain criteria pertaining to the main functionalities of the payload and how they contribute to the success of the experiment were selected. For each criterion, the designs were scored linearly so that the criteria are minimized, with a 10 being the worst score. The qualitative scores were determined according to the criteria defined in section 3 of this report.

Various objectives were considered when determining the best system for up righting the camera system. The main objectives considered include aerodynamic impact, risk in points of failure, complexity, cost, environmental factors, and risk to launch vehicle. The concepts had to be nearly fully designed in order to measure the cost and complexity. The aerodynamic risks were measured qualitatively in how many exposing holes were necessary to be milled in the airframe to allow cameras to pop out, because the aerodynamic effects of the holes cannot accurately be modeled in OpenRocket or simulated for flight dynamics.

The exposed holes are ones that cannot have retainment housing underneath due to design constraints, whereas unexposed holes have retainment housing to protect the launch vehicle from undesirable aerodynamic forces. In addition to the number of holes required, the team considered the design's accuracy relative to what can be modeled in simulation.

Points of failure were measured in the number of motors required, as those contribute the most heavily to the mechanical risk. Complexity was measured qualitatively as the combination of hours spent designing to a certain point that overcame the desired challenges set by the team and in the least number of mechanical components required to make the design work. The design challenges were a list of preliminary ideas that the team determined could be detrimental to the design or lose the spirit of the competition. Some designs required significantly more research and debate to generate concepts. These designs were more complex with respect to requirements, and generally required more manufacturing and designing time than alternatives.

The cost was estimated by compiling pricing data on the required parts for each design. The environmental factors were determined by considering which designs would be affected by outside factors that cannot be mitigated by design. Risk associated with the launch vehicle was a determined through a thorough consideration of how the launch vehicle would or would not be affected by a failure or malfunction in the payload.

Material durability was determined from open-source data regarding resistance to fatigue, heat, and chemicals (Table 23). According to the Material Selection matrix, the best choice for the material is PET-G. Its durability was considerably better suited for the design than any other choice. Acrylic may have been ideal for a design centered on visibility through its enclosure, but after considering the uncontrollable factors of dirt, sun glare, or surface deterioration, the team decided that the disadvantages using a translucent vessel would not be able to be mitigated by design.

Test	Measurement	PLA	PET-G
Stiffness	difficult bend /10	7.5	5
Durability	fatigue/heat/chemical resistance /10	4	8
Max Surface Temperature	before bending under load celsius	52	73

Table 24: Standard Materials Data

Threaded inserts were chosen as the best option for fastening the payload systems to the airframe as shown in the matrix. The thickness for the airframe was determined to be too small for countersunk fasteners. The threaded inserts also mitigate any concern with external protrusion's effects on stability.

Up Righting System			**Spring Loaded Hinge**			**Linear Extension**			**Externally Mounted**		
Objective	Weighting Factor	Parameter	Mag.	Score	Value	Mag.	Score	Value	Mag.	Score	Value
Aerodynamics	0.3	Holes	Great	10	3	Poor	2	0.6	Fair	4	1.2
Motor Count	0.3	Motors	2	8	2.4	6	2	0.6	1	10	3
Complexity	0.2	Hours	Great	10	2	Okay	6	1.2	Poor	2	0.4
Cost	0.2	Dollars	29.99	8	1.6	60	2	0.4	19.99	10	2
Overall value					**9**			**2.8**			**6.6**
Material Selection			**PLA**			**PET-G**			**Acrylic**		
Objective	Weighting Factor	Parameter	Mag.	Score	Value	Mag.	Score	Value	Mag.	Score	Value
Material Cost	0.2	Unit price	19.99	4	0.8	29.99	2	0.4	7	10	2
Durability	0.5	Resistance	Fair	4	2	Great	10	5	Poor	2	1
Manufacturability	0.3	Hours	5	10	3	5	10	3	15	2	0.6
Overall value					**6.2**			**8.4**			**3.6**
Fasteners			**Threaded Inserts**			**Countersunk**			**Exterior Nut**		
Objective	Weighting Factor	Parameter	Mag.	Score	Value	Mag.	Score	Value	Mag.	Score	Value
Cost	0.2	Dollars	9.00	2	0.4	8.00	6	1.2	5	10	2
Aerodynamic Impact	0.5	Area	Great	10	5	Fair	4	2	Poor	2	1
Thickness	0.3	Binary	1	10	3	1	10	3	2	10	3
Overall value					**8.4**			**5.2**			**6**

4.1.2.2 Camera Rotation System

Since the camera needs to rotate around z-axis following the RF commands, the payload needs a system to generate rotational motion. Several concepts were considered for rotating the spring hinge mechanism about the z-axis. The team considered using a servo motor, a brushed DC (Direct Current) motor, or a stepper motor. The mechanical structure of rotation system will be the same for any motor since the camera will be attached to the motor shaft directly. The motor that is selected, on the other hand, is essential for the accurate and efficient functioning of the rotation system.

4.1.2.2.1 Camera Rotation Objectives

The accuracy, range, and ease of control of motors were identified as objectives of motor selection. Accuracy refers to how accurately a motor can rotate when provided with a certain degree to rotate. Range refers to the angle through which a motor can rotate. Since the camera needs to rotate in 60-degree increments around the circle, the range of the motor must be at least 300°. Ease of control refers to the complexity of the software and the control circuit required to operate the motor.

4.1.2.2.2 Camera Rotation Advantages and Disadvantages

Two types of servo motors were considered for the rotation system: traditional servo motors and 360° continuous servo motors. Traditional servo motors receive a Pulse Width Modulation (PWM) and rotate to a certain position according to the duty cycle of PWM signal. This means the control of the motor is simple, since the PWM signals from the Raspberry Pi can be connected directly to the motor. Most traditional servos also employ an internal potentiometer as a feedback signal for position, which allows for accurate position control. However, because a potentiometer is used and most potentiometers only have a range of 180°, traditional servo motor's also only have a range of 180°. This means a traditional servo cannot be used for the rotation system. A 360° continuous servo motor, on the other hand, removes the potentiometer as position feedback and it can rotate continuously. However, this means the position of the motor cannot be accurately controlled without the addition of extra sensors. Most continuous servos do not have these sensors, which makes them inaccurate for position control. Additional sensors can be added into the control circuit but will make the control circuit and software significantly more complex. Furthermore, for the few continuous servos with position feedback built in, their large size makes their use prohibitive due to space constraints of payload bay.

Brushed DC motors were also considered as a method of rotating the camera. Brushed DC motor can be controlled easily by using an H-bridge, since it just needs a DC current to rotate. It also has a range greater than 300°. However, this motor does not have any position feedback, and the speed varies significantly with outside resistance and DC voltage. Accurate position control is difficult for this type of motor. Therefore, these motors were also not selected for the rotation system.

A stepper motor is controlled by giving the number of steps to rotate. One step corresponds to a certain degree of rotation. For example, if a stepper motor has 360 steps, then each step corresponds to 1 degree of rotation. Stepper motors only rotate through the number of steps given by command, which makes their accuracy very high. The range of a stepper motor is continuous, which satisfies the criteria. The stepper motor requires a specific stepper motor controller and programming for specific controllers, which adds complexity to control circuits and software. However, because stepper motors do not require position feedback to determine the current position, accurate control is simpler compared to continuous servo motors and DC motors. Therefore, stepper motors were selected as the method to generate rotational motion in camera rotation system.

4.1.2.3 Camera Retention System
For a spring-loaded hinge system, the camera needs to be locked in payload bay until landing. To securely lock the camera during flight and successfully unlock the camera after landing, a shaft can be extended into and retracted out of the camera arm to lock and unlock it. The linear motion used here can either be generated from rotational motion using a lead screw system or obtained directly from motor. For the lead screw system, a brushed DC motor paired with a long lead screw was considered. For linear motion directly from motor, linear actuators and solenoids were considered.

4.1.2.3.1 Camera Retention Objectives
The purpose of camera retention system is to hold the camera securely in the payload airframe during flight and release the camera after landing. Therefore, the objectives determined to be important were size, mechanical complexity, and control. Size refers to the space occupied by the motors inside the payload bay. This objective also considers the orientation and position of this occupied space. Mechanical complexity refers to how complex the mechanical system is with that specific motor. Control refers to how complex the control circuit and the control software is.

4.1.2.3.2 Camera Retention Advantages and Disadvantages
The simplest mechanical solution was also the cheapest and most secure. The PET-G camera cover will be fastened to the camera, and that system will be fastened to the camera mount flush with the airframe.

The lead screw system contains a brushed DC motor with reduction gear box. The gear box is then connected to the lead screw. Three locking mechanisms will be connected to the lead screw. The three latches will be unlocked at the same time. However, the advantage of this design only exists when the lead screw is in the center of the payload bay. The design of payload bay has tubs that are placed non-concentric and interfere with each other. This means one single lead screw cannot control all three latches. As a result, 3 DC motor and lead screws are needed. This means the lead screw will take a significant amount of space in the payload bay. Additional mechanical threaded parts are needed for this concept to work. Therefore, the mechanical complexity is also very high. Furthermore, the brushed DC motor needs a feedback circuit so that the Raspberry Pi knows when to stop supplying the voltage. This means the control circuit is also complex. As a result, the lead screw system is not chosen.

The linear actuator system involves using a linear actuator to generate linear motion to lock and unlock the latches. This means the mechanical system required is not complex. Feedback will be needed for the electrical system, so the control circuit will be complex. However, any linear actuator with the appropriate stroke length has a size that is prohibitively large. Therefore, it is not possible to use linear actuator as the mechanism to lock and unlock the latches.

The solenoid system uses a solenoid to lock and unlock the latch. The tongue of solenoid extended directly into the latch to lock it. As a result, the mechanical system required for this system is very simple. Feedback will not be needed for this system; therefore, the electrical control circuit will also be very simple. Finally, the solenoid with appropriate stroke length is much smaller than either lead screw system or linear actuators.

4.1.2.4 Radio System
The radio system dictates the operations of the payload once it lands and therefore makes it a critical system of the payload design. Due to this criticality, the team considered 3 ways to observe the radio commands sent by NASA RAFCO. The first way is to use of the shelf (OTS) integrated radio transceiver like Xbee. The second way is to

use the Integrated Chips (IC) radio receiver and then building a whole support circuit around it. The third way is to use the Software Defined Radio (SDR) radio dongle.

4.1.2.4.1 Radio Objectives

The radio system must be able to receive APRS radio signals transmitted by NASA. It needs to be able to tune to the desired frequency range of 144.9 MHz to 145.1 MHz. While the radio signals are being received, it should be able to actively decode the signal as encoded by APRS. It will output the APRS message, decoded and parsed to the main software payloads program to be used in further subsystems.

4.1.2.4.2 Radio Advantages and Disadvantages

The first alternative assessed by the team was to use existing Xbee based radio systems. These systems seemed to be advantageous as the libraries are commonly available and a lot of documentation exists on how to implement them with a Raspberry Pi. However, it became apparent that the Xbee radios would not work due to inability to tune to the frequency range as required by NASA. With that being a critical part of the payload operations, this radio system was discarded as a design option.

The second alternative that was investigated was an integrated circuit radio provided by Silicon Labs. This radio meets all the requirements needed by NASA, specifically being able to tune to the frequency range of 144.9 MHz to 145.1 MHz. Using this alternative provided some advantages as it contains extensive documentation and was able to interface with the Raspberry Pi via GPIO pins. The main disadvantage is that significantly more electrical components are required to use the device, and additional software is needed to decode the input stream since the chip is not capable of doing processing such as APRS decoding.

The third alternative was using an SDR dongle. This alternative meets all the requirements by NASA and it also has no electrical components since it connects with the microprocessor via USB2.0 port. However, this design does need additional software for APRS decoding. Overall, the use of SDR dongle is the simplest design that meets all of the NASA requirements.

4.1.2.5 Software System

The payload software must be responsible for interacting with all external electrical devices and utilizing those components to meet all NASA payload requirements. The overall payload system is split into four distinct subsystems: sensor, motor, radio, and camera. When designing the payload software system, each of these four subsystems went through individual design iterations. These iterations were also considered in the global context of the software system since a change in one of the subsystems will impact how the other subsystems operate.

4.1.2.5.1 Software Objectives

Each of the four software subsystems have their own set of objectives, but each of these can be summarized by an overall software system objective to interact with the electrical and mechanical systems to serve as the controller to complete all payload requirements. This overall system will need to orchestrate the interactions between each separate component and subsystem.

To start, the sensor subsystem's objectives are to continuously monitor the sensor reading from the IMU and barometer to detect launch, apogee, and landing. This subsystem will be the first and only system active when the payload is powered on. Therefore, it will be responsible for enabling the other systems once landing has been detected.

The motor subsystem will have two additional subsections that have their own objectives. The first subsection being the solenoid motors, which needs to trigger the release of the correct camera latch. This objective needs to be met so that the specified camera is in the correct orientation to take photos. Secondly, the stepper motors need to be able to rotate the camera 360° around the Z-axis while being able to stop at any 60° increment.

The radio system needs to be able to tune to the frequency required by NASA, decode the APRS message, and send the final commands to the other software subsystems.

Finally, the camera subsystem's objectives are to take a photo with the proper camera, apply the filters required by NASA, apply a custom filter chosen by the team, and add a timestamp to all photos taken.

4.1.2.5.2 Software Advantages and Disadvantages

4.1.2.5.2.1 Software Radio System Advantages and Disadvantages

When looking at the four main software subsystems, the one that went through the most iterations was the radio subsystem. The first software radio alternative was a Python library called *kiss*, which implements the KISS protocol to communicate with TNC radio devices. This is a very simple library for reading data frames from a USB radio transceiver. The advantage of this library is that it provides the radio input data with a minimal amount of configuration of software overhead. However, it was determined that it would be better to use the software library made directly for the RTL-SDR directly. This is because another program named Dire Wolf exists which simplifies the conversion of the APRS radio message to a human readable message. The RTL-SDR software can output directly to Dire Wolf and therefore provides an even easier radio message decoding pipeline compared to the *Kiss* Python library. Additionally, not using the *Kiss* library means that the entire software codebase can be consolidated into just C++, which provides many benefits in terms of code organization, management, and testing.

Once the decision was made to move away from the Python *kiss* library and utilize a direct RTL-SDR to Dire Wolf connection, an additional library called *Dirus* became available. This library would strictly act as background process to manage the interconnect between the RTL-SDR radio and Dire Wolf. The proposed benefit of this software is that the radio for decoding pipeline could be configured once and then *Dirus* would manage it without any additional intervention. However, it provides no real benefit to the software system besides serving as a helper program and does not contribute to any of the objectives. Therefore, it was decided that the radio message decoding pipeline would be set up manually to not overcomplicate the number of software libraries needed. Doing so means relying less on third party configuration options and less software to manage and update.

4.1.2.5.2.2 Software Camera System Advantages and Disadvantages

For the camera subsystem, the gphoto2 Python library was considered as the main method for interfacing with the onboard cameras and capturing photos. It provides the ability to take photos and save them to the Raspberry Pi which is the bare minimum needed for the camera subsystem. However, compared to similar options, such as OpenCV, it fails to provide as many features built in. Specifically, OpenCV outshines gphoto2 in its ability to apply filters and even append the timestamp, both of which are requirements for the payload. Therefore, gphoto2 was ruled out as a viable camera subsystem alternative since the subsystem would need even more libraries to accomplish all objectives.

4.1.2.5.2.3 Software Sensor System Advantages and Disadvantages

The sensor subsystem has a unique software design since the types of sensors chosen were made to interface with Arduino's instead of Raspberry Pi's and therefore the vendor provided drivers and software libraries are not immediately compatible. One alternative to fix this problem was to install an Arduino to RaspberryPi/C++ conversion library that can translate the Arduino header files into code that can compile as a regular C++ program and interface with the Raspberry Pi GPIO pins. The benefit of this approach is that it does not require any changes to the code since the compatibility layer should handle all the translation. However, this alternative was rejected as it makes more sense to just directly interface with the electrical components and not rely on translational middleware. Even though not using a translation library will increase the development and testing needs of the payload, in the long-term, it will benefit both the rocket and the reliability of the software.

4.1.2.5.2.4 Software Motor System Advantages and Disadvantages

Finally, for the motor controller, a Python library called *RpiMotorLib* was considered to act as the main motor controller. This motor library aims to simplify the operation of stepper motors, DC motors, and servos and was chosen as a possibility because it has the advantage of simplifying the interface to manage and move the motors. However, this library only has a certain number of motors that have been tested and that poses a limit to the electrical subteam decision in motors. Specifically, if this library was used and then later it was found that it did not operate properly with the specific motors that were chosen, then the motor subsystem would need to be written from scratch. Therefore, by writing all the motor controllers manually in C++, it gives the software subteam more insight into the payload software and the exact operations the subsystem will execute while in flight and once landed. Additionally, not using this library will allow for the entire software system to be written in C++ as stated above for the radio subsystem.

4.1.3 Leading Payload Design

4.1.3.1 Mechanical Leading Payload Design

The leading design consists of three camera systems that will be positioned 120° apart so that one will always be aligned with the z-axis upon landing (Figure 37)(Figure 39). Each camera system will have a camera housing that integrates a camera, camera mount, and motors. The airframe has three cut-outs that each camera system will rotate out of. The camera mount sits flush with the cut-out airframe so that each camera can exit the airframe upon landing. An Inertial Measurement Unit (IMU) will detect the orientation of the launch vehicle and determine which camera to activate so that only one camera will be in use when taking photos of the surroundings. Each camera system will be mounted inside the airframe with threaded inserts and ¼-20 fasteners so that the outer surface of the mount is flush with the airframe. The camera mount will be 3D printed so the upper surface is flush with the original curvature of the airframe. Upon landing, one camera will rotate out of the airframe and a stepper motor will rotate the camera about the z-axis (Figure 37)(Figure 38). A Software Defined Radio (SDR) dongle will be incorporated in the payload to receive Automatic Package Reporting System (APRS) commands from NASA. The payload will use the Raspberry Pi and custom software to manage and control all the motors, cameras, sensors, and radios. The software will begin running when the Raspberry Pi is powered on and will be a state-based system interacting with specific software subsystems.

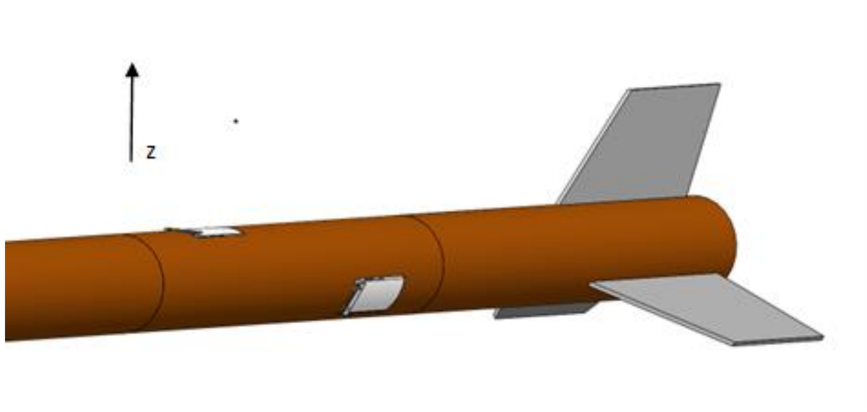

Figure 37: Launch Vehicle Orientation Upon Landing Prior to Camera System Deployment

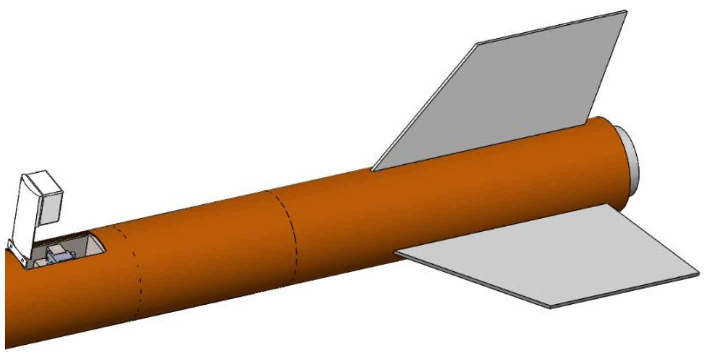

Figure 38: Launch Vehicle with Camera System Deployed

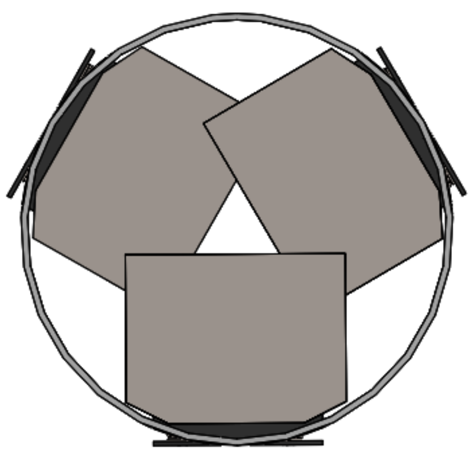

Figure 39: Longitudinal view: Payload camera orientation in airframe

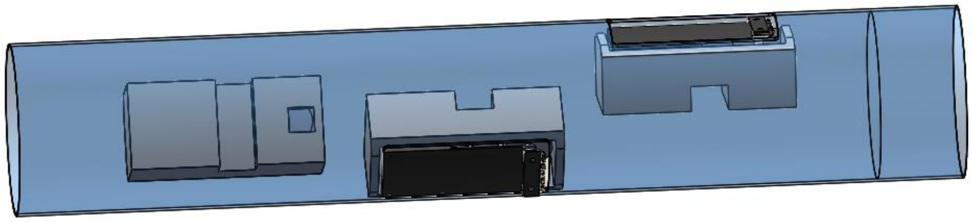

Figure 40: Side view: Payload camera orientation in airframe

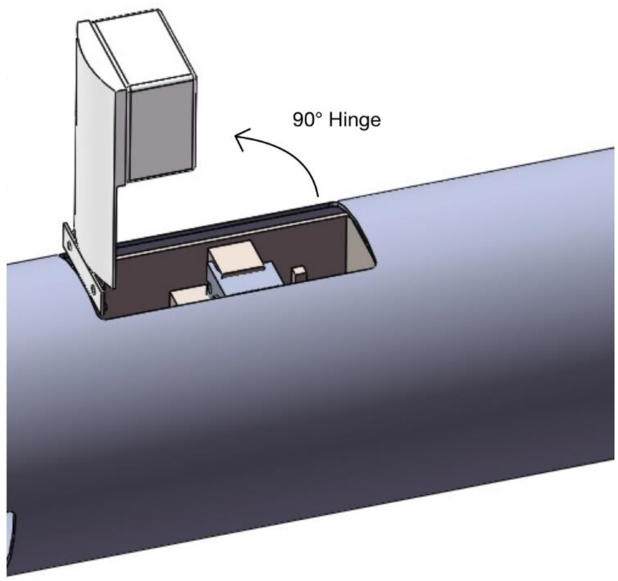

Figure 41: Spring-loaded hinge

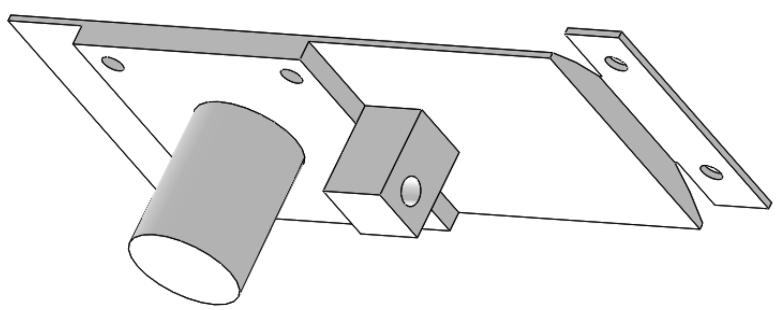

Figure 42: Camera mount isometric view

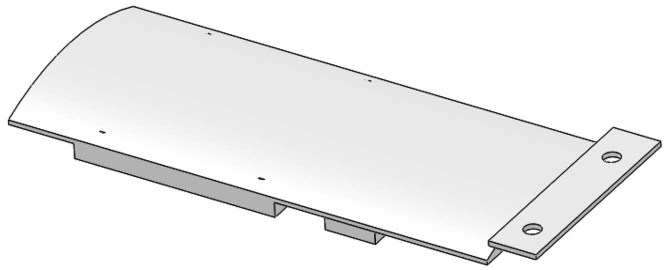

Figure 43: Camera mount isometric view of surface flush with airframe

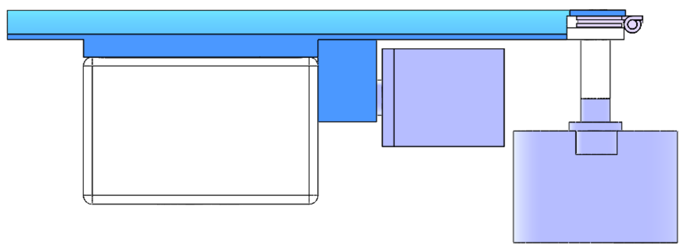

Figure 44: Side view: Payload assembly

The camera system includes a camera mounted to the PET-G camera mount and is enclosed by a camera cover fastened to the inside of the airframe (Figure 43). Each camera system will be mounted on a 90° spring-loaded hinge with No. 6 screws and bolts, so that it lays flush in the launch vehicle during flight and can rotate out of the airframe on the hinge once the vehicle has landed. The spring-loaded hinge is secured closer to the forward end of the airframe so that the direction of the streamlines will always push the hinge closed during flight. This is to protect the launch vehicle and ensure that mechanical failures will have no effect on the aerodynamics of the launch vehicle. The base of the mount has a small cutout for the hinge to be fastened to a flat rigid lip. The spring-loaded hinge is fastened with No. 6 screws to the surface of the camera mount that is flush with the airframe. One side of the hinge is fastened underneath the contacting surface of the camera mount, and on the other side to a motor mount. The motor mount is fitted on the stepper motor that will rotate the camera, mount, locking lug, and spring system when prompted by RF commands (Figure 44)(Figure 45)(Figure 46).

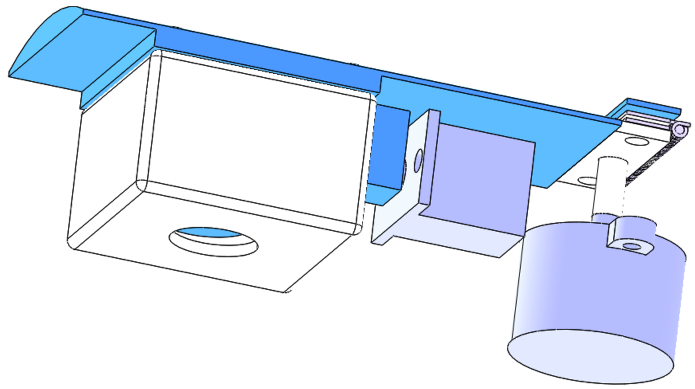

Figure 45: Isometric view: Payload assembly

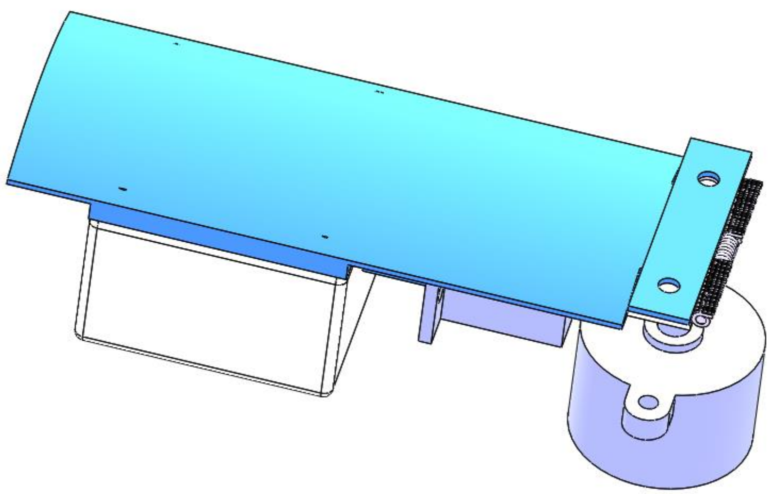

Figure 46: Isometric view: Payload assembly surface flush with airframe

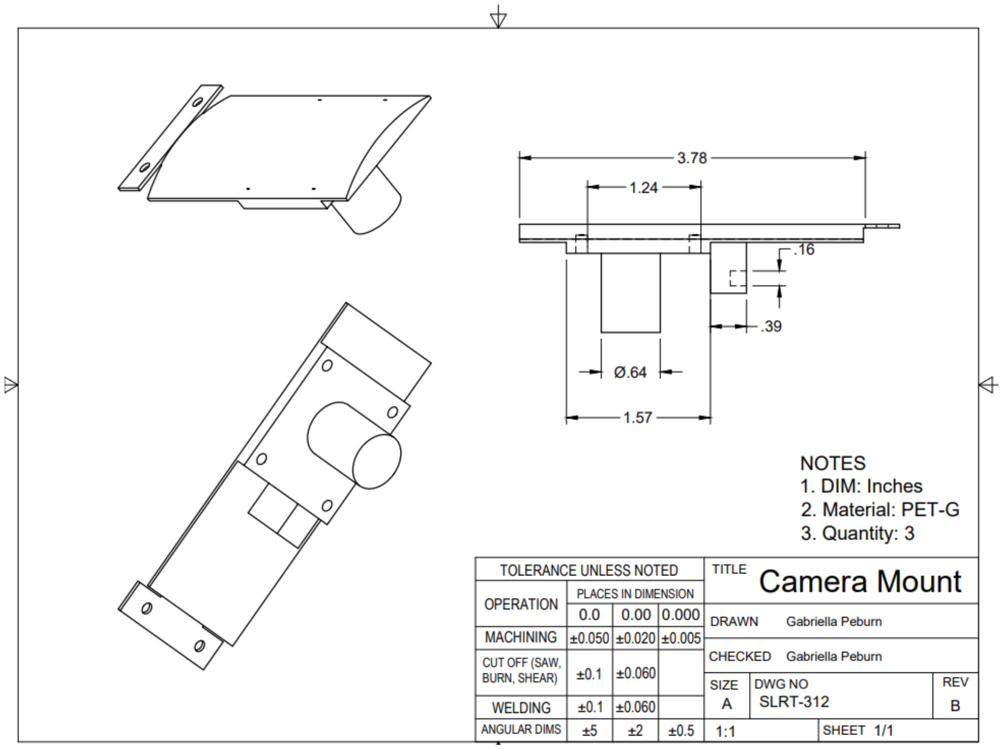

Figure 47: Drawing: Camera mount

The PET-G camera mount includes a locking lug as an extrusion inside the airframe next to the camera cover (). The lug extrusion features a cylindrical cut-out for a mini solenoid tongue to fit into the hole. The camera system is held down by the tongue of the solenoid motor, and it will retract into itself, out of the lug after the launch vehicle lands. The retraction of the tongue releases the hinge and springs the camera system up. The solenoid tongue is extended by default, so the system is locked while powered off. The solenoid must be powered on to retract, so the camera systems cannot be extended mid-flight, providing mechanical safety for electronic failure (Figure 48)(Figure 50)(Figure 51).

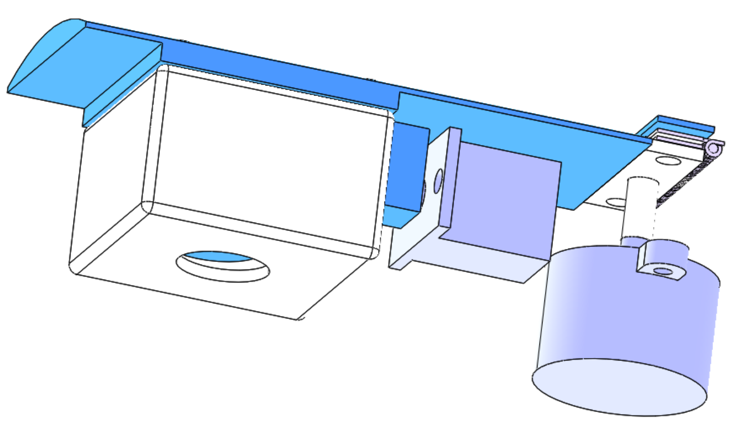

Figure 48: Locking lug on camera mount

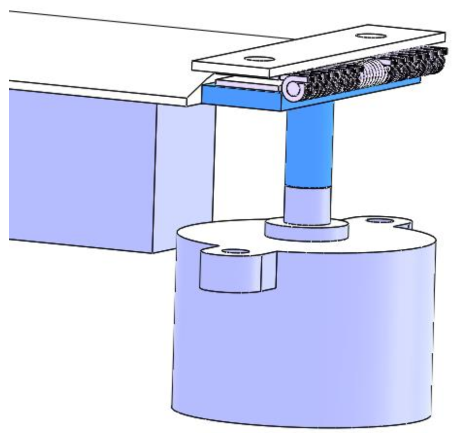

Figure 49: Motor mount

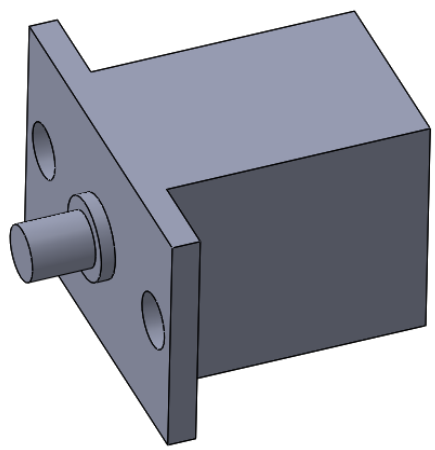

Figure 50: Solenoid

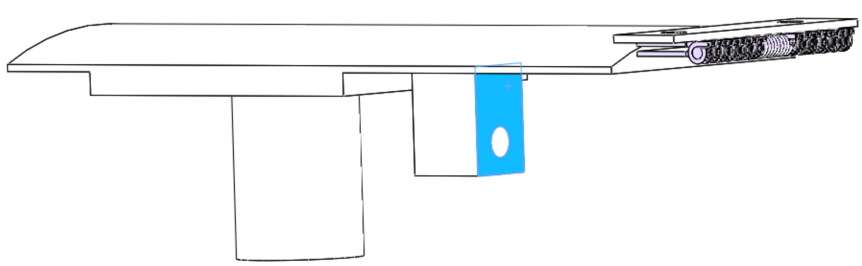

Figure 51: Locking lug

When the solenoid is retracted, the camera mount system will rotate up so the spring-loaded hinge will spring to its naturally released state up from the airframe. The spring-loaded hinge is fastened to a motor mount that is secured to a stepper motor that rotates the camera system about the z-axis. The stepper motor aligned with the top fin will receive commands for the payload challenge (Figure 49)(Figure 52). An IMU accelerometer will determine which camera mount is rotated up, and only that camera will receive the commands and capture images. The camera servo will rotate the entire camera system including the hinge at the surface of the airframe.

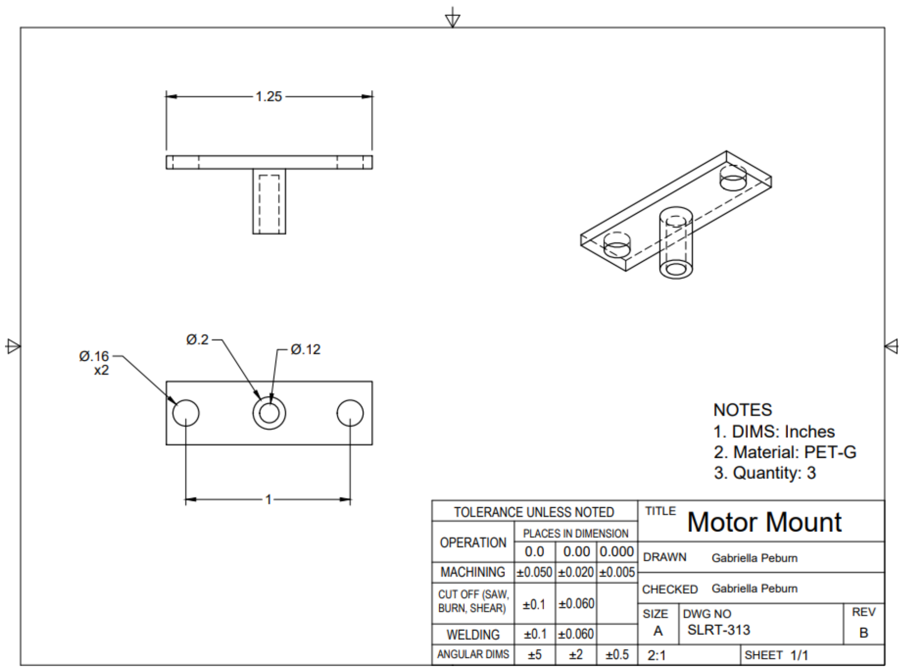

Figure 52: Drawing: Motor mount

The camera servo is fastened to a box-like frame that encloses the entire payload under the airframe. Each of the three camera systems has its own housing (Figure 54)(Figure 55)(Figure 56). Each housing has a small hole in its base for camera and motor wires to pass through. The housing serves the purpose of securing the motors and fasteners while also protecting the launch vehicle from unwanted uncertainties like mechanical failure. The outside of the frame will house the Raspberry Pi and a Raspberry Pi cover. The batteries and battery covers will be housed under the bottom face of the frame at the forward end of the frame. All these components are secured with fasteners for easy assembly and testing.

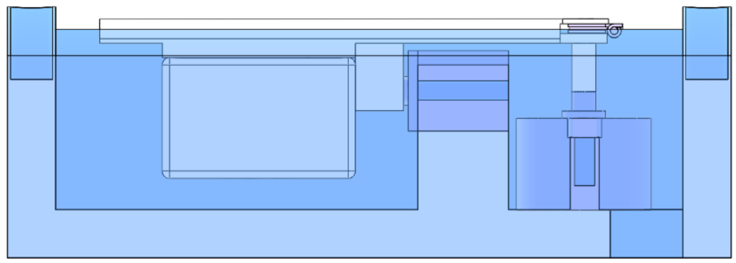

Figure 53: Front View: Payload Assembly Housing

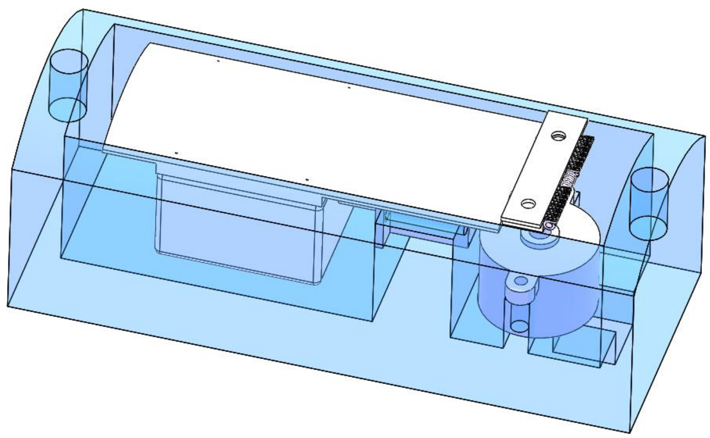

Figure 54: Isometric view: Payload assembly in housing

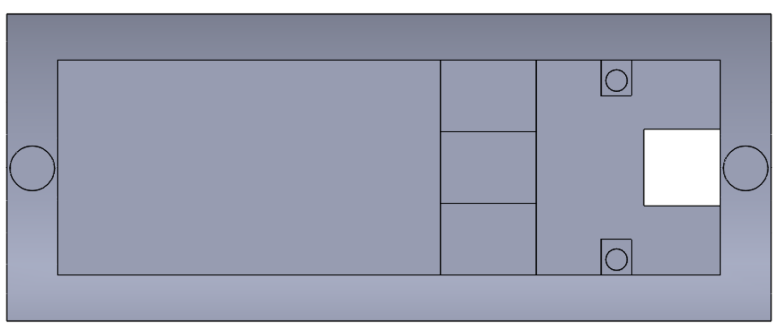

Figure 55: Top view: Payload housing

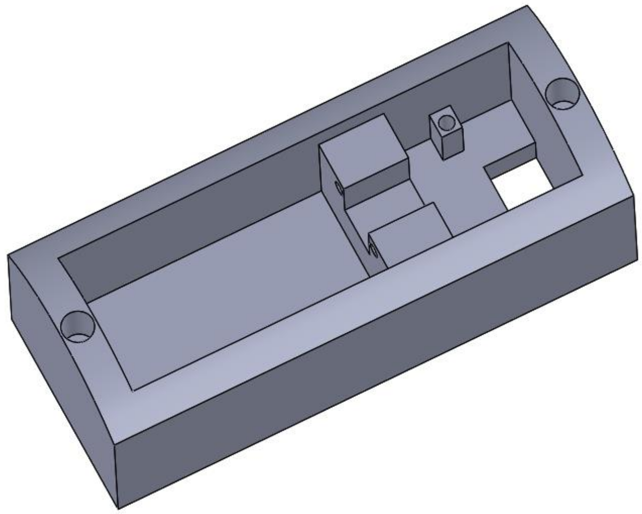

Figure 56: Isometric view: Payload housing

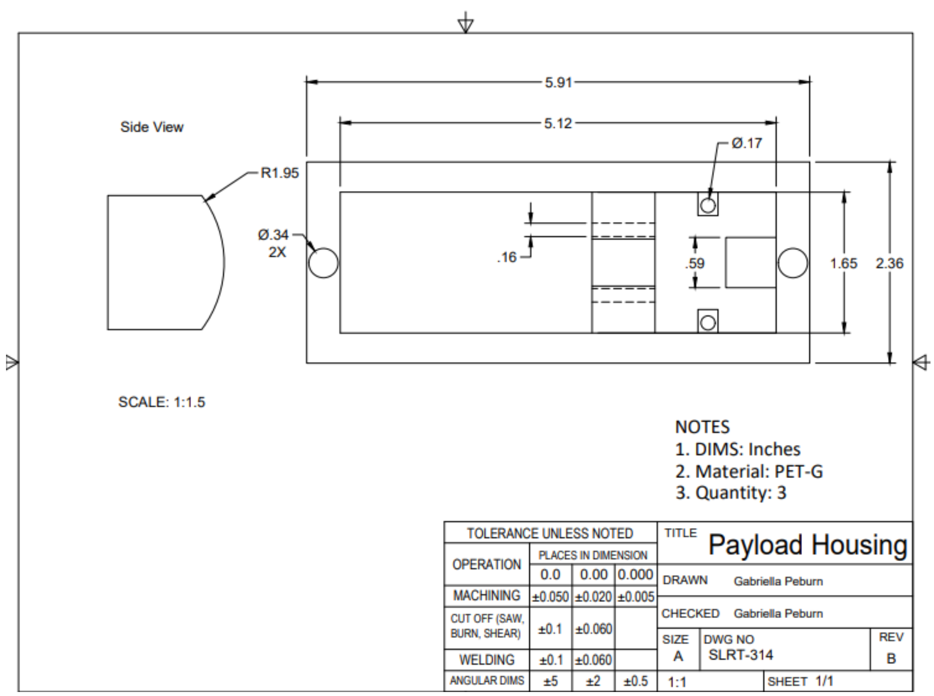

Figure 57: Drawing: Payload housing

The PET-G camera mount will weigh approximately 0.923 oz; the motor mount will weigh 0.0353 oz; camera cover will weigh 0.485 oz, and housing will weigh 8.27 oz. The low-carbon steel hinge will weigh 0.15 oz.

Once the mechanical alternatives were considered and the selection was made, the team moved on to consider electronics alternatives. The stepper motor that will rotate the camera about the z-axis carries a load of about 2.232 oz. The estimated torque the motor supplies is 15e-3 N*m, the shaft diameter is 5 mm, and the gravitational acceleration near the surface of the earth is assumed to be 9.81 m/s^2. The definition of torque was used to find that $T_L = M*g*R$, where T is linear torque, M is mass, g is gravitational acceleration, and R is radius of the shaft. The maximum mass that can be supported as the load is about 21.55 oz. This is about five times more than it will have to support.

4.1.3.2 Electronics Leading Payload Design

The payload uses a Raspberry Pi 4 as the microprocessor. The electronics connected to the Raspberry Pi can be separated into 4 subsystems: a camera subsystem, a sensor subsystem, an actuator subsystem, and a radio subsystem. Figure 58 shows all electronic components and their relation to each other. The camera subsystem and radio subsystem are connected to the Raspberry Pi with Universal Serial Bus (USB), while the sensor subsystem and actuator subsystem are connected to Raspberry Pi through General Purpose Input/Output (GPIO) pins.

Figure 59Figure 59shows how the sensor and actuator subsystems are connected to the Raspberry Pi through GPIO pins. All connections shown in Figure 59 will be implemented on a Printed Circuit Board (PCB) designed by the team for improved integration. The camera subsystem and radio subsystem are not connected through GPIO pins and are therefore not shown in Figure 59. Similarly, the power supply for the Raspberry Pi is supplied through a USB-C power cable, so it is also not shown in Figure 59.

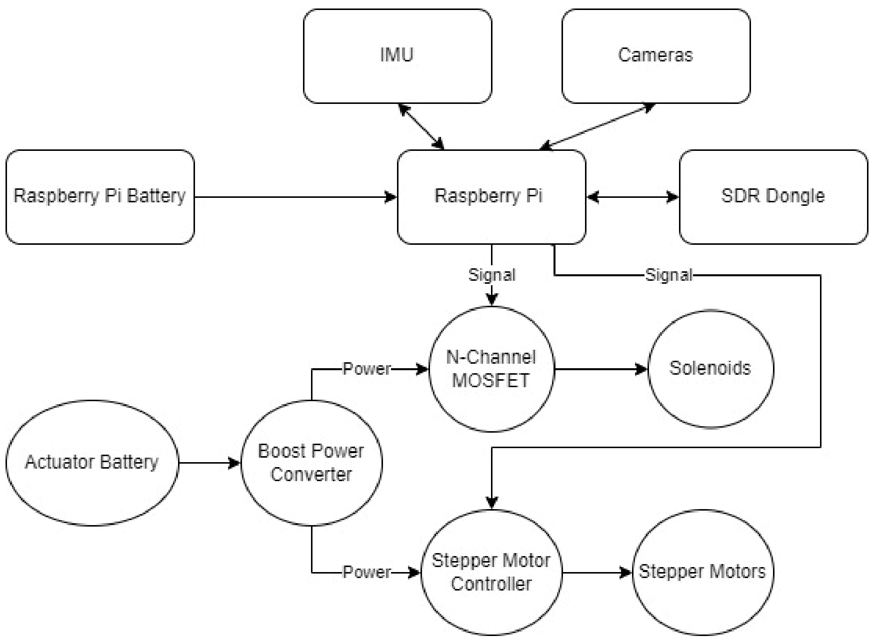

Figure 58: Block Diagram of Electrical Components

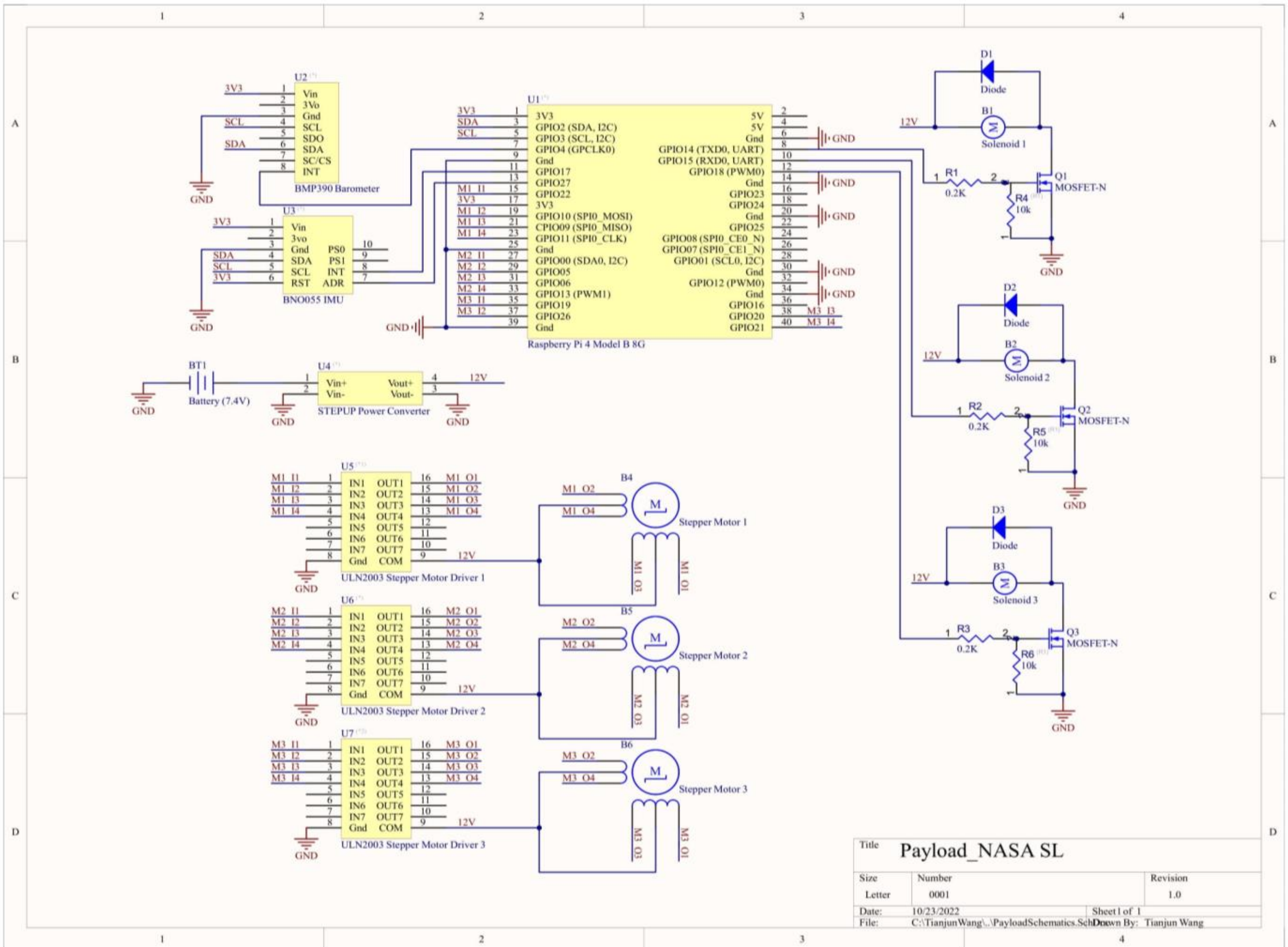

Figure 59: Electrical Schematics with GPIO Pin Connections

4.1.3.2.1 Microprocessor

The Raspberry Pi 4 Model B with 8GB of Random Access Memory (RAM) is used as the microprocessor for the payload. It contains 4 USB2.0 female adaptors, 3 of which will be used to connect with the 3 cameras, and the fourth will be used to connect with the Software Defined Radio (SDR) dongle. Power for the Raspberry Pi is supplied through a battery bank rated with 5V and 10000mAh. The battery bank is connected to the Raspberry Pi through a USB-C cable. As a result, the 5V power pins on the Raspberry Pi are not connected. 3.3V power pins on the Raspberry Pi are used to supply power to the sensor subsystem. The actuator subsystem's power is supplied through another battery (Figure 59) to prevent high current draw from motors to affect the Raspberry Pi. SDA (Serial Data) and SCL (Serial Clock) are used to control and pull data from the sensor subsystem. The rest of GPIO pins are used to supply control signals to the motor subsystem.

4.1.3.2.1.1 Component Selection Justification

A few different microprocessors were considered for the payload. A decision matrix was used to determine the microprocessor (Table 25). Qualitative score assignment will follow Table 3.

Microprocessor			Raspberry Pi 4 Model B			Arduino Uno Rev3		
Objective	Weighting Factor	Parameter	Mag.	Score	Value	Mag.	Score	Value
Performance	0.5	DIMPs	9450	10	5	8	0.08	0.04
IO	0.2	# of pins	40	10	2	14	3.5	0.7
Ease of use	0.2	Experience	Good	8	1.6	Great	10	2
Cost	0.1	dollars	163.00	1.7	0.2	27.60	10	1
Overall value					**8.8**			**3.7**

Microprocessor			Libre Computer Board AML-S905X-CC		
Objective	Weighting Factor	Parameter	Mag.	Score	Value
Performance	0.5	DMIPs	3450	3.65	1.83
IO	0.2	# of pins	40	10	2
Ease of use	0.2	Experience	Okay	6	1.2
Cost	0.1	dollars	60.00	4.6	0.5
Overall value					**5.5**

Table 25: Microprocessor Decision Matrix Assessment

Performance is measured in Dhrystone Millions of Instructions per second (DIMPs). The components were evaluated on a qualitative scale that considers each of those metrics. The single core DIMPs/MHz is multiplied by the maximum frequencies of the processor to get the DIMPs. The multiple cores are not accounted since not all the software running on the Raspberry Pi supports multi-thread. The Performance was weighted at 50% because the radio needs a significant amount of processing power to decode the radio signals into useful commands. The processor with the highest DIMPs received a score of 10 out of 10.

IO refers to the number of pins the microprocessor contains. The number of pins directly determines the number of GPIO pins the microprocessor has. For example, the Raspberry Pi 4 has 40 pins, 27 of which are GPIO pins. The sensor and actuator subsystem all use GPIO pins to interact with the microprocessor. 20 GPIO pins are needed to connect all the subsystems to the microprocessor. Therefore, the number of pins was assigned a weight of 20%. The processor with the highest IO count received a score of 10 out of 10.

Ease of Use is a qualitative assessment referring to how easy the platform can be learned. For example, a device with more thorough documentation and more available software is preferred. Third party instructions were considered but are valued less than the document from the original manufacturer. The ease of use was weighted at 20% because of its significant effect on software development time. The processor that is easier to use received a score of 10 out of 10.

Cost refers to the price (USD) of microprocessor. It is not a priority of the payload design since it does not affect performance; however, since the team must adhere to a budget, price is one of the things that must be optimized. Thus, it was given a weight of 10%. The processor with the lowest cost received a score of 10 out of 10.

4.1.3.2.1 Camera Subsystem

The camera subsystem consists of three 8 Megapixel USB2.0 cameras that are positioned along the 3 fins so that one of the cameras will always face up. All cameras are connected to the Raspberry Pi directly through the USB2.0 port. Therefore, the connections are easy to implement and are not shown in electrical schematics (Figure). This method of connection is chosen because of the lack of GPIO pins on the Raspberry Pi.

4.1.3.2.1.1 Component Selection Justification

A decision matrix was used to choose the specific camera used in the payload (Table 26).

Camera			**16MP Autofocus Camera for Raspberry Pi**			**Arducam 8MP IMX179 USB M12 Lens Camera Module**		
Objective	Weighting Factor	Parameter	Mag.	Score	Value	Mag.	Score	Value
Cost	0.3	USD	126.0	3.5	1.0	61.0	7.2	2.2
Complexity	0.3	# of GPIO	6	1.7	0.5	0	10	3
Area	0.2	in^3	0.037	10	2	0.088	4.2	0.8
Resolution	0.2	megapixels	16	10	2	8	5.0	1.0
Overall value					5.5			**7.0**

Camera			**Spedal Wide Angle USB Webcam**		
Objective	Weighting Factor	Parameter	Mag.	Score	Value
Cost	0.3	USD	44.0	10.0	3
Complexity	0.3	# of GPIO	0	10	3
Area	0.2	in^3	0.797	3.0	0.6
Resolution	0.2	megapixels	2	1.3	0.3
Overall value					**6.9**

Table 26: Camera Decision Matrix Assessment

Cost refers to the price (USD) of the material. This is given a weight of 30% because 3 cameras are needed, and therefore their price affect the total price more significantly than other normal components. The lowest price received a score of 10 out of 10.

Complexity refers to how many GPIO pins are required to set up the camera. They are measured in the number of GPIO pins. Some cameras require GPIO pins to connect to the Raspberry Pi, while other cameras connect to Raspberry Pi through USB2.0 port, in which case they require 0 GPIO pins. The number of pins determine the complexity of connection on the field. As a result, the ease of connection is very important and is given a weight of 30%. The component with the lowest pin count received a score of 10 out of 10.

Area refers to the area of the board of the camera measured in square inch. Since the space in payload bay is limited, the surface area of the camera is important. It is important that the camera has a small surface area to fit in the 3D printed housing. However, the area does not affect the functionality of the camera. Therefore, the objective was weighted at 20%. The smallest surface area received a score of 10 out of 10.

Resolution refers to the number of pixels (megapixels) the camera has. A higher number of pixels corresponds to higher quality images, which is important for the final image output of the surroundings. Therefore, resolution was weighted at 20%. The camera with the highest number of pixels received a score of 10 out of 10.

4.1.3.2.2 Sensor Subsystem

The sensor subsystem consists of BNO055 Inertial Measurement Unit (IMU) and BMP390 Barometer. The IMU is used to measure the acceleration for launch detection and gravity vector to determine orientation. The barometer is used as a redundancy to the IMU. The Raspberry Pi will only have a launch detection when it detects large accelerations from the IMU and a significant change in barometric pressure from the barometer. This limits the consequences of noise that the IMU can potentially generate.

Both the IMU and barometer are connected to the Raspberry Pi through GPIO pins. The Raspberry Pi supplies power through its 3V3 pins. SCL and SDA pins are wired with corresponding GPIO pins on the Raspberry Pi. The interrupt (INT) pins are each connected to GPIO pins for potential use. Reset (RST) pin on the IMU is wired to 3V3 to prevent reset from happening.

4.1.3.2.2.1 Component Selection Justification

4.1.3.2.2.1.1 BNO055 IMU

A decision matrix was used to select the specific IMU used in the payload (Table 27).

IMU			Adafruit BNO055			Adafruit LSM9DS1		
Objective	Weighting Factor	Parameter	Mag.	Score	Value	Mag.	Score	Value
Cost	0.2	USD	33.4	6.0	1.2	40.0	5.0	1.0
Size	0.4	In^2	0.8	9.6	3.9	1.0	7.8	3.1
Data variety	0.4	Number of data types	8	10.0	4.0	3	3.8	1.5
Overall value					**9.1**			**5.6**

IMU			Adafruit LSM6DSOX + LIS3MDL		
Objective	Weighting Factor	Parameter	Mag.	Score	Value
Cost	0.2	USD	20.0	10.0	2.0
Size	0.4	In^2	0.8	10.0	4.0
Data variety	0.4	Number of data types	3	3.8	1.5
Overall value					**7.5**

Table 27: Inertial Measurement Unit Decision Matrix Assessment

Cost refers to the price (USD) of the IMU. Since the performance related requirements (excepting # of data type) of the IMU are not very stringent for this specific payload, the cost was given a comparably high weight of 20%. The component with the lowest price received a score of 10 out of 10.

Size refers to the area of the sensor in square inches. Since the sensors are integrated to a PCB board, the thickness is not a concern. As a result, the board size is used evaluate the sensor. The size of the PCB board directly affects the size of overall PCB board of the payload. Therefore, size was given a weight of 40%. The component with the smallest size received a score of 10 out of 10.

Data variety refers to the number of different data types that the sensor can provide. The BNO055 barometer can give out absolute orientation, gravity vector, angular velocity, and 5 other different types of data directly. The more types of data the sensor can provide, the easier it is to use the sensor since less calculations need to be done to obtain those data. Therefore, data variety was given a weight of 40%. The IMU with the greatest number of data types received a score of 10 out of 10.

4.1.3.2.2.1.2 BMP390 Barometer

A decision matrix was used to select the specific barometer used in the payload electronics (Table 28).

Barometer			Adafruit BMP390			MPL3115A2 Barometer		
Objective	Weighting Factor	Parameter	Mag.	Score	Value	Mag.	Score	Value
Cost	0.2	dollars	10.95	10.00	2.00	15.49	6.00	1.20
Size	0.2	mm^2	468.00	7.31	0.73	342.00	10.00	2.00
Accuracy	0.4	meters	0.25	10.00	4.00	0.30	8.33	3.33
Extra Requirements	0.2	components	0.00	10.00	2.00	3.00	3.33	0.67
Overall value					**8.73**			**7.20**

Barometer			Adafruit BME280 I2C		
Objective	Weighting Factor	Parameter	Mag.	Score	Value
Cost	0.2	dollars	14.95	7.32	2.20
Size	0.2	mm^2	2086.56	1.64	0.16
Accuracy	0.4	meters	1.00	2.50	1.00
Extra Requirements	0.2	components	0.00	10.00	2.00
Overall value					**5.36**

Table 28: Barometer Decision Matrix Assessment

Cost refers to the price (USD) of the barometer. Since the performance related requirements (excepting accuracy) of the barometer are not very stringent for this specific payload, the cost was given a comparably high weight of 20%. The component with the lowest price received a score of 10 out of 10.

Size refers to the area of the barometer in square inches. Since the sensors are integrated to a PCB, the thickness is not a concern. As a result, the board size is used evaluate the sensor. The size of the PCB directly affects the size of the overall PCB of the payload. Therefore, it is given a weight of 20%. The component with the smallest size received a score of 10 out of 10.

Accuracy refers to the error at which the barometer can measure the altitude in meters. It is essential for the barometer to be able to accurately measure to function as a redundancy for the IMU. Therefore, it is given a weight of 40%. The barometer with the smallest error received a score of 10 out of 10.

Extra Requirements refers to the number of extra electrical components needed to wire the sensor up with the Raspberry Pi 4. Most sensors can just be directly wired with Raspberry Pi, but others may need external resistors and capacitors, which will increase the complexity of the design. Therefore, extra requirements was given a weight of 20%. The barometer that requires the lowest number of extra electrical components received a score of 10 out of 10.

4.1.3.2.3 Actuator Subsystem

The actuator subsystem consists of 6 motors in total, 3 solenoid and 3 stepper motors. Each camera will have 1 solenoid to lock and unlock the latch and 1 stepper motor to rotate around the z-axis after the arm spring up. All motors are controlled through the GPIO pins on the Raspberry Pi.

Solenoids are controlled by an N-channel MOSFET. A diode is used to prevent the high voltage pulse from damaging the MOSFET when the solenoid returns by the spring. A pulldown resistor is used at the gate of the MOSFET to make sure the solenoid is locked until a signal is sent out from Raspberry Pi.

Stepper motors are controlled by ULN2003 Stepper Motor controller. Each controller has 4 input pins that are connected to 4 GPIO pins on Raspberry Pi. The 4 output pins are connected directly to the stepper motor.

4.1.3.2.3.1 Component Selection Justification

4.1.3.2.3.1.1 Solenoid

A decision matrix was used to select the specific solenoid used in the payload (Table 29).

Solenoid			**Adafruit Small Push-Pull Solenoid**			**Adafruit Lockstyle Solenoid**		
Objective	Weighting Factor	Parameter	Mag.	Score	Value	Mag.	Score	Value
Body Length	0.3	inches	1.5	5.4	1.6	2.1	3.8	1.1
Mass	0.3	ounces	1.4	7.1	2.1	5.1	1.9	0.6
Stroke Length	0.2	inches	0.2	9.0	1.8	0.2	9.0	1.8
Cost	0.2	dollars	7.5	10.0	2.0	15.0	5.0	1.0
Overall value					**7.5**			**4.5**
Solenoid			**4.5mm Push-Pull Solenoid**					
Objective	Weighting Factor	Parameter	Mag.	Score	Value			
Body Length	0.3	inches	0.8	10.0	3.0			
Mass	0.3	ounces	1.0	10.0	3.0			
Stroke Length	0.2	inches	0.2	10.0	2.0			
Cost	0.2	dollars	10.0	7.5	1.5			
Overall value					**9.5**			

Table 29: Solenoid Decision Matrix Assessment

Body Length refers to the length of the solenoid body in inches. The length directly affects the length of the tub and thus affects the length of the payload bay. Therefore, body length was given a weight of 30%. The component with the shortest body length received a score of 10 out of 10.

Mass refers to the mass of the motor in ounces. Some solenoid motors can be very heavy, and they can significantly shift the center of gravity of the rocket. Therefore, mass was given a higher weight of 30%. The component with the lightest weight received a score of 10 out of 10.

Stroke Length refers to how far the solenoid can extend and retract measured in inches. This directly affect the contact area between the solenoid motor and the lock on the latch, which will affect the security of the lock.

Therefore, stroke length was given a weight of 20%. The component with the longest stroke length received a score of 10 out of 10.

Cost refers to the price (USD) of the solenoid motor. Since 3 solenoids need to be purchased, cost was given a higher weight of 20%. The component with the lowest price received a score of 10 out of 10.

4.1.3.2.3.1.2 Stepper Motor

A decision matrix was used to select the specific stepper motor used in the payload (Table 30).

Stepper Motor			28BYJ-48 Reduction Gear			NEMA-17 Motor		
Objective	Weighting Factor	Parameter	Mag.	Score	Value	Mag.	Score	Value
Volume	0.3	In^3	1.1	6.5	1.9	5.1	1.3	0.4
Cost	0.3	dollars	8.5	10.0	3.0	14.0	6.1	1.8
Mass	0.2	ounces	1.3	10.0	2.0	13.8	0.9	0.2
Torque	0.2	oz*in	1.0	0.1	0.0	84.0	10.0	2.0
Overall value					**7.0**			**4.4**

Stepper Motor			NEMA-8 Motor		
Objective	Weighting Factor	Parameter	Mag.	Score	Value
Volume	0.3	In^3	0.7	10.0	3.0
Cost	0.3	dollars	20.3	4.2	1.3
Mass	0.2	ounces	2.1	6.2	1.2
Torque	0.2	oz*in	2.3	0.3	0.1
Overall value					**5.5**

Table 30: Stepper Motor Decision Matrix Assessment

Volume refers to the space the stepper motor will take inside the tub measured in cubic inches. It directly affects the size of the tub, which affects the length of the payload airframe. Since it was important to minimize the amount of space the payload required, it was given a weight of 30%. The component with the smallest volume receives a score 10 out of 10.

Cost refers to the price (USD) of the selected component. Since 3 stepper motors need to be purchased, cost was given a higher weight of 20%. The component with the lowest price received a score of 10 out of 10.

Mass refers to the mass of the motor in ounces. Some stepper motor can be very heavy, and they can significantly shift the center of gravity of the rocket. Therefore, mass was given a weight of 30%. The component with the lightest weight received a score of 10 out of 10.

Torque refers to the amount of rotating force the motor can generate in oz*in. Since the load on top of the motor is not extremely high, it was given a smaller weight of 20%. The component with the smallest torque received a score of 10 out of 10.

4.1.3.2.4 Radio Subsystem

The radio subsystem is consisted of an SDR dongle that serves as a receiver of the APRS radio frequencies. The SDR dongle is connected to the Raspberry Pi through the USB2.0 port on the Raspberry Pi. The connection is not shown in the electrical schematics in Figure. The SDR dongle converts the radio waves into a digital signal and sends them to the Raspberry Pi through USB2.0 port. Upon receiving digital signal, the Raspberry Pi converts the signal back to a radio signal in *rtl_fm* and then hands them off to *Dire Wolf* to decode into text commands.

4.1.3.2.4.1 Component Selection Justification

Several different types of alternative radio systems are considered for the radio receiver. Integrated Internet of Things (IoT) receivers like Xbees are considered for the payload. They were the first choice because they can decode the radio directly to text command and then send them to the Raspberry Pi. This has the potential to greatly decrease the complexity of the software system and requirement of microprocessor. However, no such IoT radio receiver chips can be found that are compatible with the 144.90 MHz to 145.10 MHz frequency range. Therefore, this solution is not chosen for the payload.

The second alternative solution is buying an Integrated Chip (IC) radio receiver and then use them. This requires building an entire circuit around the IC chip and then writing custom drivers based on the datasheet provided by the manufacturer. The IC chip would convert the radio signal to digital signal and send them to Raspberry Pi. After receiving the digital signal, the Raspberry Pi would need to convert the digital signal back to radio signal and then decode them. Compared to the SDR radio solution, the software required is slightly more complex due to the use of custom drivers, but the hardware is significantly more complex. Therefore, the IC chip solution is not chosen.

4.1.3.3 Software Leading Payload Design

The software system will be divided into four subsystems: sensor, motor (solenoid and stepper), radio, and camera (Figure 60). The sensor system will run from the beginning, monitoring input from the IMU and barometer. It will detect launch, apogee, and landing. Once there is constant acceleration (due to gravity) from the IMU, it will detect the landing and begin to activate other subsystems. Based on the launch vehicle orientation, determined from the IMU data, the sensor system will choose which motor and camera is upright and will be activated. The solenoid motor subsystem will activate to release the upright camera, then turn off. The radio system will then be activated. This subsystem will turn on the radio receiver using the program *rtl_fm* and tune it to the range of 144.90 MHz to 145.10 MHz. The program's output gets sent to another program, *Dire Wolf*, that decodes radio signals and outputs the decoded APRS message in a log file. The radio subsystem will parse this log file for the relevant commands and stop listening for more. Once the program has commands, the stepper motor system and camera subsystem will be turned on. The stepper motor will rotate the camera as needed while the camera system, which uses the library OpenCV, takes images and applies filters according to instructions. Once there are no more commands to complete, these systems will turn off.

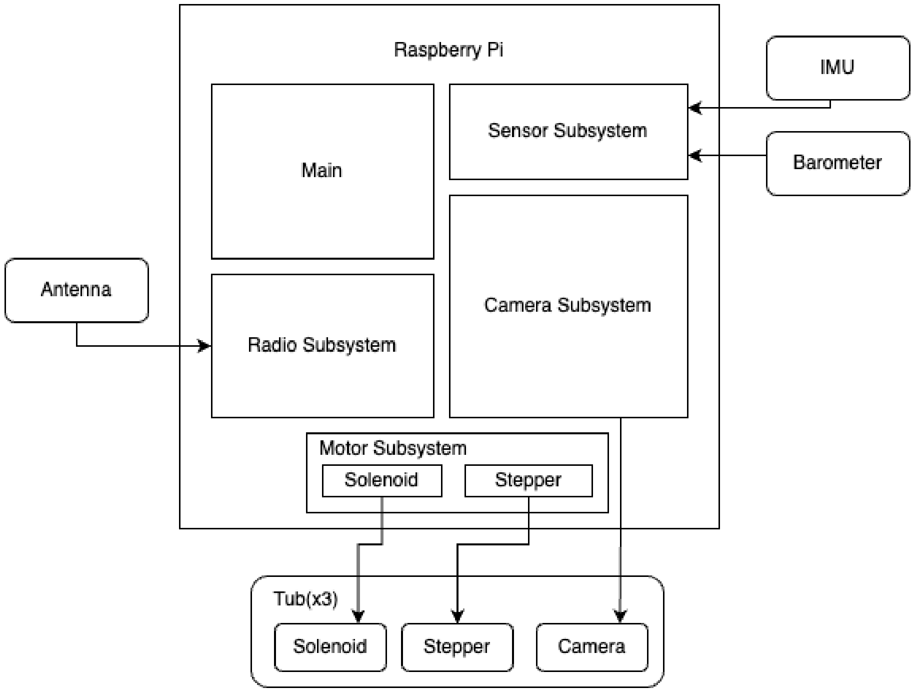

Figure 60: Overview of software subsystems with inputs and outputs

4.1.3.3.1 Payload Sensor System

The payload sensor system runs continuously in the background the entire flight, receiving data from the IMU and barometer (Figure 61). It remains the only system online until it detects a landing, when the barometer reads constant pressure and the IMU indicates constant acceleration due to gravity. Once this occurs, the sensor system will determine which camera housing is facing upward based on the orientation of the IMU provided by the three-dimensional gravity vector. Once this is determined, the sensor system will call for the activation of the solenoid motor to release the upright camera. It will then activate the radio system to begin receiving transmissions, as well as the respective stepper motor and camera systems. Once all these steps have been completed, the sensors will be deactivated.

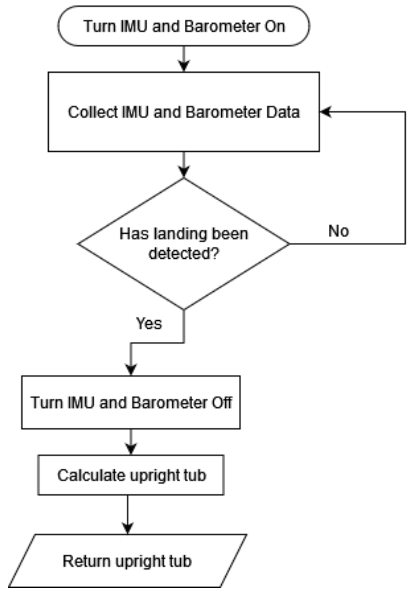

Figure 61: Sensor Software Subsystem Process Sequence

4.1.3.3.2 Payload Motor System

The motor system is composed of a solenoid section and stepper motor section (Figure 62). The solenoid system is only activated once when the sensor system detects a landing. The sensor system will decide which camera-motor system is upright and trigger the solenoid to unlatch for the upright one. Once this is completed, the solenoid is no longer needed. The second section, the stepper motor, will remain active for as long as the radio and camera systems are active. Depending on the command received via radio, the stepper motor will rotate the camera to the left or right a specified number of degrees. For example, the APRS transmission A1 will cause the stepper motor to rotate the camera 60 degrees to the right. Naturally, the only stepper motor activated will be the upright one.

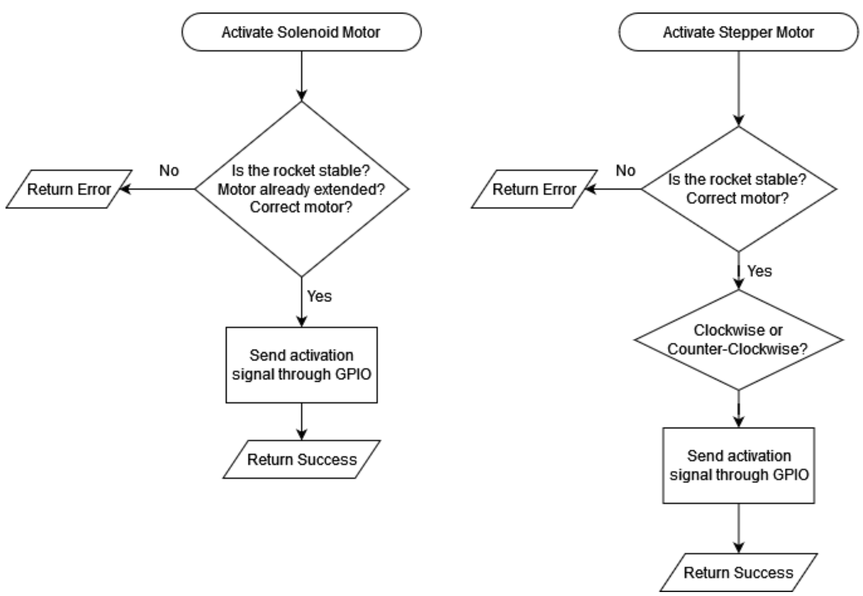

Figure 62: Motor Software Subsystem Process Sequence

4.1.3.3.3 Payload Camera System

The OpenCV library provides pre-built camera capturing and photo manipulation functions that will make image processing much smoother (Figure 63). The system will wait for commands issued by the radio subsystem and will keep track of which filters should be applied to any new images captured. An example of some of the filters that will be applied by OpenCV is the grayscale (radio command D4) and image flipping 180° (radio command F6). It also allows for the appending of the timestamp to a section of the photo which is required for all photos taken. Once all photos are captured, filters applied, and timestamp added, the resulting files will be saved to the Raspberry Pi for inclusion in the Post Launch Assessment.

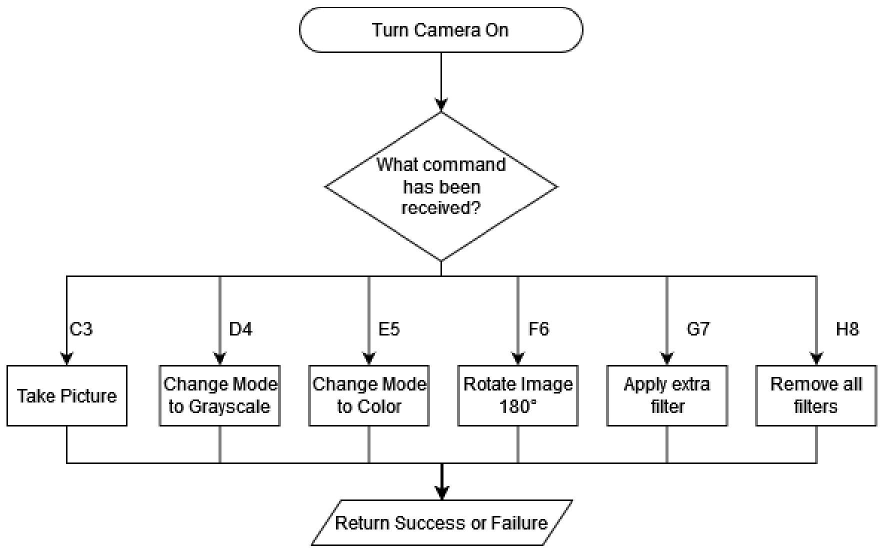

Figure 63: Camera Software Subsystem Process Sequence

4.1.3.3.4 Payload Radio System

The radio system will run until the message sent by NASA RAFCO have been received and interpreted. NASA will send out the message every two minutes, so this subsystem is expected to only be enabled for, at the longest, a little over two minutes (Figure 64). However, it will keep running if the software fails to properly analyze and decode the messages. The program *rtl_fm* allows for the capture of radio signals but does not perform any processing or decoding. Therefore, the program *Dire Wolf* will also be utilized to decode the APRS signals and output the message to a log file. The log will contain plenty of text irrelevant for the rest of the payload system, so there will a custom parser to find the desired payload commands.

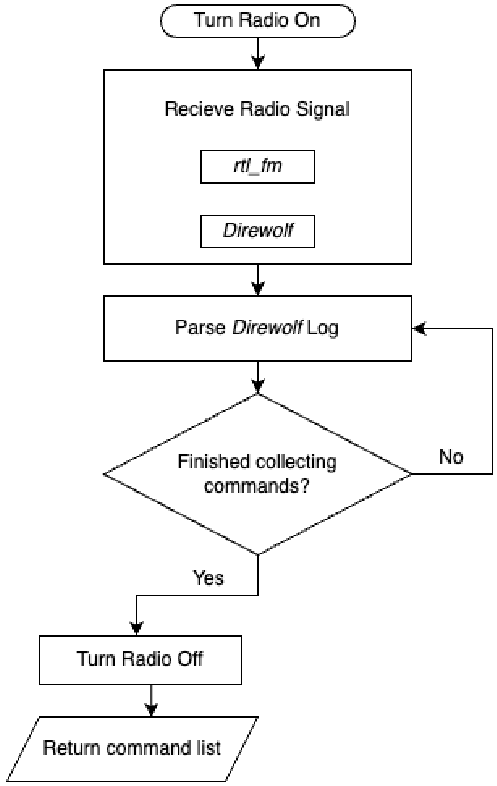

Figure 64: Radio Software System Process Sequence

5. Safety

Given the nature of this competition, safety will be highly prioritized for this project. This section details the protocols established to maximize cognizance of potential hazards and to mitigate all feasible risks.

To accomplish these goals, a safety plan has been developed that encompasses all aspects of project activities: design, manufacturing, assembly, testing, and launch attempts for the duration of the competition. The entire team has been briefed on the current safety plan through meetings hosted by the leads. Any updates to the safety plan will be communicated via the team Slack channel. However, significant updates to the plan will be communicated through meetings hosted by the Safety Officer or leads.

5.1 Safety Team Responsibilities

The Safety Team is led by the Safety Officer, Luka Bjellos. It also comprises of Safety Stewards certified by the University of Florida Mechanical and Aerospace Engineering (MAE) department.

5.1.1 Safety Officer Responsibilities

The safety team is led by the Safety Officer and will also comprise of Safety Stewards certified by the University of Florida Mechanical and Aerospace Engineering (MAE) department.

1. The Safety Officer will monitor team activities to emphasize safe practices and hazard mitigation.
    a. Safety-related feedback on launch vehicle and payload design choices
    b. Supervision of manufacturing activities
        i. Impose adherence to machine and tool standard operating procedures as defined by the respective user manuals
    c. Supervision of launch vehicle and payload assembly

            i. Implement proper launch-day assembly procedure, which will be determined by the safety officer and the respective leads
    d. Supervision of ground testing
        i. NAR/TRA mentor shall also supervise ground tests
    e. Supervision of subscale launch testing
        i. Adhere to launch preparation procedure
            1. Confirm all checks are carried out and redundancies are in place
    f. Supervision of full-scale launch testing
        i. Adhere to launch preparation procedure
        ii. Confirm all checks are carried out and redundancies are in place
        iii. NAR/TRA mentor shall also supervise launch day procedure
    g. Supervision of team activities on Launch Day
        i. Hazard recognition around team launch vehicle and vehicles of others
        ii. Compliance with NAR/TRA policies
        iii. NAR/TRA mentor shall also supervise launch day procedure
    h. Supervision of recovery activities after launch attempt
        i. Close observation of launch vehicle descent and landing
        ii. Implement caution around launch vehicle debris
    i. Verification of hazard mitigation strategies in place for STEM engagement
        i. Supervise if active hazard mitigation is required
2. The Safety Officers shall verify the team has developed procedures for actively mitigating potential hazards. The Officers shall also enforce the implementation of the procedures.
3. The Safety Officers shall manage and maintain current revisions of the team's safety documentation.
    a. Personnel Hazard Analysis
    b. Failure Modes and Effects Analysis
    c. Environmental Concerns
    d. Project Risks
4. The Safety Officers shall assist in the writing and development of the team's new safety documentation.
    a. Revisions or updates to hazard analyses
    b. Failure mode analyses for the updated payload and launch vehicle designs
    c. Launch procedures for the updated payload and launch vehicle designs

5.1.2 Safety Steward Responsibilities

Safety Stewards will assist the Safety Officer with the supervision of team members during work in the Student Design Center. This will ensure hazard mitigation strategies are being followed. A certified and experienced Safety Steward is qualified to supervise a team manufacturing process without the presence of the Safety Officer, but at least two of the Safety Stewards/Officer will always perform supervision together. New Safety Stewards with less experience supervising relevant processes will be aided by the Safety Officer. Additionally, the Safety Stewards will have multiple methods of quick communication with the Safety Officer, such as phone or Slack direct message. The official responsibilities of the Safety Stewards have been provided by the MAE Facilities Operations Specialist, Daniel Preston.

1. Safety Stewards shall enforce all protocols outlined in the SDC's Rules for Facility Use document. This includes policies for personal safety; equipment uses; facility cleanliness, organization, and respect; proper language; use of the Material & Tool List and Broken / Lost Tooling List; and all other miscellaneous policies.
2. Safety Stewards must have a strong understanding of each machine at the SDC.

3. Safety Stewards shall train students on machines, administer knowledge quizzes, and sign authorization sheets to allow future supervised equipment use.
4. Safety Stewards shall verify students are trained and authorized on each machine they use.
5. Safety Stewards shall set up each approved equipment each time a user works on a new part.
6. Safety Stewards shall keep watch of powered machinery as it is being used.
7. Safety Stewards shall manage access to common-use tools via the Material & Tool Use List.
8. Safety Stewards shall ensure students clean machines after each use and accept responsibility for stations not up to SDC cleaning standards.
9. Safety Stewards shall ensure students keep the team's bay neat and clean.

5.1.3 NAR/TRA Safety Procedures

5.1.3.1 NAR Safety Procedures

The following measures will be taken as a team to ensure compliance with requirements from the NAR High Power Rocket Safety Code (effective August 2012). The safety measures are specified by NAR as follows:

1. **Certification.** I will only fly high power rockets or possess high power rocket motors that are within the scope of my user certification and required licensing.
2. **Materials.** I will use only lightweight materials such as paper, wood, rubber, plastic, fiberglass, or when necessary ductile metal, for the construction of my rocket.
3. **Motors**. I will use only certified, commercially made rocket motors, and will not tamper with these motors or use them for any purposes except those recommended by the manufacturer. I will not allow smoking, open flames, nor heat sources within 25 feet of these motors.
4. **Ignition System.** I will launch my rockets with an electrical launch system, and with electrical motor igniters that are installed in the motor only after my rocket is at the launch pad or in a designated prepping area. My launch system will have a safety interlock that is in series with the launch switch that is not installed until my rocket is ready for launch and will use a launch switch that returns to the "off" position when released. The function of onboard energetics and firing circuits will be inhibited except when my rocket is in the launching position.
5. **Misfires.** If my rocket does not launch when I press the button of my electrical launch system, I will remove the launcher's safety interlock or disconnect its battery and will wait 60 seconds after the last launch attempt before allowing anyone to approach the rocket.
6. **Launch Safety.** I will use a 5-second countdown before launch. I will ensure that a means is available to warn participants and spectators in the event of a problem. I will ensure that no person is closer to the launch pad than allowed by the accompanying Minimum Distance Table. When arming onboard energetics and firing circuits I will ensure that no person is at the pad except safety personnel and those required for arming and disarming operations. I will check the stability of my rocket before flight and will not fly it if it cannot be determined to be stable. When conducting a simultaneous launch of more than one high power rocket I will observe the additional requirements of NFPA 1127.
7. **Launcher.** I will launch my rocket from a stable device that provides rigid guidance until the rocket has attained a speed that ensures a stable flight, and that is pointed to within 20 degrees of vertical. If the wind speed exceeds 5 miles per hour, I will use a launcher length that permits the rocket to attain a safe velocity before separation from the launcher. I will use a blast deflector to prevent the motor's exhaust from hitting the ground. I will ensure that dry grass is cleared around each launch pad in accordance with the accompanying Minimum Distance table and will increase this distance by a factor of 1.5 and clear that area of all combustible material if the rocket motor being launched uses titanium sponge in the propellant.

8. **Size.** My rocket will not contain any combination of motors that total more than 40,960 N-sec (9208 pound-seconds) of total impulse. My rocket will not weigh more at liftoff than one-third of the certified average thrust of the high-power rocket motor(s) intended to be ignited at launch.
9. **Flight Safety.** I will not launch my rocket at targets, into clouds, near airplanes, nor on trajectories that take it directly over the heads of spectators or beyond the boundaries of the launch site and will not put any flammable or explosive payload in my rocket. I will not launch my rockets if wind speeds exceed 20 miles per hour. I will comply with Federal Aviation Administration airspace regulations when flying and will ensure that my rocket will not exceed any applicable altitude limit in effect at that launch site.
10. **Launch Site.** I will launch my rocket outdoors, in an open area where trees, power lines, occupied buildings, and persons not involved in the launch do not present a hazard, and that is at least as large on its smallest dimension as one-half of the maximum altitude to which rockets are allowed to be flown at that site or 1500 feet, whichever is greater, or 1000 feet for rockets with a combined total impulse of less than 160 N-sec, a total liftoff weight of less than 1500 grams, and a maximum expected altitude of less than 610 meters (2000 feet).
11. **Launcher Location.** My launcher will be 1500 feet from any occupied building or from any public highway on which traffic flow exceeds 10 vehicles per hour, not including traffic flow related to the launch. It will also be no closer than the **appropriate Minimum Personnel Distance from the accompanying table from any boundary of the launch site.**
12. **Recovery System**. I will use a recovery system such as a parachute in my rocket so that all parts of my rocket return safely and undamaged and can be flown again, and I will use only flame-resistant or fireproof recovery system wadding in my rocket.
13. **Recovery Safety.** I will not attempt to recover my rocket from power lines, tall trees, or other dangerous places, fly it under conditions where it is likely to recover in spectator areas or outside the launch site, nor attempt to catch it as it approaches the ground.

MINIMUM DISTANCE TABLE

Installed Total Impulse (Newton-Seconds)	Equivalent High Power Motor Type	Minimum Diameter of Cleared Area (ft.)	Minimum Personnel Distance (ft.)	Minimum Personnel Distance (Complex Rocket) (ft.)
0 — 320.00	H or smaller	50	100	200
320.01 — 640.00	I	50	100	200
640.01 — 1,280.00	J	50	100	200
1,280.01 — 2,560.00	K	75	200	300
2,560.01 — 5,120.00	L	100	300	500
5,120.01 — 10,240.00	M	125	500	1000
10,240.01 — 20,480.00	N	125	1000	1500
20,480.01 — 40,960.00	O	125	1500	2000

Figure 65: NAR Minimum Personnel Distance Based on Motor Type (taken from NAR website)

5.1.3.2 TRA Safety Procedures

The following measures will be taken as a team to ensure compliance with requirements from the TRA High Power Rocket Safety Code (effective May 1, 2022). The safety measures are specified by TRA as follows:

1. Although Tripoli Launches involve several layers of safety rules which are intended to increase safety, FLIERS ARE ULTIMATELY RESPONSIBLE FOR THEIR ROCKET AND FLIGHT, including but not limited to the following:
    a. Construction; rockets shall be built using lightweight materials and construction techniques that are suitable for the planned flight.
    b. Stability; the flier shall document the location of the center of pressure and be able to demonstrate the center of gravity.
    c. Every rocket shall include a recovery system sufficient to allow the rocket to land at a safe velocity.
    d. The thrust-to-weight ratio of a rocket typically should be at least 5:1. However, the RSO may approve a thrust-to-weight as low as 3:1 ratio. Initial thrust-to-weight ratios lower than 3:1 may only be authorized by an RSO if an active stability system is included.
    e. Range Personnel designated by the RSO shall inspect all rockets flown at Tripoli Launches. Only rockets approved for flight as a result of this inspection process shall be allowed to fly. The inspection shall minimally consist of verification of the following:
        i. Adequate construction methods
        ii. Positive stability or acceptable glider trim.
        iii. Appropriate recovery system.
        iv. Sufficient Thrust to Weight ratio
2. While installing an igniter, and at all times afterward, the rocket must remain pointed in a safe direction (away from all people.)
3. Rockets must launch from a stable platform which guides the rocket in a safe direction until it has reached the velocity necessary for stable flight.
4. Rockets shall not be intentionally launched over the flight line.
5. When needed, blast deflectors must be used to prevent damage or reduce the risk of fire.
6. Blast deflectors shall be oriented such that any ejected motor parts shall not endanger people.
7. Launch Control Systems used at *Tripoli Launches* shall:
    a. Include an arming switch with a removable key or interlock, which disables the entire launch control system when removed.
    b. Use a momentary switch to command the rocket motor ignition.
    c. Only be used with rockets which they can safely and quickly ignite.
8. The motor igniter shall not be connected to the launch system until all other flight electronics are active.
9. Rockets flown at Tripoli Launches may not carry any of the following:
    a. Vertebrate animals
    b. Hazardous Payloads including those which are poisonous, flammable, incendiary, or explosive.
10. Range activity shall cease whenever a thunderstorm has been detected within ten miles of the launch site.
11. *Spectators* shall follow all directives by launch personnel. Failure to comply will result in being required to leave.

Safe Distance Table

Motor Designation	Total Installed Impulse **Newton-seconds**		Single Motor		Complex	
			feet	**meters**	**feet**	**meters**
A-G	0.01	80	50	15	50	15
A-G Class 1 HP*	0.01	80	100	30	200	60
H-J	80.01	1,280	100	30	200	60
K	1,280.01	2,560	200	60	300	90
L	2,560.01	5,120	300	90	500	150
M	5,120.01	10,240	500	150	1,000	300
N	10,240.01	20,480	1,000	300	1,500	460
O	20,480.01	40,960	1,500	460	2,000	610
P-T	40,960.01	890,000	2,000	610	2,500	760

*Class 1 High Power are motors which fall into the Class 1 impulse range, but are regulated as High Power motors because they have greater than 80 Newtons average thrust, contain metal particles to make them sparkies, or contain more than 125 grams of propellant.

Figure 66: TRA Minimum Personnel Distance Based on Motor Type (taken from TRA website)

5.2 Personnel Hazards Analysis

The personnel hazards analysis evaluates the level of risk to safety of team members and equipment and risk mitigation strategies. Each hazard will be assigned a risk score ranging from 1 to 100, with 1 representing the lowest possible severity and likelihood, and 100 representing the highest possible severity and likelihood. The risk score is calculated by multiplying the severity value 'S' of each risk (1-10) by its likelihood value 'L' (1-10) (Table 31) (Table 32).

	Severity (S)	Likelihood (L)
1, 2	Little to no equipment damage/very minor or no injury	1-20% occurrence, very unlikely
3, 4	Minor equipment damage/minor injury	21-40% occurrence, unlikely
5, 6	Moderate equipment damage/mild injury	41-60% occurrence, uncertain likelihood
7, 8	Major equipment damage/mild to major injury	61-80% occurrence, likely
9, 10	Irreparable equipment damage/major injury or death of personnel	81-100% occurrence, very likely

Table 31: Risk Assessment Chart (RAC)

		Likelihood									
		1	2	3	4	5	6	7	8	9	10
	1	1	2	3	4	5	6	7	8	9	10
	2	2	4	6	8	10	12	14	16	18	20
	3	3	6	9	12	15	18	21	24	27	30
	4	4	8	12	16	20	24	28	32	36	40
Severity	5	5	10	15	20	25	30	35	40	45	50
	6	6	12	18	24	30	36	42	48	54	60
	7	7	14	21	28	35	42	49	56	63	70
	8	8	16	24	32	40	48	56	64	72	80
	9	9	18	27	36	45	54	63	72	81	90
	10	10	20	30	40	50	60	70	80	90	100

Table 32: Risk Assessment Score Chart

5.2.1 Chemical Hazards

Chemical hazards are those posed by the team’s chemical inventory. Potential occurrences for chemical hazards and their respective effects, risk score, and mitigation strategy were evaluated (Table 33).

Hazard	Cause	Effect	S	L	Score	Mitigation Strategy
All-purpose cement contact	Exposure to fumes	Dizziness	5	1	5	Use of PPE per MSDS in well-ventilated areas
All-purpose cement ignites	Liquid form exposed to heat source	Burns, inhalation of smoke	8	2	16	Keep in well-ventilated, cool storage. Keep away from heat sources/oxidizers
Cleaning agent contact	Use of cleaning agents	Irritation, possible blindness if sprayed in eyes	4	4	16	Use of PPE per MSDS
Epoxy contacts skin	Exposure of skin to epoxy	Skin irritation	5	6	30	Use of PPE per MSDS when handling epoxy
Gelcoat compound ignites	Liquid form exposed to heat source	Burns ranging from 1st to 3rd degree, smoke inhalation	9	2	18	Keep in well-ventilated, cool storage. Keep away from heat sources/oxidizers
Gelcoat fume inhalation	Prolonged toxic fume exposure	Dizziness	4	1	4	Use of PPE per MSDS in well-ventilated areas
Paint thinner contact	Spills, accidental touch with bare skin	Irritation, possible blindness if sprayed in eyes	7	1	7	Use of PPE per MSDS. Keep lid closed when not in use
Paint thinner ignites	Liquid form exposed to heat source	Burns ranging from 1st to 3rd degree, smoke inhalation	9	2	18	Keep in well-ventilated, cool storage. Keep away from heat sources/oxidizers
Spray paint can explodes	Compressed gas in paint can exposed to heat	Hearing damage and lacerations or organ damage from debris	9	1	9	Use of PPE per MSDS, keep spray paint can away from heat sources
Spray paint contact with skin	Paint sprayed onto skin	Skin Irritation	2	5	10	Use of PPE per MSDS, spray down and away from persons in area
Spray paint contact with eyes	Paint sprayed onto eyes	Eye irritation, possible blindness	3	5	15	Use of PPE per MSDS, spray down and away from persons in area
Spray paint ignites	Paint in air exposed to heat source	Burns ranging from 1st to 3rd degree, smoke inhalation	9	4	36	Use of PPE per MSDS, keep spray paint aerosols away from heat sources
Spray paint inhalation	Paint aerosols are inhaled	Dizziness, respiratory inhalation	5	4	20	Use of PPE per MSDS, use spray paint in ventilated areas

Table 33: Chemical Hazard Identification

5.2.2 Physical Hazards

Physical hazards are those posed by manufacturing processes, launch preparation, and launching (Table 34) (Table 35) (Table 36).

5.2.2.1 Manufacturing Hazards

Hazard	Cause	Effect	S	L	Score	Mitigation Strategy
Bandsaw blade contact	Hand close to blade when cutting materials	Skin laceration	8	2	16	Keep hands out of blade path when cutting materials, use respective operators' manual
Live drill contact	Hand under or too close to drill bit	Skin laceration	9	1	9	Keep hands away from cutting tools when machine is powered, use respective operators' manual
Sharp tool contact	Contact between tool and bare hands	Skin laceration	6	2	12	Use a rag as a buffer when handling sharp tools
Vise Pinches	Hand or fingers placed inside the vice while vise is being tightened	Pinching or minor skin laceration	5	2	10	Keep hands away from machine when in use, keep observers away from machine when tightening vises
Hammer Injury	Hand or finger under hammer	Pinching or contusion, possible skin laceration	5	2	10	Ensure that body parts are away from workpiece before swinging hammer, avoid swinging with excessive force
Waterjet stream contact	Hand or finger in waterjet stream	Skin laceration, potential bone and nerve damage	9	1	9	Check waterjet for leaks, use of PPE per MSDS, stand far from machine, use respective operators' manual
Waterjet boom injury	Standing too close to boom during operation	Minor blunt trauma to the head, potential concussion	6	1	6	Stand far from machine when in use, use respective operators' manual
Machining noise exposure	Proximity to loud machines	Hearing damage	5	1	5	Use of PPE and either noise cancelling headphones, earmuffs, or earplugs
Metal chips contact	Touching metal chips with bare hands	Skin laceration	5	1	5	Wear long pants and close toed shoes, use compressed air or rag to remove excess chips. Use

						gloves only when working with sheet metal
Fiberglass debris contact	Hands touch fiberglass dust	Skin irritation or skin laceration	**4**	**1**	**4**	Wear gloves, long sleeves, and pants when handling fiberglass
Fiberglass inhalation	Exposure to fiberglass dust in air	Respiratory irritation, cancer	**9**	**1**	**9**	Wear particulate respirators when machining and cutting fiberglass
Soldering injury	Exposure to hot solder	Skin burns, primarily 1st degree	**4**	**1**	**4**	Wear gloves and PPE, keep away while observing
Battery acid contact	Broken or punctured battery casing	Skin irritation	**2**	**1**	**2**	Handle and store batteries carefully, keep away from sharp objects

Table 34: Manufacturing Hazard Identification

5.2.2.2 Launch Preparation Hazards

Hazard	Cause	Effect	S	L	Score	Mitigation Strategy
Premature motor ignition	Ignition during motor loading	Premature launch of vehicle, severe blunt trauma, or impaling	**9**	**1**	**9**	Keep away from heat sources, smoke, and sources of static electricity. Store in cool, dry environment
Black powder ignition	Exposure to heat source/static electricity	Blunt trauma or lacerations from flying debris	**8**	**1**	**8**	Keep away from heat sources, smoke, and sources of static electricity. Store in cool, dry environment
Premature altimeter activation	Sudden pressure differential or faulty assembly	Premature ignition of ejection charges, causing blunt trauma or flying debris	**7**	**1**	**7**	Ensure proper avionics bay assembly, avoid activating altimeters with sudden pressure changes, ensure proper key switch activation
Live wiring contact	Improper payload and avionics bay assembly	Skin burns, primarily 1st degree	**5**	**2**	**10**	Wear safety glasses and PPE when soldering, avoid bare skin contact with any live systems

Table 35: Launch Preparation Hazard Identification

5.2.2.3 Launching Hazards

Hazard	Cause	Effect	S	L	Score	Mitigation Strategy
Ballistic launch vehicle	Improper assembly/risky design choices	Severe impact injury	**9**	**1**	**9**	Maintain proper stand-off distance
	Launch vehicle fails to separate	Severe impact injury	**9**	**1**	**9**	Use redundant altimeters and ejection charges, ground test ejection charges before launching, maintain proper stand-off distance

Falling debris	Premature or faulty ejection charges, lack of parachute deployment or function	Impact injury or skin laceration	6	1	6	Use redundant altimeters and ejection charges, ground test ejection charges before launching, maintain proper stand-off distance
	Recovery harness failure	Impact injury or skin laceration	6	1	6	Select a recovery harness that is sufficiently strong to withstand separation forces, inspect recovery harness for tears or fraying before use
	Eyebolt failure and subsequent detachment during ejection	Impact injury or skin laceration	6	1	6	Ensure eyebolts are properly fastened to PVC bulkheads with properly torqued steel nuts, and that sufficient epoxy is properly set on a sanded, clean surface
Launch site fire	Premature motor ignition	Burns, 1st and 2nd degree (3rd degree for prolonged exposure), smoke inhalation	6	1	5	
	Premature ejection charges	Burns, 1st and 2nd degree (3rd degree for prolonged exposure), smoke inhalation	6	1	5	

Table 36: Launch Operations Hazard Identification

5.2.3 Biological Hazards

Biological hazards are threats posed by bacteria or other living organisms (Table 37).

Hazard	Cause	Effect	S	L	Score	Mitigation
Spread of COVID-19 and other illnesses	Not sanitizing hands frequently, refusal to stay home/follow CDC guidelines	Member gets COVID-19 or other illness	5	3	15	Provide accessible sources of sanitation, tell sick members to stay at home, and keep members updated on current CDC guidelines
Sun damage	Prolonged sun exposure	Skin irritation, sun burns	2	4	8	Provide sunscreen; wear long sleeves, long pants, hats, and sunglasses

Table 37: Biological Hazard Identification

5.3 Failure Mode and Effects Analysis

Failure mode and effects analysis (FMEA) is the process of reviewing as many components, assemblies, and subsystems as possible to identify potential failure modes in a system and their causes and effects. By identifying failure modes, corrective actions can also be applied to mitigate risk. FMEAs have been created for the following categories: Structures (Table 40)Payload (Table 41)(Table 42)(Table 43), Avionics and Recovery (Table 44) and Flight Dynamics (Table 45Table 45). Three ratings are given to each failure mode to quantify the significance of the failure: severity, likelihood, and detection. Severity (S) is rated from 1 to 10 where a rating of 1 means that the failure has no effect while a rating of 10 is a catastrophic failure. Likelihood (L) is rated from 1 to 10 where a rating of 1 means that the failure has little to no chance of occurring while a 10 indicated it is incredibly likely to occur. Detection (D) is rated from 1 to 10 where a 1 is a failure that has a high likelihood of detection while a 10 is a failure that has an extremely low likelihood of detection. A risk priority number (RPN, 1-1000) is calculated as the product of the ratings and will be used to inform the team where mitigation strategies are needed, and which risks should be mitigated first. Severity, Likelihood, Detection, and RPN will be visualized using the following charts (Table 38)(Table 39).

	Severity (S)	**Likelihood (L)**	**Detection (D)**
1, 2	Little to no effect on flight/little to no equipment damage	1-20% occurrence, very unlikely	81-100% detection chance, very likely detection
3, 4	Slight effect on flight/minor equipment damage	21-40% occurrence, unlikely	61-80% detection chance, likely detection
5, 6	Moderate effect on flight/moderate equipment damage	41-60% occurrence, uncertain likelihood	41-60% detection chance, uncertain detection
7, 8	Major effect on flight/major equipment damage	61-80% occurrence, likely	21-40% detection chance, unlikely detection
9, 10	Complete vehicle loss/irreparable equipment damage	81-100% occurrence, very likely	1-20% detection chance, very unlikely detection

Table 38: Risk Priority Number Chart

RPN Score

1-100	101-200	201-300	301-400	401-500	501-600	601-700	701-800	801-900	901+

Table 39: RPN Score Chart

5.3.1 Structures

Component	**Function**	**Failure Mode**	**Failure Cause**	**Failure Effects**			**S[1]**	**L[2]**	**D[3]**	**RPN[4]**	**Corrective Actions**
				Local Effects	**Next Higher Level**	**System Effects**					
Bulkhead	Protect the bays from heat of ejection charges and keeps them separate from the rest of the launch vehicle.	Breaks	Manufacturing defects such as not complying to drawings which determine the size of the bulkheads.	Fails to sufficiently seal components such as electronics, parachutes, or camera housings.	Ejection charges fail to separate vehicle	Parachutes are not deployed and/or internal components are damaged	**9**	**2**	**2**	**36**	Inspect launch vehicle before and after each launch.
Bulkhead	Protect the bays from heat of ejection charges and keeps them separate from the	Epoxy fails	Improper application	Fails to sufficiently seal components such as	Ejection charges fail to separate vehicle	Parachutes are not deployed and/or internal components are damaged	**9**	**2**	**2**	**36**	Follow proper procedures for applying epoxy.

	rest of the launch vehicle.			electronics, parachutes, or camera housings.							
Fins	Provide launch vehicle stability.	Epoxy fails	Improper application	Launch vehicle loses stability and flight orientation	Uncontrollable flight	Launch vehicle drifts, becomes uncontrollable, and creates a hazard	**8**	**2**	**5**	**80**	Follow proper procedures for applying epoxy.
Centering Rings	Supports and aligns motor tube.	Breaks	Manufacturing defect	Launch vehicle loses stability and flight orientation	Uncontrollable flight	Launch vehicle drifts, becomes uncontrollable, and creates a hazard	**10**	**2**	**5**	**100**	Inspect immediately after manufacturing and inspect launch vehicle before and after each launch.
Centering Rings	Supports and aligns motor tube.	Epoxy fails	Improper application	Launch vehicle loses stability and flight orientation	Uncontrollable flight	Launch vehicle drifts, becomes uncontrollable, and creates a hazard	**10**	**2**	**6**	**120**	Follow proper procedures for applying epoxy.
Airframe	Hold electronic components, hardware, recovery equipment, and payload.	Breaks	Manufacturing defect and/or poor transportation	Fails to contain internal components	Launch vehicle assembly fails	Launch vehicle is unrecoverable and a hazard to those nearby due to falling debris	**10**	**3**	**2**	**60**	Members must follow the procedure of transporting components and inspect the launch vehicle before and after launch.
Coupler	Contains vehicle avionics bay and payload electronics.	Breaks	Manufacturing defect and/or improper transportation	Fails to contain internal components	Launch vehicle assembly fails	Launch vehicle is unrecoverable	**10**	**3**	**2**	**60**	Inspected component for defects after manufacturing and before and after launch.
Shear Pins	Allows launch vehicle to remain connected until separation events.	Shears too early	Excessive pressure and force from previous events during launch.	Airframe and couplers separate	Early separation and premature parachute deployment	Reduced altitude	**7**	**3**	**9**	**189**	Test ejection charges and ensure pins are housed correction so does not shear prematurely.
Shear Pins	Allows launch vehicle to remain connected until separation events.	Do not break	Insufficient strength of ejection charge during separation	Parachutes do not deploy	Rapid descent of launch vehicle with a large impact force	Launch vehicle is unrecoverable	**10**	**2**	**8**	**160**	Test ejection charges to find enough force necessary to shear the pins.
Motor	Produces thrust for flight of launch vehicle	Breaks	Improper Installment	Payload with sustain severe damage and mission will fail	Launch vehicle assembly fails	Launch vehicle is unrecoverable and pose a hazard to those nearby	**10**	**3**	**3**	**90**	Motors will be inspected before installment and installed by someone trained.

Table 40: Structures FMEA

5.3.2 Payloads

5.3.2.1 Payload Mechanical

Component	**Function**	**Failure Mode**	**Failure Cause**	**Failure Effects**			**S[1]**	**L[2]**	**D[3]**	**RPN[4]**	**Corrective Actions**
				Local Effects	**Next Higher Level**	**System Effects**					

Camera mount and hook	Acts as airframe and holds camera and hinge system	Cracking and breaking	Forces upon landing impact	Camera housing is not stable	Camera housing breaks off	The payload is unable to view the surrounding areas.	**8**	**2**	**1**	**16**	Impact testing, high infill in 3D print
Spring-loaded Hinge	Allows camera to deploy out of the airframe.	Hinge breaks off from the mount	Hinge applies excessive torque for the rigid motor mount body	Hinge breaks	Camera housing breaks off	The payload is unable to view the surrounding areas.	**7**	**2**	**2**	**28**	Torque calculations, prototype testing
Solenoid Motor	Latches on to the camera mount hook and holds spring-loaded hinge system down to be flush with airframe	Torque failure	Not enough or too much torque for the stresses from the load from the hinge.	Motor fails	Payload does not rise out of the airframe	Payload Challenge fails	**7**	**3**	**1**	**21**	Motor torque calculations, prototype testing
Stepper Motor	Rotates camera system	Torque failure	Not enough or too much torque for the stresses from the camera mount load.	Motor fails	Cameras do not rotate	Payload Challenge fails	**7**	**3**	**1**	**21**	Motor torque calculations, prototype testing

Table 41: Payload Mechanics FMEA

5.3.2.2 Payload Electronics

Component	**Function**	**Failure Mode**	**Failure Cause**	**Failure Effects**			**S[1]**	**L[2]**	**D[3]**	**RPN[4]**	**Corrective Actions**
				Local Effects	**Next Higher Level**	**System Effects**					
Actuator Battery	Provide power to electrical components of payload	Short circuit	Unintended contact between positive and ground terminal	Battery experience thermal runaway and fails	Payload failure due to the loss of power	Fire and loss of launch vehicle	**9**	**2**	**4**	**72**	Use PCB to reduce the number of jumper wires used, make sure no metal is exposed and all wires are securely connected
Stepper Motor	Rotate the camera about the z-axis	Motor failure	Incorrect wiring	Motor is unresponsive to the Raspberry Pi	Camera cannot rotate around z-axis	Payload failure	**5**	**3**	**2**	**30**	Use connectors on the field to prevent incorrect wiring, conduct built-in default software health check that will rotate motors every time Raspberry Pi is powered on
Solenoid	Unlock the latch to allow camera spring up	Motor failure	Unexpected motor damage	Motor stops working	Camera cannot deploy	Payload failure and possible damage due to stepper motor turning inside tub	**6**	**3**	**2**	**36**	Built-in default software health check that will retract solenoid when Raspberry Pi is powered on
RTL-SDR Radio	Receive APRS command from NASA	Interference	Magnetic field created by motors and Raspberry Pi	Noisy signals	Raspberry Pi doesn't receive command	Payload failure	**2**	**4**	**4**	**32**	Place radio antenna away from Raspberry Pi and motors to avoid interference,

											and make sure software does not read the signals received when motors are on
IMU	Detect launch and landing as well as the orientation of the rocket	Excessive noise	Static noise in the electronics and irregular movement created during launch preparation	IMU gives incorrect reading	Raspberry Pi incorrectly detects landing and initiate payload	Payload failure and possible launch vehicle failure	**8**	**1**	**1**	**8**	Use software filter to get rid of noises, and use a barometer as a redundancy
Raspberry Pi	Process radio signals and controls cameras and motors	Unstable voltage supply	Transient voltage created by motors	Raspberry Pi reboots and enters launch detection mode	Raspberry Pi won't reach radio command listening loop, and payload will not receive command	Payload failure	**3**	**3**	**4**	**36**	Use separate power supply for motors to ensure a stable current and voltage for Raspberry Pi

Table 42: Payload Electronics FMEA

5.3.2.3 Payload Software

Component	**Function**	**Failure Mode**	**Failure Cause**	**Failure Effects**			**S**[1]	**L**[2]	**D**[3]	**RPN**[4]	**Corrective Actions**
				Local Effects	**Next Higher Level**	**System Effects**					
Raspberry Pi	Controls payload operations	Software error	Unaccounted edge case in software, causing system to crash	The flight computer reboots and attempts to restore to previous state	No data is saved and the device reboots to the initial condition	The payload is unable to complete the assigned objective	**3**	**3**	**4**	**36**	Incorporate failure modes into software design
RTL-SDR Radio	Receives incoming radio signals	Device fails to send accurate data to Pi	Device configured improperly or unable to send data to controller	No signals will be sent to the Raspberry Pi	The Raspberry Pi fails to change state with incoming commands	The payload is unable to receive commands and therefore fails to perform assigned operations	**2**	**4**	**4**	**32**	Reboot and reconnect the USB device and reconfigure the receive frequency
TArduCam Camera	Take photos of local environment	Camera fails to listen to controller and is unable to take photos	Software configuration error not allowing proper inaction between camera and Raspberry Pi	Unable to take photo of environment	NASA radio transmissions will go without a response	The payload requirement to take photos would not be met	**2**	**4**	**4**	**32**	Reboot and reconnect the USB device and reload photo software

Table 43: Payload software FMEA

5.3.3 Avionics and Recovery

Component	**Function**	**Failure Mode**	**Failure Cause**	**Failure Effects**			**S**[1]	**L**[2]	**D**[3]	**RPN**[4]	**Corrective Actions**
				Local Effects	**Next Higher Level**	**System Effects**					
Altimeter	Determine the altitude of the launch vehicle at all points throughout flight to accurately set off ejection charges and	Sudden power loss	In-flight motions disconnect altimeter and battery	The altimeter stops monitoring and recording the launch	Ejection charges are not set off parachutes do not deploy	The launch vehicle descends with no deployed parachutes, high chance of significant	**10**	**1**	**6**	**60**	Secure altimeters, their respective batteries, and wiring in the avionics bay.

	deploy parachutes at the proper altitudes.			vehicle's altitude		damage to the launch vehicle upon landing					
Altimeter	Determine the height of the launch vehicle at all points throughout flight to accurately set off ejection charges and deploy parachutes at the proper altitudes.	Parachute deployment order reversed (main deployed at apogee)	Improper wiring of the altimeter (main ejection charge wiring attached to drogue terminal)	The main parachute is deployed at apogee instead of the drogue	The launch vehicle descends at a slow speed for the entire descent	The launch vehicle drifts much further than intended, resulting in a longer recovery and possible loss of the launch vehicle	**6**	**2**	**2**	**24**	Clear labeling of all wiring terminals, inspection of wiring prior to launch
Altimeter	Determine the height of the launch vehicle at all points throughout flight to accurately set off ejection charges and deploy parachutes at the proper altitudes.	Detonation of ejection charges on the launch pad	Improper wiring resulting in reversal of polarity of the battery	Instant detonation of ejection charges when altimeters are armed	Sections of the launch vehicle separate on the ground, potentially falling on and injuring nearby students	Unable to launch, possible damage to launch vehicle and injury to students near the pad	**10**	**2**	**2**	**40**	Test wiring of the altimeters before attaching ejection charges
Ejection Charges	Provides force necessary to cause separation of launch vehicle sections	Ejection charges do not detonate or fail to provide sufficient force to cause separation	Altimeters fail to set off ejection charge, ejection charge too small to cause separation, igniter failure, wires between the altimeters and ejection charges become disconnected	Launch vehicle sections do not separate	Parachutes are not deployed at the correct altitude or at all	Possible ballistic descent of the launch vehicle, high chance of damage to launch vehicle upon landing	**10**	**1**	**3**	**30**	Conduct ejection testing (test ID LV-R-5 and LV-R-6) to determine sufficient charge size, perform corrective actions for altimeters prior to launch
Recovery Harness	Tether sections of the launch vehicle to each other and to the parachutes after separation	Tears or breaks in the recovery harness	Use of a recovery harness that is damaged or has insufficient strength to remain functional after parachute deployments, melting of recovery harness due to ejection gases	Two or more sections of the launch vehicle become untethered	Sections not tethered to a parachute descend rapidly	Possible damage to sections not tethered to parachutes	**7**	**1**	**3**	**21**	Select recovery harnesses with sufficient strength and heat resistance, inspect recovery harnesses prior to use
Main Parachute	Slows the launch vehicle to its final descent velocity	Tears or holes in parachute	Insufficient protection from sharp objects, failure or improper use of parachute protector	Parachute is less efficient at slowing the launch vehicle	The launch vehicle descends at a faster velocity than designed	Possible damage to launch vehicle upon landing	**5**	**1**	**3**	**15**	Inspect parachute prior to use and patch holes as necessary
Main Parachute	Slows the launch vehicle to its final descent velocity	Tangled lines	Improper folding of parachute	Parachute is unable to fully inflate	The launch vehicle descends at a faster velocity than designed	Possible damage to launch vehicle upon landing	**5**	**3**	**2**	**30**	Store carefully to prevent tangling lines during storage, inspect

											packed parachute before using a parachute protector or putting it in the launch vehicle, conduct parachute deployment testing (LV-R-4) to evaluate packing effectiveness
Parachute Protector	Shields parachute from ejection gases during deployment	Holes or tears in parachute protector	Insufficient protection from sharp objects, damage and wear from previous use	Parachutes are not protected from ejection gases	Holes and burns may be made in parachutes due to ejection gases	Launch vehicle descends faster than anticipated	**6**	**2**	**1**	**12**	Inspect parachute protectors prior to use
Drogue Parachute	Slows initial descent of the launch vehicle and is deployed at apogee	Tears or holes in parachute	Insufficient protection from sharp objects, failure of parachute protector	Drogue parachute is less efficient at slowing the launch vehicle	The descent speed of the launch vehicle isn't slowed prior to main parachute deployment	Possible damage to launch vehicle during main parachute deployment	**5**	**1**	**3**	**15**	Inspect drogue parachute prior to use, ensure that parachute protector is used correctly
Drogue Parachute	Slows initial descent of the launch vehicle and is deployed at apogee	Tangled lines	Improper folding of parachute	Parachute is unable to fully inflate	The launch vehicle descends at a faster velocity than designed	Possible damage to launch vehicle upon landing	**5**	**3**	**2**	**30**	Store carefully to prevent tangling lines during storage, inspect packed parachute before using a parachute protector or putting it in the launch vehicle, conduct parachute deployment testing (LV-R-4) to evaluate packing effectiveness
Recovery Hardware (Eyebolt)	Connect recovery harness to payload and avionics bay bulkheads	Breaks during parachute deployment	Improper epoxying of hardware into bulkheads, insufficient strength of recovery hardware	Two or more sections of the launch vehicle become untethered	Sections not tethered to a parachute descend rapidly	Possible damage to sections not tethered to parachutes	**7**	**1**	**1**	**7**	Select recovery hardware strong enough to withstand deployment forces

Table 44: Avionics and recovery FMEA

5.3.4 Flight Dynamics

Component	Function	Failure Mode	Failure Cause	Failure Effects			S¹	L²	D³	RPN⁴	Corrective Actions
				Local Effects	Next Higher Level	System Effects					
Propellant	Generates thrust to propel the rocket.	Propellant Failure	Grain Defects, Improper storage, Water Damage.	Improper propellant burn.	Abrupt changes in thrust.	The launch vehicle has unpredictable trajectory/flight, or the rocket doesn't take off. Additional risks of over pressuring.	9	3	4	108	Ensure the integrity of the propellant grains by visually checking for defects. Store motors in a Climate Regulated room, and handle with care.
Nozzle	Controls the mass flow rate of the propellant burn.	Nozzle Deformation	Structural failure of the nozzle.	The nozzle exit area, nozzle exhaust pressure, and the mass flow rate change.	Abrupt changes in the thrust vector, and impulse.	The launch vehicle has an altered trajectory creating potential danger to bystanders	9	3	5	135	Ensure defects are not present on the nozzle by visually checking for them. Always handle the nozzle with care.
Motor Case (including the forward and aft closures)	Encloses the propellant grain and maintains pressure.	Case Deformation	Structural failure of the motor case including the forward or aft enclosures.	Internal pressure is not maintained, and propellant interacts with other components.	Motor assembly is damaged, and integrity of the motor and launch vehicle are compromised.	The launch vehicle is prone to having an unpredictable flight.	7	2	8	112	Ensure the integrity of the case by visually inspecting for defects. Always handle the motor case with care, and always have a protective cover over the casing until launch.
Motor Tube	Encloses the motor assembly in the correct position.	Motor Tube is dislodged.	Structural failure of the motor tube.	The motor case is not held in the correct position.	Risk of motor case forced through the launch vehicle, and misaligned thrust vector.	The launch vehicle is damaged, and the flight trajectory is altered.	6	3	6	108	Ensure the alignment of the tube by visually inspecting for defects. Always handle the motor tube with care.
Motor Retainer	Retains the motor inside the rocket.	Motor Retainer cracks or breaks.	Structural failure of the motor retainer or unfastened screws.	The motor case assembly is not held in place.	Risk of motor case assembly forced through the launch vehicle.	The launch vehicle is damaged, and the motor's function is lost.	7	4	7	196	Ensure the motor is retained by tightening the screws.
Thrust Plate	Transfers the thrust from through the centering rings and to the airframe.	Thrust Plate cracks or breaks.	Structural failure of the thrust plate.	The integrity of the centering rings and the airframe are compromised.	Centering rings are damaged, and risk of damage to airframe.	The launch vehicle is damaged, and the flight trajectory is altered.	5	4	7	140	Ensure the thrust plate is properly fastened by visually inspecting for defects. Always handle the thrust plate with care.

Table 45: Flight dynamics FMEA

5.4 Environmental Concerns

Environmental hazards are those that the vehicle and environment impose on each other (Table 46) (Table 47). This also uses the same scoring system as the Personnel Hazards Analysis.

5.4.1 Effect of Environment on Launch Vehicle

Hazard	Cause	Effect	S	L	Score	Mitigation
Precipitation soaks launch vehicle	Dramatic humid conditions at launch site	Electronic Disruption and Energetics Leakage	8	3	24	Supply a canopy/large tent for prep area

Descent into body of water	Launch vehicle drifts out of range	Failed Recovery	**9**	**2**	**18**	Minimize drift with drogue, angle launch rail into wind
Launch vehicle lands in unknown terrain	Excessive drift	Unretrievable or Collision Damage	**8**	**3**	**24**	Check launch site for obstacles
Wind	Drift or trajectory change	Unretrievable	**5**	**2**	**10**	Angle launch rail into wind, scrub launch if wind reaches unsafe speed
Dryness	Brittle adhesive at epoxy joints	Fins, centering rings, and bulkheads crack or loosen	**7**	**3**	**21**	Manufacture with long curing time
High Temperatures	Electrical Components Overheat	Avionics and payload fail	**7**	**4**	**28**	Canopy at prep site

Table 46: Effects of Environment on Launch Vehicle

5.4.2 Effect of Launch Vehicle on Environment

Hazard	Cause	Effect	S	L	Score	Mitigation
Fire at launch prep site	Black powder spills and ignites	Fire damages private property	**8**	**3**	**24**	Ensure black powder is separated from electronics and any ignition sources during prep; store in ammo box until use
Fire at launch pad	Motor exhaust ignites surrounding grass	Fire damages private property	**3**	**6**	**18**	Remove dry grass from area directly around launch pad
Litter	Trash or components left on launch field	Pollution of local area	**2**	**6**	**12**	Inspect launch prep area before leaving to ensure no litter is left on the ground, and use garbage pack to collect litter
Launch vehicle/debris from launch vehicle	Parts of the launch vehicle separate completely and are lost, or the entire launch vehicle is lost	Pollution of local area	**10**	**2**	**20**	Have redundancies in the recovery system to prevent ballistic descent, conduct ground testing to ensure that recovery components are sufficiently strong
Chemical Leaks	Punctured batteries	Chemicals harm local plants and wildlife	5	2	**10**	Handle batteries with care and store them insecure areas away from sharp objects.

Table 47: Effects of Launch Vehicle on Environment

5.5 Project Risks

A project risk is any uncertain event that may or may not occur during a project. Given the challenges of this competition, we can break these down into risks due to time, resources, and general scope of the project. For determining their severities, Impact (I, 1-10) and Likelihood (L, 1-10) scoring charts can be developed like those in the Personnel Hazards Analysis. Using these scores, we can also develop a risk assessment score (RA, 1-100) (Table 48)(Table 49)(Table 50).

	Impact (I)	**Likelihood (L)**
1, 2	Very minor setback in project plan, very high possibility of prompt launch eligibility/little or no design changes	1-20% occurrence, very unlikely
3, 4	Minor setback in project plan, high possibility of prompt launch eligibility/minor design changes	21-40% occurrence, unlikely
5, 6	Moderate setback in project plan, moderate possibility of prompt launch eligibility/necessity for slight redesign	41-60% occurrence, uncertain likelihood
7, 8	Major setback in project plan, low possibility of prompt launch eligibility/necessity for moderate redesign	61-80% occurrence, likely
9, 10	Complete setback in project plan, extremely low possibility of prompt launch eligibility/necessity for major redesign	81-100% occurrence, very likely

Table 48: Risk Assessment Chart (RAC)

		Likelihood									
		1	2	3	4	5	6	7	8	9	10
Impact	1	1	2	3	4	5	6	7	8	9	10
	2	2	4	6	8	10	12	14	16	18	20
	3	3	6	9	12	15	18	21	24	27	30
	4	4	8	12	16	20	24	28	32	36	40
	5	5	10	15	20	25	30	35	40	45	50
	6	6	12	18	24	30	36	42	48	54	60
	7	7	14	21	28	35	42	49	56	63	70
	8	8	16	24	32	40	48	56	64	72	80
	9	9	18	27	36	45	54	63	72	81	90
	10	10	20	30	40	50	60	70	80	90	100

Table 49: RA Score Chart

Risk	Cause	Effect	I	L	Score	Mitigation Strategy	Mitigation Effects
Payload Functionality	Flaw in payload system due to improper design and/or insufficient testing for various conditions	Payload does not function; cannot complete tasks sent by mission control and/or capture 360-degree photos of surroundings	9	6	54	Hold multiple design reviews and recruit as many new members as possible to assist in payload manufacturing, testing, and programming	Decreased likelihood of payload not functioning due to improper design
Delays/Falling Behind Project Plan	Errors/mistakes inflicted on the vehicle or payload during manufacturing	Team falls behind in project plan. Depending on timeline position, changes to manufacturing, testing, and launch plans will be delayed, changed, or scrapped entirely to remain on track	10	5	50	Create a well-detailed, time-efficient manufacturing plan that includes generous functional tolerances and room for slight errors	Lack of errors or mistakes in manufacturing, ability to move on to further tasks in project
	Team leader falls behind on completing assigned tasks					Set early deadlines for all team leaders to complete tasks, encourage communication between leads and project managers	Assigned tasks are completed on time or before the deadline
	Shipping delays for ordered parts (e.g., airframe, nose cone, parachutes)					Send shipping orders early/make use of pre-existing parts	Lack of time waiting to begin manufacturing or testing
Budget	Limited funding available from University, Department, or Student Government	Inability to secure necessary parts for manufacturing, testing, and ultimately launches	6	5	30	Utilize a cost-efficient design, secure funding from as many sources as possible early, and supplement with fund raisers	Sufficient funding to secure necessary parts for all steps in the project

Table 50: Project Risk Identification

6. Project Plan

6.1 Requirements Verification

The team has created requirements that are specific to the team's launch vehicle design, recovery system, and payload design (Table 51)(Table 52)(Table 53).

6.1.1 Vehicle Requirements

Requirement	Justification	Verification
1.1 The launch vehicle will reach an apogee of 4000 – 4600 ft.	The apogee must be within this range to ensure it does not fall below the competition minimum.	The Flight Dynamics lead will verify the apogee using simulations to ensure the launch vehicle will meet this

		requirement in different launch conditions.
1.2 The airframe section containing the payload will retain sufficient structural strength to endure forces of flight and recovery.	For safe flight, airframe must not experience structural failure during launch, and must remain undamaged for multiple launches.	A payload housing compressive strength test (P-D-3) will determine the compressive strength of the modified airframe.

Table 51: Team Derived Vehicle Requirements

6.1.2 Recovery Requirements

Requirement	Justification	Verification
2.1 The drogue parachute will have a descent rate of 80.1 ft/s.	This descent rate will ensure that the launch vehicle will not be damages upon landing.	The parachute drag test (LV-R-1) will ensure that the parachute will induce enough drag.
2.2 The main parachute will have a descent rate of 17.2 ft/s.	This descent rate will ensure that the launch vehicle will not be damages upon landing.	The parachute drag test (LV-R-2) will ensure that the parachute will induce enough drag.
2.3 The recovery harnesses will be at least 2.5 times the length of the total length of the airframe.	The recovery harnesses must be sufficiently long enough to ensure that the different sections of the launch vehicle do not collide during descent.	The Avionics and Recovery lead will measure the length of the recovery harness to verify that it is correct.
2.4 The secondary drogue ejection charge will activate 1 second after the primary ejection charge.	The secondary ejection charge must activate quickly enough to ensure drogue deployment occurs at a safe velocity; however, over pressurization may occur if charge activates too quickly.	The altimeter accuracy test (LV-A-2) will be performed to ensure the altimeter activates at the correct time.
2.5 The secondary main ejection charge will activate 50 feet lower than the primary ejection charge.	The secondary ejection charge must activate quickly enough to ensure drogue deployment occurs at a safe velocity; however, over pressurization may occur if charge activates too quickly.	The altimeter accuracy test (LV-A-2) will be performed to ensure the altimeter activates at the correct altitude.
2.6 The secondary ejection charges will be 25% larger by weight than the primary ejection charges.	Secondary ejection charges are included in the design to ensure separation in the event that the primary charges fail, and as such must be slightly more powerful.	Ejection charges will be prepared with the proper amount of black powder using a scale, and the Avionics and Recovery lead will verify the quantity of black powder used.

Table 52: Team Derived Recovery Requirements

6.1.3 Payload Requirements

Requirement	Justification	Verification
3.1 The horizon line will be within 10 degrees of parallel with the bottom of the image.	Ensure that the camera is perpendicular to the ground and is able to take level images of the surroundings.	Simulate representative recovery scenarios to gather image data and ensure that the horizon line is parallel to the bottom border of the image.
3.2 Latch release mechanism will have sufficient strength to release camera arm.	Latch release must be strong enough so that the correct camera can be released into the upright position.	The latch release test (P-CF-5) will be conducted to ensure latch release is reliably able to release the camera arm.
3.3 Payload will be able to recover from a brief power loss event.	Power may temporarily fail while payload awaits launch, or during launch when payload is subject to elevated forces. The payload must be able to recover from such an event and accomplish mission goal.	The power loss recovery demonstration (P-SF-5) will be conducted to ensure that payload can reliably recover from power loss events.
3.4 Payload will be able to remain idle for a minimum of two hours, with sufficient battery power for operation at the conclusion of the two hours.	Launch vehicle may remain on launch pad for as long as two hours prior to launch, and must be able to complete the mission despite this delay.	The payload battery life test (P-SF-1) will be performed to ensure the payload is capable of retaining sufficient battery power after significant delays.
3.5 Payload electronics will be able to resist acceleration forces during launch.	Electrical and structural connections within the payload must be able to withstand the forces of launch in order to carry out the mission objective.	The payload acceleration resilience test (P-D-4) will be performed to ensure the payload is able to withstand accelerations similar to those experienced during launch.
3.6 Payload must be able to detect landing.	Payload must be able to detect landing so camera can be deployed and other mission objectives started.	The landing detection test (P-SF-6) will be performed to ensure payload is capable of detecting landing.

Table 53: Team Derived Payload Requirements

6.2 Testing Plan

A comprehensive testing plan has been compiled to certify compliance with all requirements set forth by NASA in the student handbook and team-derived requirements included in this report. All testing will be overseen by the testing lead, safety officer, and adult educators as necessary to ensure the safe and successful execution of testing.

Information for each test has been tabulated for quick reference (Table 55, Table 56). Each line describes the rationale for completing the test, a summary of the planned procedure, and required materials. In addition to a title, each test has been assigned a test ID, which provides a method for referencing tests elsewhere in project documentation. The test ID is assigned based on the type of test it describes (Table 54). Safety information for each test is organized separately (Table 57, Table 58).

ID Abbreviation	Category
LV	Launch Vehicle Test
P	Payload Test
MS	Material Strength
MP	Material Property
SP	System Property
A	Avionics
R	Recovery
L	Launch Related
CF	Component Functionality
SI	System Integration
D	Durability
SF	System Functionality

Table 54: Test ID Abbreviations

6.2.1 Vehicle Testing Plan

Test ID	Title	Overview of Procedure	Rationale	Required Materials
LV-MS-1	Airframe Material Compression Test	Use Instron UTM to experimentally determine maximum compressive strength of a section of airframe.	Ensure that airframe material is capable of withstanding compressive forces during flight and landing.	Instron UTM, airframe material sample
LV-MS-2	Fin Material Bend Test	Use Instron UTM to experimentally determine maximum flexural strength of a sample of fin material through a four-point flexural test.	Ensure fin material is capable of withstanding forces from ground impact upon landing.	Instron UTM, fin material sample
LV-MS-3	Bulkhead Material Strength Test	Use Instron UTM to experimentally determine maximum tensile strength of bulkhead and eyebolt assembly.	Ensure bulkhead assembly is capable of withstanding force of parachute ejection	Instron UTM, bulkhead material, eyebolt
LV-MS-4	Epoxy Strength Test	Use Instron UTM to experimentally determine maximum shear strength of epoxy through a lap shear test.	Ensure epoxy is capable of withstanding forces of vehicle operation.	Instron UTM, epoxy, material sample
LV-MS-5	Recovery Harness Knot Efficiency Test	Use Instron UTM to experimentally determine the efficiency of several knots used to secure recovery harness to eyebolts.	Ensure recovery harness attachments are capable of withstanding force of parachute ejection.	Instron UTM, recovery harness material sample

LV-MS-6	Recovery Harness Material Strength Test	Use Instron UTM to experimentally determine maximum yield strength of recovery harness material.	Ensure recovery harness material is capable of withstanding force of parachute ejection.	Instron UTM, recovery harness material sample
LV-MS-7	Airframe Material Impact Resistance Test	Drop section of airframe from a height that simulates flight recovery conditions.	Ensure airframe is capable of withstanding forces during vehicle recovery.	Airframe material sample
LV-MS-8	Bulkhead Impact Resistance Test	Drop a bulkhead attached to a weighted airframe from a height that simulates flight recovery conditions.	Ensure bulkheads are capable of withstanding forces during vehicle recovery.	Airframe material sample, bulkhead
LV-MS-9	Airframe Material Zippering Resistance Test	Apply brief force to airframe and recovery harness assembly to simulate ejection conditions.	Ensure airframe material can withstand forces during parachute ejection.	Airframe material sample, recovery harness
LV-MP-1	Epoxy Density Inspection	Prepare a known volume of epoxy, and once cured, measure weight.	Obtain density of epoxy for use in computer simulations.	Epoxy, scale
LV-MP-2	Epoxy Environmental Exposure Test	Prepare epoxy sample and, once cured, place outside for a minimum of two hours before testing shear strength.	Ensure epoxy does not weaken significantly from exposure to likely launch day conditions .	Instron UTM, epoxy, material sample
LV-SP-1	Rotation and Rolling Analysis	Simulate launch vehicle behavior in radial and axial direction.	Identify and correct stability issues in launch vehicle.	MATLAB, OpenRocket
LV-SP-2	Launch Vehicle Drag Analysis	Simulate launch vehicle aerodynamics to measure drag.	Identify and correct issues arising from excess or undesirable drag.	SolidWorks
LV-SP-3	Center of Gravity Inspection	Balance rocket along axis and record location.	Ensure launch vehicle will be stable in flight.	Launch vehicle, rope
LV-SP-4	Vehicle Vibration Test	Simulate vibrations vehicle is likely to experience during launch.	Ensure launch vehicle can withstand vibrations during flight.	Launch vehicle

LV-SP-5	Fastening Hardware Vibration Test	Simulate vibrations D-links and nuts and bolts used in launch vehicle are likely to experience during launch.	Ensure fastening hardware will remain secure during flight.	D-links, nuts, bolts
LV-A-1	Altimeter Functionality Demonstration	Place altimeter in a jar that can be pressurized using a syringe. Pressurize and record change in volume of air to calculate change in pressure.	Verify that altimeter responds to differing pressure.	Altimeter, modified jar, syringe, tubing
LV-A-2	Altimeter Accuracy Test	Move altimeter to several known altitudes and record altimeter reading.	Verify altimeter functionality.	Altimeter
LV-A-3	Avionics Battery Life Test	Run avionics instrumentation on standby until battery is depleted , and record time to depletion.	Ensure launch vehicle can remain launch-ready for required period of time.	Avionics assembly
LV-A-4	Avionics Bulkhead Explosive Resistance Test	Fire ejection charge against bulkheads of varying thicknesses to determine necessary size of bulkhead for avionics bay.	Ensure avionics bay bulkheads are capable of withstanding ejection charges.	Bulkheads, airframe, ejection charge, 9V battery, test stand
LV-A-5	Avionics Interference Test	Perform altimeter accuracy test with avionics bay assembly in final configuration with operational payload in close proximity.	Ensure avionics bay will not suffer interference from payload operation.	Payload assembly, avionics bay assembly
LV-R-1	Drogue Parachute Drag Test	Drop weighted parachute from height to simulate vehicle recovery conditions.	Ensure parachute provides sufficient drag to safely eject main parachute.	Parachute, weight
LV-R-2	Main Parachute Drag Test	Drop weighted parachute from height to simulate vehicle recovery conditions.	Ensure parachute provides sufficient drag to safely recover launch vehicle.	Parachute, weight
LV-R-3	Parachute Preparation Test	Fold drogue and main parachute and install in launch vehicle.	Determine best way to ensure parachutes can	Launch vehicle, drogue and main parachute

			be properly loaded into the launch vehicle.	
LV-R-4	Parachute Deployment Test	Drop folded and weighted parachute from a height to simulate vehicle recovery conditions.	Ensure that parachute will properly deploy during vehicle recovery.	Drogue and main parachute, weight
LV-R-5	Drogue Parachute Ejection Demonstration	Prepare vehicle in launch configuration and manually fire ejection charges.	Ensure vehicle separates and parachute properly deploys.	Launch vehicle, drogue parachute, recovery insulation, ejection charge, wire, test stand, 9V battery
LV-R-6	Main Parachute Ejection Demonstration	Prepare vehicle in launch configuration and manually fire ejection charges.	Ensure vehicle separates and parachute properly deploys.	Launch vehicle, main parachute, recovery wadding, ejection charge, wire, test stand, 9V battery
LV-L-1	Launch Rehearsal Demonstration	Prepare full-scale launch vehicle assembly and payload assembly in launch configuration (excepting motor).	Ensure launch vehicle and payload can be prepared in allotted time.	Launch vehicle, payload, and associated components
LV-L-2	Subscale Demonstration Launch	Launch subscale vehicle.	Ensure subscale design can be successfully launched and recovered.	Subscale model
LV-L-3	Vehicle Demonstration Launch	Launch full-scale vehicle in final configuration.	Ensure launch vehicle can be successfully launched and recovered.	Launch vehicle

Table 55: Vehicle Testing Plan

6.2.2 Payload Testing Plan

Test ID	Title	Overview of Procedure	Rationale	Required Materials
P-CF-1	Raspberry Pi Functionality Demonstration	Connect keyboard, mouse, and monitor to Raspberry Pi and confirm that it is fully functional.	Ensure Raspberry Pi can run necessary commands.	Raspberry Pi, laptop

P-CF-2	Camera Functionality Demonstration	Instruct camera to take a photo.	Ensure camera is responsive to commands.	Camera, Raspberry Pi, software
P-CF-3	Radio Reception Test	Transmit radio instructions to payload receiver and determine if instructions were received.	Ensure payload can successfully receive transmissions.	Radio, Raspberry Pi
P-CF-4	Image Manipulation Software Unit Test	Manipulate images in required ways (rotate, apply filters) using software.	Ensure payload software can execute required image manipulation commands.	Payload software
P-CF-5	Latch Release Test	Instruct solenoid to release the latch securing the camera assembly inside the payload.	Ensure solenoid is responsive to software commands and has sufficient power to release latch.	Latch assembly, Raspberry Pi, software
P-CF-6	Camera Rotation Test	Instruct motor to rotate camera around z-axis through software.	Ensure that camera can be rotated through software commands.	Camera assembly, Raspberry Pi, software
P-CF-7	Camera Deployment Test	Initiate camera deployment through software commands.	Ensure that camera can be successfully deployed from the payload housing.	Payload assembly
P-CF-8	IMU Accuracy Test	Record IMU readings for several acceleration scenarios and compare to correct values.	Ensure IMU yields accurate readings for use by payload systems.	IMU
P-SI-1	Raspberry Pi Camera Integration Test	Perform multiple commands on Raspberry Pi to take photos using cameras.	Ensure that Raspberry Pi can interface with the cameras.	Cameras, Raspberry Pi
P-SI-2	Raspberry Pi Motor Integration Test	Perform multiple commands on Raspberry Pi to manipulate all motors contained in payload.	Ensure that Raspberry Pi can successfully control payload hardware.	Motors, Raspberry Pi
P-SI-3	Raspberry Pi Radio Integration Test	Transmit signal to radio and verify that Raspberry Pi received the signal.	Ensure that radio can receive transmissions and relay them to the Raspberry Pi.	Radio, Raspberry Pi

P-SI-4	Radio Integration Test	Perform payload functions while radio signal is being transmitted.	Ensure that radio does not interfere with payload function.	Payload, radio transmitter
P-D-1	Ejection Demonstration	Assemble rocket in launch configuration with payload and ignite ejection charge.	Ensure payload is undamaged by ejection events.	Launch vehicle, payload assembly
P-D-2	Electronics Vibration Test	Subject payload to vibrations similar to those experienced during launch and verify that payload is undamaged.	Ensure that payload will not be damaged during flight.	Payload assembly
P-D-3	Payload Housing Compressive Strength Test	Use Instron UTM to experimentally determine maximum compressive strength of payload housing.	Ensure that payload assembly can withstand forces present during flight.	Instron UTM, Airframe section altered to simulate payload assembly
P-D-4	Payload Acceleration Resilience Test	Subject payload to G-forces similar to those experienced during launch and verify that payload still functions.	Ensure that payload will retain functionality after flight.	Payload assembly, rope
P-D-5	Payload Impact Resistance Test	Drop payload section from height to simulate recovery conditions.	Ensure that payload can withstand forces present during recovery of the launch vehicle.	Payload assembly, parachute
P-SF-1	Payload Battery Life Test	Operate payload on standby until battery depletion occurs.	Ensure payload can operate on standby for two-hour minimum requirement.	Payload assembly
P-SF-2	Overheating Test	Operate payload for a minimum of two hours outside while monitoring internal temperature.	Ensure payload will not overheat when subject to launch day conditions.	Payload assembly
P-SF-3	Payload Performance Test	Command payload to execute several commands, and time how long it takes to accomplish commands.	Ensure payload can accomplish all goals in the necessary time frame.	Payload assembly, software, radio

P-SF-4	Camera Angle Inspection	Simulate recovery scenarios and determine the angle at which the camera rests following landing.	Ensure camera is oriented nearly straight upright.	Payload assembly, launch vehicle aft section.
P-SF-5	Power Loss Recovery Demonstration	Temporarily disconnect power from the payload. Verify that once power is reconnected, payload is able to restart.	Ensure payload can recover from temporary power loss.	Payload assembly
P-SF-6	Landing Detection Test	Simulate landing conditions and determine whether payload detected landing.	Ensure payload can determine when to commence mission processes.	Payload assembly
P-L-1	Payload Demonstration Flight	Launch payload in final configuration in full-scale launch vehicle.	Ensure payload is able to operate after flight.	Launch vehicle, payload

Table 56: Payload Testing Plan

6.2.3 Testing Safety

6.2.3.1 Launch Vehicle Testing Safety

Test ID	Safety Measures
LV-MS-1	Only trained and qualified individuals will operate the Instron. Team members present for the test will follow all instructions from trained and qualified individuals.
LV-MS-2	Only trained and qualified individuals will operate the Instron. Team members present for the test will follow all instructions from trained and qualified individuals.
LV-MS-3	Only trained and qualified individuals will operate the Instron. Team members present for the test will follow all instructions from trained and qualified individuals.
LV-MS-4	Only trained and qualified individuals will operate the Instron. Team members present for the test will follow all instructions from trained and qualified individuals.
LV-MS-5	Only trained and qualified individuals will operate the Instron. Team members present for the test will follow all instructions from trained and qualified individuals.
LV-MS-6	Only trained and qualified individuals will operate the Instron. Team members present for the test will follow all instructions from trained and qualified individuals.
LV-MS-7	Samples will be dropped from safe location. Landing zone will be carefully controlled to ensure it is kept clear of people.
LV-MS-8	Samples will be dropped from safe location. Landing zone will be carefully controlled to ensure it is kept clear of people.
LV-MS-9	Relevant PPE will be worn during test. Team members not required for execution of test will stand back a safe distance.
LV-MP-1	Gloves, eye protection, and other relevant PPE will be worn while preparing the epoxy sample in a well-ventilated area.
LV-MS-5	Only trained and qualified individuals will operate the Instron. Team members present for the test will follow all instructions from trained and qualified individuals.

LV-SP-1	Minimal inherent risk.
LV-SP-2	Minimal inherent risk.
LV-SP-3	Minimal inherent risk.
LV-SP-4	Members not actively involved in test will stand back, eye protection and other necessary PPE will be worn by test operators.
LV-SP-5	Members not actively involved in test will stand back, eye protection and other necessary PPE will be worn by test operators.
LV-A-1	Minimal inherent risk.
LV-A-2	Minimal inherent risk.
LV-A-3	Minimal inherent risk.
LV-A-4	Members will stand well back from launch vehicle while test is underway. A fire extinguisher will be readily accessible during test.
LV-A-5	Minimal inherent risk.
LV-R-1	Parachutes will be dropped from safe location. Landing zone will be carefully controlled to ensure it is kept clear of people.
LV-R-2	Parachutes will be dropped from safe location. Landing zone will be carefully controlled to ensure it is kept clear of people.
LV-R-3	Minimal inherent risk.
LV-R-4	Parachutes will be dropped from safe location. Landing zone will be carefully controlled to ensure it is kept clear of people.
LV-R-5	Members will stand well back from launch vehicle while test is underway. A fire extinguisher will be readily accessible during test.
LV-R-6	Members will stand well back from launch vehicle while test is underway. A fire extinguisher will be readily accessible during test.
LV-L-1	Minimal inherent risk.
LV-L-2	All range safety guidelines and Range Safety Officer directives will be followed.
LV-L-3	All range safety guidelines and Range Safety Officer directives will be followed.

Table 57: Launch Vehicle Testing Safety

6.2.3.2 Payload Testing Safety

Test ID	Safety Measures
P-CF-1	Minimal inherent risk.
P-CF-2	Minimal inherent risk.
P-CF-3	Radio operator will possess required license(s) for operation, and all relevant radio guidelines will be adhered to.
P-CF-4	Minimal inherent risk.
P-CF-5	Minimal inherent risk.
P-CF-6	Minimal inherent risk.
P-CF-7	Minimal inherent risk.
P-CF-8	Minimal inherent risk.
P-SI-1	Minimal inherent risk.
P-SI-2	Minimal inherent risk.
P-SI-3	Radio operator will possess required license(s) for operation, and all relevant radio guidelines will be adhered to.

P-SI-4	Radio operator will possess required license(s) for operation, and all relevant radio guidelines will be adhered to.
P-D-1	Members will stand well back from launch vehicle while test is underway. A fire extinguisher will be readily accessible during test.
P-D-2	Members not actively involved in test will stand back, eye protection and other necessary PPE will be worn by test operators.
P-D-3	Only trained and qualified individuals will operate the Instron. Team members present for the test will follow all instructions from trained and qualified individuals.
P-D-4	Member conducting test will wear required PPE. Other members not actively involved will stand well back from the testing.
P-D-5	Payload will be dropped from safe location. Landing zone will be carefully controlled to ensure it is kept clear of people.
P-SF-1	Minimal inherent risk.
P-SF-2	Test will be run in fire-safe area, under close supervision. A fire extinguisher will be readily accessible during test.
P-SF-3	Minimal inherent risk.
P-SF-4	Minimal inherent risk.
P-SF-5	Minimal inherent risk.
P-SF-6	Minimal inherent risk.
P-L-1	All range safety guidelines and Range Safety Officer directives will be followed.

Table 58: Payload Testing Safety

6.3 Completed Tests

6.3.1 Completed Vehicle Tests

Airframe Material Impact Resistance Test

Test ID: LV-MS-7

Recovery of the launch vehicle—specifically the landing—is a launch phase in which airframe components are subjected to potentially damaging forces upon impact with the ground at high velocities. Thus, it is necessary to evaluate different airframe material samples for their impact durability.

Success criteria: The test is deemed successful if the airframe material has no damage after landing.

Materials:

- G-12 Fiberglass Airframe Section
- Phenolic Airframe
- Quantum Airframe Tubing
- Blue Tube Airframe

Possible alternatives for airframe material must be exposed to high velocity collisions with the ground to ensure that no permanent damage will occur in flight scenarios. To test this, each potential airframe material was launched downwards from the top floor of a parking garage, an approximate height of 33 feet and 5 inches, into a grass-covered area free of people and objects.

Based on the height at which each airframe sample was dropped, an estimate of the impact velocity of the samples can be calculated. Determining the drag for a cylindrical object tumbling in the air is prohibitively complex, but by disregarding air resistance it is estimated that each airframe sample impacted the ground with an approximate velocity of 46 ft/s (Equation 4). While this is an overestimate due to the fact air resistance was not considered, since this is a significantly greater velocity than the expected ground hit velocity of the launch vehicle under typical launch conditions it is expected that these methods will yield an acceptably accurate demonstration of actual performance.

$$v = \sqrt{v_o + 2a\Delta x} \sim \sqrt{(0) + 2(32\,\mathrm{ft/s^2})(33\,\mathrm{ft})} \sim 46\,\mathrm{ft/s}$$

Equation 4: Estimate for Impact Velocity of Airframe Samples

Following each individual drop test, the airframe materials sample were collected and inspected thoroughly for signs of damage. None of the airframe tubes showed any sign of damage after landing (Figure 67). Therefore, all airframe materials demonstrated sufficient impact strength to meet the success criteria for this test.

Figure 67: Airframe Samples Following Impact Resistance Test

Epoxy Density Inspection

Test ID: LV-MP-1

Epoxy is used extensively on both the inside and outside of the rocket to adhere certain components, such as fins. Determining the density of the different epoxy brands used will improve the accuracy of computer simulations. Both JB-Weld and RocketPoxy will be tested. As of the writing of this review, only the JB-Weld density inspection has been completed.

JB-Weld Density Inspection

Materials:

- JB-Weld two-part steel and hardener epoxy
- Scale
- Stirring utensil & receptacle
- 2 pieces of flat test material
- Ruler

Approximately 1 ounce of JB Weld epoxy was prepared by thoroughly mixing equal amounts by weight of steel and hardener in a small container. The flat test material samples were weighed, then filleted together with epoxy at a right angle (Figure 68).  At least 6 hours were allowed for the epoxy to set.

Figure 68: Epoxy Fillet

Once cured, the slabs were weighed again. The linear density of the epoxy, λ, was calculated by subtracting the mass of the bare slabs, m_1 and m_2, from the mass of the slabs with epoxy, M_f, and dividing by the length of the slab spanned by the epoxy fillet, L (Equation 5).The calculated linear mass density of the JB Weld epoxy was found to be 0.0748 oz/in (Table 59).

$$\lambda = \frac{M_E}{L} = \frac{M_f - (m_1 + m_2)}{L}$$

Equation 5: Formula for Linear Density of Epoxy Fillet

Description	Variable	Measured Value
Mass of test material 1	m_1	2.755 oz
Mass of test material 2	m_2	2.751 oz
Mass of epoxied test material	M_f	5.859 oz
Mass of epoxy	M_E	0.353 oz
Length of material	L	4.719 in
Linear density of epoxy	λ	0.075 in

Table 59: Results of JB Weld Density Inspection

6.4 Budgeting and Timeline

6.4.1 Project Schedule

The development of the project will be based around this scheduled timeline (Figure 69). The schedule has been developed to meet the deadlines set by NASA, and the team's own internal deadlines.

Task Name	Duration	Start	Finish
Launch Vehicle / Payload Design	11 days	Fri 8/19/22	Fri 9/2/22
Proposal Draft	8 days	Mon 9/5/22	Wed 9/14/22
Proposal Revisions	2 days	Thu 9/15/22	Fri 9/16/22
Proposal Submission	0 days	Mon 9/19/22	Mon 9/19/22
PDR Design Revisions	12 days	Mon 9/19/22	Tue 10/4/22
Subscale Vehicle Design	7 days	Wed 10/5/22	Thu 10/13/22
Subscale Vehicle Purchase Order	1 day	Fri 10/14/22	Fri 10/14/22
PDR Draft & Presentation Development	12 days	Wed 10/5/22	Thu 10/20/22
PDR Revisions	2 days	Fri 10/21/22	Mon 10/24/22
PDR Submission	0 days	Tue 10/25/2	Tue 10/25/22
PDR Conference / Presentation	15 days	Tue 11/1/22	Mon 11/21/22
Subscale Vehicle Manufacturing	12 days	Mon 11/14/2	Tue 11/29/22
Subscale Launch	0 days	Sat 12/3/22	Sat 12/3/22
Payload Prototype Manufacturing	7 days	Mon 12/12/2	Tue 12/20/22
Subscale Corrections	5 days	Mon 12/12/2	Fri 12/16/22
CDR design revisions	3 days	Sun 12/11/2	Tue 12/13/22
CDR Draft & Presentation Development	8 days	Wed 12/14/22	Fri 12/23/22
Subscale Backup Launch	0 days	Sat 12/17/22	Sat 12/17/22
CDR Revisions	6 days	Sun 1/1/23	Fri 1/6/23
CDR Submission	0 days	Mon 1/9/23	Mon 1/9/23
Fullscale Vehicle / Payload Purchase Order	1 day	Mon 1/9/23	Mon 1/9/23
CDR Conference / Presentation	16 days	Mon 1/9/23	Mon 1/30/23
Fullscale Manufacturing	9 days	Mon 1/16/23	Thu 1/26/23
Fullscale Testing	4 days	Fri 1/27/23	Wed 2/1/23
Payload Manufacturing	5 days	Wed 2/1/23	Tue 2/7/23
Payload Testing (Ground)	4 days	Wed 2/8/23	Mon 2/13/23
FRR Draft	6 days	Tue 1/31/23	Tue 2/7/23
Vehicle & Payload Demonstration Flight	0 days	Sat 2/18/23	Sat 2/18/23
FRR Revision	4 days	Wed 3/1/23	Sat 3/4/23
FRR Submission	0 days	Sun 3/5/23	Sun 3/5/23
Vehicle & Payload Demonstration Flight 2	0 days	Sat 3/18/23	Sat 3/18/23
FRR Addendum Draft (Window)	12 days	Sun 3/19/23	Sat 4/1/23
FRR Addendum Submission	0 days	Sun 4/2/23	Sun 4/2/23
LRR	1 day	Wed 4/12/23	Wed 4/12/23
Launch Week	4 days	Wed 4/12/23	Sun 4/16/23
PLAR Draft	6 days	Wed 4/19/23	Wed 4/26/23
PLAR Revision	3 days	Thu 4/27/23	Sat 4/29/23
PLAR Submission	0 days	Sun 4/30/23	Sun 4/30/23

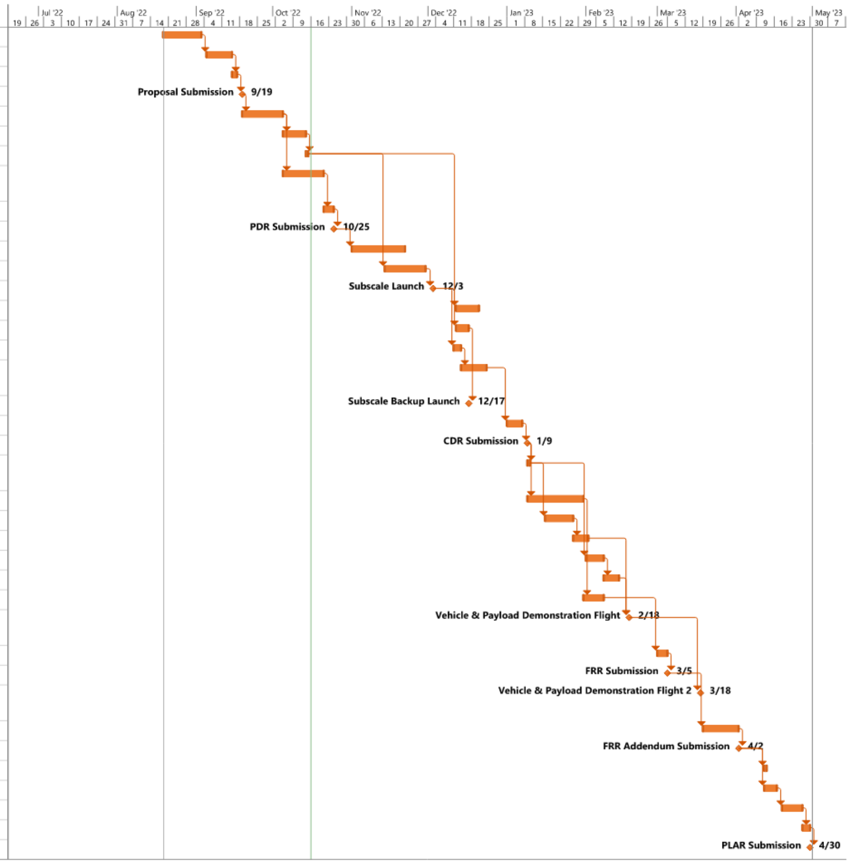

Figure 69: Project Timeline

6.4.2 Funding

This project will be primarily funded by the University of Florida's Mechanical and Aerospace Engineering Department along with the support of our sponsors, who provide both monetary and material donations. The team is sponsored by Blue Origin, Aerojet Rocketdyne, and Hands On Gainesville. The team is actively seeking more corporate sponsorships by developing a sponsorship plan and reaching out to potential sponsors. To accomplish this, the team has developed a corporate sponsorship package that will be sent to potential sponsors. The current sponsorships range from $250 to $2,000, with additional material donations. Between the funding received from the University of Florida's Mechanical and Aerospace Engineering Department and corporate sponsorships, the team will have approximately $8,800.00 to utilize for the project.

Additional funding is raised by the team through working with local businesses to create fundraisers to benefit the business and the organization. Funding will first be received by our faculty advisors, Dr. Lind and Dr. Niemi, and will then be allocated to our group. Additionally, the team has started an alumni program to stay connected with dedicated members who have graduated, encouraging them to stay involved and support the future of the group.

6.4.3 Budget

The team's total expected budget for the 2022-2023 year is $7,100.00 (Figure 70) (Table 60). This budget is derived from total vehicle component costs of the subscale and full-scale vehicles (Table 61) (Table 62), as well as testing and general costs (Table 66) (Table 65). Testing costs are anything associated with testing campaigns for both vehicles. General costs are any costs that pertain to the development of both vehicles, excluding testing. This budget allows for a $1,700.00 contingency in the event of necessary changes, damage repair, or further testing.

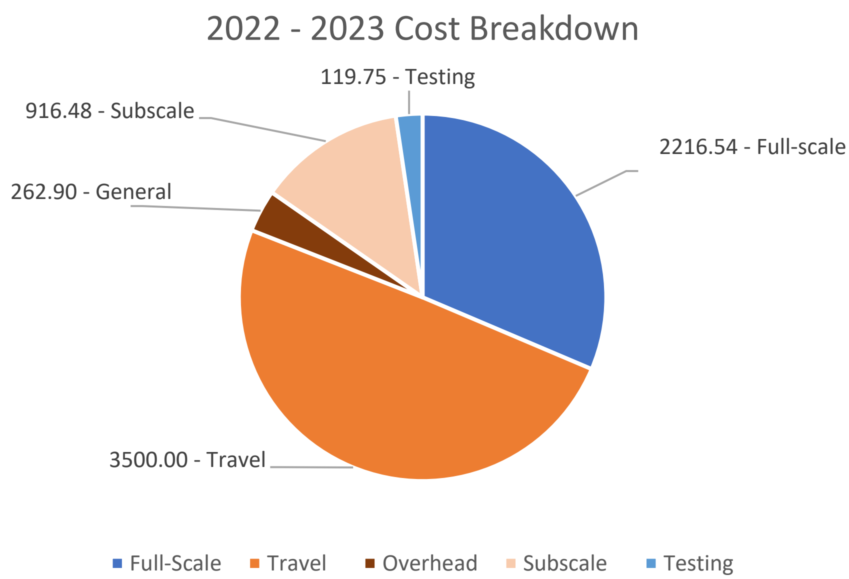

Figure 70: 2022-2023 Cost Breakdown

Cost Category	Total Cost ($)
Full-Scale	2216.54
Travel	3500.00
Overhead	262.90
Subscale	916.48
Testing	119.75
Total:	**7015.67**

Table 60: 2022-2023 Budget

Subteam	Total Cost ($)
Structures	411.68
Avionics & Recovery	72.37
Flight Dynamics	342.68
Testing	89.75
Total:	**916.48**

Table 61: Subscale Costs by Subteam

Subteam	Total Cost ($)
Structures	635.33

Avionics & Recovery	34.75
Flight Dynamics	1224.25
Testing	30.00
Payload	292.21
Total:	**2216.54**

Table 62: Full-Scale Costs by Subteam

Item Description	Vendor	Subteam	Unit Price	Quantity	Total
Fiberglass Airframe G12-3.0	Wildman	Structures	$90.24	2	$180.48
Fiberglass Coupler G12-3.0	Wildman	Structures	$2.54	24	$60.69
Nosecone	Wildman	Structures	$64.90	1	$64.90
E-matches	Wildman	Testing	$17.95	5	$89.75
Fiberglass Airframe G12-2.1	Wildman	Structures	$31.68	1	$31.68
Rail Buttons	Apogee	Structures	$11.73	2	$23.46
Aerotech J415W-14A	Apogee	Flight Dynamics	$131.60	1	$131.60
Motor Hardware	Apogee	Flight Dynamics	$211.08	1	$211.08
3'' PVC Rod	McMaster	Structures	$50.47	1	$50.47
Eyebolts	McMaster	Recovery	$4.90	8	$39.20
Terminal Blocks	Amazon	Recovery	$13.99	1	$13.99
Keylock Switch	Amazon	Recovery	$9.59	2	$19.18
G10 Fiberglass	Inventory	Structures	$0.00	1	$0.00
1/2 in Plywood	Inventory	Structures	$0.00	1	$0.00
				Total	**$916.48**

Table 63: Subscale Line-Item Budget

Item Description	Vendor	Subteam	Unit Price	Quantity	Total
USB Camera	Amazon	Payload	$60.99	3	$182.97
Solenoid motor (4.5mm stroke)	Harfington	Payload	$9.81	4	$39.24
Stepper motor	Harfington	Payload	$7.83	4	$31.32
Radio Dongle (transceiver)	Ebay	Payload	$30.99	1	$30.99
Radio antenna	Amazon	Payload	$13.99	1	$13.99
Battery bank (raspberry pi)	Amazon	Payload	$13.99	1	$13.99
USB extension cable	Amazon	Payload	$5.84	1	$5.84
Radio adaptor kits	Amazon	Payload	$6.29	1	$6.29
USB-C Power cable 3.3ft	Amazon	Payload	$7.99	1	$7.99
DC-DC stepup converter	Amazon	Payload	$15.00	1	$15.00
PCB	JLC PCB	Payload	$10.00	1	$10.00
STEMMA QT 4-pin Female	Adafruit	Payload	$0.95	2	$1.90
STEMMA QT 4-pin to Male	Adafruit	Payload	$0.95	2	$1.90
Adafruit BMP390	Adafruit	Payload	$10.95	1	$10.95
N-Channel MOSFET Gates	Digikey	Payload	$1.99	5	$9.95
JST SM Connector (20pc)	Walmart	Payload	$9.07	1	$9.07

Diodes	Digikey	Payload	$0.14	20	$2.80
Raspberry Pi	Inventory	Payload	$0.00	1	$0.00
Adafruit BNO055 IMU	Inventory	Payload	$0.00	1	$0.00
Li-Po Battery (Actuators)	Inventory	Payload	$0.00	1	$0.00
MPL3115A2 Barometer	Adafruit	Payload	$9.95	1	$9.95
Baofeng UV-5R Radio	Amazon	Testing	$30.00	1	$30.00
Nosecone	Wildman	Structures	$75.90	1	$75.90
Airframe	Wildman	Structures	$102.47	3	$307.41
Couplers	Wildman	Structures	$2.86	20	$57.20
Motor Tube	Wildman	Structures	$45.12	2	$90.24
Bulkheads	McMaster	Structures	$81.12	1	$81.12
Rail Buttons	Apogee	Structures	$11.73	2	$23.46
Eyebolts	McMaster	Recovery	$4.90	4	$19.60
D links	McMaster	Recovery	$2.78	2	$5.56
Terminal Blocks	Amazon	Recovery	$9.59	1	$9.59
Payload Hinge	McMaster	Payload	$14.52	3	$10.32
Motor Retainer	Apogee	Flight Dynamics	$75.83	1	$75.83
Motor Forward Closure	Apogee	Flight Dynamics	$111.82	1	$111.82
Motor Aft Closure	Apogee	Flight Dynamics	$108.74	1	$108.74
Motor Casing	Apogee	Flight Dynamics	$329.18	1	$329.18
Thrust Plate	Apogee	Flight Dynamics	$46.71	1	$46.71
Aerotech K1000T-PS	Csrocketry	Flight Dynamics	$183.99	3	$551.97
				Total	**$2216.54**

Table 64: Full-scale Line-Item Budget

Item Description	Vendor	Subteam	Unit Price	Quantity	Total
PETG 3D Printer Filament	PRUSA	Payload	29.99	3	$89.97
Rivets	Apogee	Testing	$0.74	50	$37.05
Shear Pins	McMaster	Testing	$0.09	100	$8.74
RocketPoxy	Apogee	Structures	$67.14	1	$67.14
JBWeld	Amazon	Structures	$20.00	3	$60.00
				Total	**$262.90**

Table 65: General Project Line-Item Budget

Item Description	Vendor	Subteam	Unit Price	Quantity	Total
E-matches	Wildman	Testing	$17.95	5	$89.75
Baofeng UV-5R Radio	Amazon	Testing	$30.00	1	$30.00
				Total	**$119.75**

Table 66: Testing Line-Item Budget

6.5 Conclusion

In conclusion, Swamp Launch Rocket Team is confident in the primary designs identified in this preliminary design review and their ability to meet the requirements set by NASA and the team.